Cyclodepsipeptides from a Kenyan Marine Cyanobacterium

A thesis submitted in fulfilment of the requirements for the degree of

MASTER OF SCIENCE

of

Rhodes University

by

Thomas Mwambire Dzeha

November 2002

Acknowledgements

It has been my ardent pleasure to work with Prof. Mike Davies-Coleman whose relentless support and supervision throughout my research in the laboratory and in this thesis has been of great help. I wish to thank my colleagues of the Marine Natural Products Research Group (Prof. D.E.A. Rivett, Greg, Edith, Chris, Meke, Carole and Andrew) and the Organic Chemistry discussion group especially Prof. Kaye, Musa and Kevin who motivated me to work harder by example. Dr. Denzil Beukes (Faculty of Pharmacy, Rhodes) and Prof. Kerry McPhail (Oregon State University) encouraged me to proceed with my research. Collection of *Lyngbya majuscula* samples was possible because of the support of Shadrack Tunje and Gaya Chibundi of the Kenya Marine and Fisheries Research Institute (KMFRI) with who I shared turbulent currents at the Shimoni channel. Pamela Ochieng (KMFRI) provided me with the map of Kenya. Stereochemical studies were successful because of the assistance of Mr. Aubrey Soneman (Rhodes). Dr. Denver (University of Cape Town) performed the biological studies on homodolastatin 16. Dr. Marcel Jaspars (University of Aberdeen, Scotland, U.K) in whose laboratory I was a research fellow in 2000 prepared me to face the challenges of research at Rhodes. I wish to acknowledge emeritus Professor Shmuel Halevy (Hebrew University, Israel) for introducing me to natural products research in March 1996. My research at Rhodes would not have been possible if it were not for Professor John Faulkner (Scripp's Institution of Oceanography, University of California, San Diego) who provided me with a scholarship from the National Cooperative Drug Discovery Grant (NCDDG) of the US National Institutes of Health. I am thankful to Dr. Johnson Kazungu (director KMFRI) for granting me a study leave. The fortitude and perseverance of my dear wife Florence and my children; Ruwa, Njira and Haydar (Daddy, do you say good morning teacher like me?) gave me hope to work harder and to compensate for my days of absence from them. Mariam Makbell has always been helpful to my family in my absence and I am grateful to her. I acknowledge my parents (Dzeha Mwamvula and Kajumwa Mwandaza) for sacrificing their monies and time to take me to school. My friends at Rhodes, Kemi and Admasu provided me with the much-needed moral support; and to those who indirectly assisted me. This thesis is dedicated to "Baha'u'llah" (the Lord of the Age) Who Has been unfailing to me at all times.

Table of Contents

List of Figures, Schemes and Tables

Figure

Scheme

Table

List of Abbreviations

1D	one dimensional
2D	two dimensional
α	alpha
β	Beta
δ	delta
γ	gamma
$[\alpha]_D$	specific rotation (determined using the sodium D line at the temperature quoted)
CD	circular dichroism
COSY	correlation spectroscopy
D-	dextrorotatory
DMSO	dimethyl sulfoxide
EtOAc	ethyl acetate
EIMS	electron impact mass spectrometry
FABMS	fast atom bombardment mass spectrometry
FDAA	1-fluoro-2,4-dinitrophenyl-5-L-alanine amide
FFDNB	1,5-difluoro-2,4-dinitrobenzene
Fn	fraction
FT-IR	fourier transform infra red
GC	gas chromatograph
GC-MS	gas chromatography-mass spectrometry
GI_{50}	median growth inhibition
HIV-AIDS	human immunodeficiency virus-acquired immune deficiency syndrome
HMBC	heteronuclear multiple bond coherence
HPLC	high performance liquid chromatography

HRFABMS	high resolution fast atom bombardment mass spectrometry
HSQC	heteronuclear single quantum coherence
HSQMBC	heteronuclear single quantum multiple bond correlation
IC_{50}	median inhibitory concentration
i.d	internal diameter
i-PrOH	isopropanol
IR	infrared spectroscopy
J	coupling constant
KB	human epidermoid – nasopharyngeal tumour cell line
L-	laevorotatory
LD_{50}	median lethal dose
LoVo	Human ovarian cancer cell line
m	multiplet
MeOH	methanol
MHz	Mega Hertz
mL	millilitre
NIH309	National Institutes of Health strain 309
nM	nanometers
NMR	nuclear magnetic resonance
nOe	nuclear Overhauser enhancement
NOESY	nuclear Overhauser enhancement spectroscopy
ODS	octadecylsilane
ORD	optical rotatory dispersion
PFPA	pentafluoropropanoic acid anhydride
ppm	parts per million

q	quartet
r	radius
ROESY	rotating-frame Overhauser enhancement spectroscopy
RP	reversed phase
s	singlet
t	triplet
TFA	trifluoroacetic acid
TLC	Thin Layer Chromatography
TOCSY	total correlation spectroscopy
tR	retention time
µ	micron
µg	micogram
UV	ultraviolet
viz	

ABSTRACT

An examination of an organic extract of the cyanobacterium *Lyngbya majuscula* collected from Wasini Island off the southern Kenyan coast led to the isolation of the known cyclodepsipeptide antanapeptin A (**7**), recently isolated from a Madagascan collection of *L. majuscula*, and a new bioactive cyclodepsipeptide, homodolastatin 16 (**42**). Although *L. majuscula* is a common, pantropical cyanobacterium this study represents the first investigation of the natural product chemistry of a Kenyan population of *L. majuscula.* The structures of the two cyclodepsipeptides were determined from 2D NMR and mass spectrometry data. The *L*- stereochemistry of the proline, valine, and N-methylphenylalanine amino acids in **7** and the *L* – proline configuration in **42**, was confirmed by Marfey's HPLC method. Chiral GC was used to determine the absolute stereochemistry of the hydroxyisovaleric acid moiety in **7** and **42**, the lactate residue in **42** and tentatively propose an *L*-stereochemistry for the *N*-methylisoleucine amino acid in **42**. Homodolastatin 16, a higher homologue of the potential anti-cancer agent, dolastatin 16, exhibited moderate activity against two oesophageal cancer cell lines.

CHAPTER ONE

INTRODUCTION

1.1 Marine organisms as a source of new pharmaceuticals

Bioprospecting for drugs from terrestrial plants, prokaryotic microbes and eukaryotic fungi has been successful in providing many useful organic medicinal compounds such as penicillin, aspirin and taxol. However, together with the ever increasing threat of drug resistance by microbes, no cure for the dreaded HIV-AIDS, some cancers, arthritis and many other diseases has been found.[1] Accordingly, scientists have over the past four decades, increasingly turned towards the oceans for new and alternative medicines because marine organisms (microbes, algae and marine invertebrates) have proved to be a rich source of novel biologically active secondary metabolites or natural products. Marine bioactive metabolites are frequently derived from biosynthetic pathways unique to the marine environment and possess structural features which are not found in terrestrial natural products. The secondary metabolites produced by certain organisms *e.g*. *Coelenterata* (soft corals, sea fans), *Porifera* (sponges), *Bryozoa* (bryozoans) and *Echinodermata* (sea stars, sea cucumbers),[2] are thought to act as antifeedants or toxins to prevent predation of the producing organism. Additional roles for these metabolites include growth inhibition of competing organisms on a marine reef. Marine reefs are very competitive environments characterized by limited nutrients and space.

Significant advances have been made since the early 1960s when scientists first began to view the oceans as a new source of potentially useful pharmaceutical compounds. Pseudopterosin C (**1**), isolated by Fenical's research group at Scripps Institution of Oceanography, San Diego, from the Caribbean sea whip *Pseudopterogorgia elisabethae,* was one of the first products to reach the market as an anti-inflammatory preparation.[3] Two marine derived drugs, dolastatin 10 (**2**) isolated from a sea hare and cryptophycin 52 (**3**) which is a synthetic derivative of a marine natural product, are in the final clinical phase for cancer therapy.[4]

In addition, approximately half of all cancer drug discovery efforts are currently focused on marine organisms.[5] Surprisingly, despite the isolation of over 13,000 novel compounds from marine organisms,[6] the numerous pharmaceuticals derived from terrestrial organisms presently still far outweigh the number of pharmaceuticals isolated from the marine environment. Marine microorganisms such as the actinomycetes and fungi, have been shown to be actively involved in the biosynthesis of highly complex marine natural products isolated from macroorganisms like sponges and tunicates.[7] Another promising source of a whole range of diverse bioactive compounds are the blue green algae, also known as cyanobacteria.

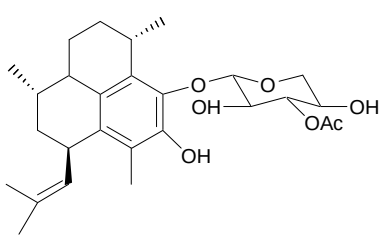

1

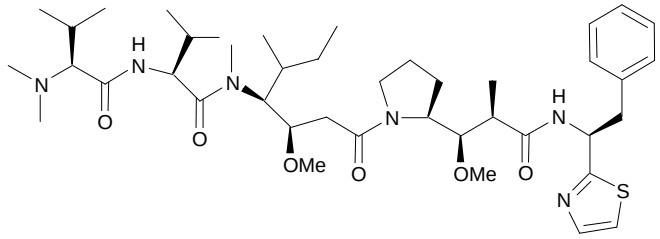

2

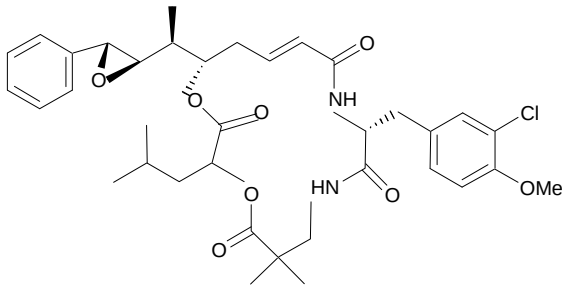

3

1.2 The marine cyanobacterium *Lyngbya majuscula*

Cyanobacteria (blue green algae) are an ancient group of photosynthetic micro-organisms which are thought to have first appeared 2.5-3.0 billion years ago.[8] Most cyanobacteria are prokaryotic obligate phototrophs. Prokaryotes lack a defined nucleus and have simplified internal organization of the cell contents.

The term obligate used here, implies that only some species of cyanobacteria can grow organotrophically and are thus capable of balancing osmotic pressure as well as resisting the denaturing effects of salts. Cyanobacteria are found either in unicellular or filamentous (branched or unbranched) forms with the latter form predominating. Generally, cyanobacteria are classified as gram-negative and are characterised by a peptidoglucan cell wall.[9] The photosynthetic mechanism in plants is thought to be derived from cyanobacterial progenitors as plants appeared only about 250 million years ago as compared to cyanobacteria which came into existence much earlier. Although photosynthetic cyanobacteria are similar in many respects to plants, their metabolic pathways are very similar to those of bacteria. The ability of cyanobacteria to survive extremely low carbon dioxide concentrations is because they are able to concentrate carbon dioxide within polyhedral structures called carboxysomes which are present in their cell walls. These carboxysomes contain the enzymes ribulose-1,5-biophosphate carboxylase and carbonic anhydrase. In addition, many species of cyanobacteria are capable of fixing nitrogen through nitrogenase enzymes which are found in specialised organelles called heterocysts. Consequently, cyanobacteria produce a unique range of defensive metabolites and are gaining importance as a useful and sustainable (cyanobacteria can be cultured relatively easily) source of new drugs. Indeed, the rate of discovery of novel compounds from cyanobacteria only appears to be constrained by the development and application of screening programmes, whether for anticancer, antimicrobial, cytotoxic or multi-drug resistance activities.

The mat forming *Lyngbya majuscula*, which is the organism studied in this thesis, is a cyanobacteria which is typically toxic and is known to cause skin dermatitis or swimmers itch, eye irritation, asthma and oral and gastrointestinal inflammation.[10] This notwithstanding, *L. majuscula* is also known to be a prolific source of a wide variety of useful bioactive secondary metabolites, some of which are antiproliferative agents, anti-HIV protease inhibitors and yet others have found applications in the pharmaceutical industry as potential anticancer agents. Recently, it has been estimated that 40% of cyanobacteria secondary metabolites tested at the National Cancer Institute possess anticancer activity.[11]

A typical metabolite isolated from *L. majuscula* that has shown promise as a potential anticancer drug is curacin A[12] (**4**). Curacin A is in Phase II clinical trials in the United States.

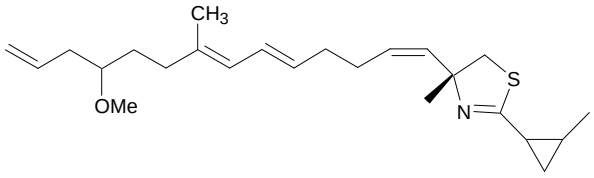

4

Barbamide (**5**),[13] which is yet another secondary metabolite originating from *L. majuscula*, has been found to have antimolluscicidal activities. *L. majuscula* has also been discovered to be a prolific producer of cyclodepsipeptides, the most recent examples of which are lyngbyabellin C (**6**)[14] and antanapeptins A-D (**7**-**10**).[15]

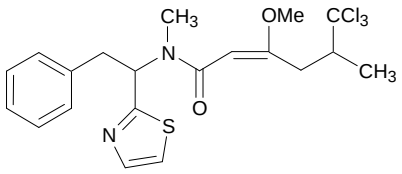

5

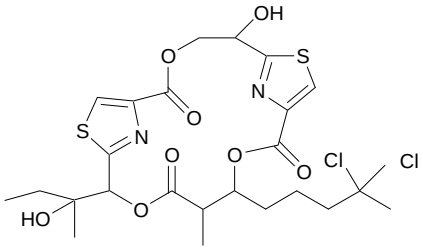

6

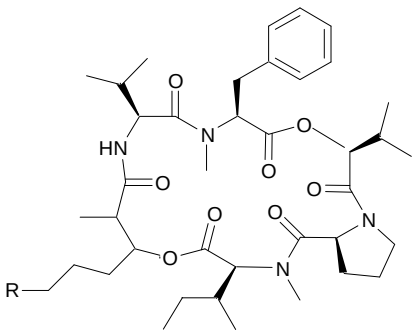

7 R = 

8 R = 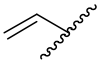

9 R = 

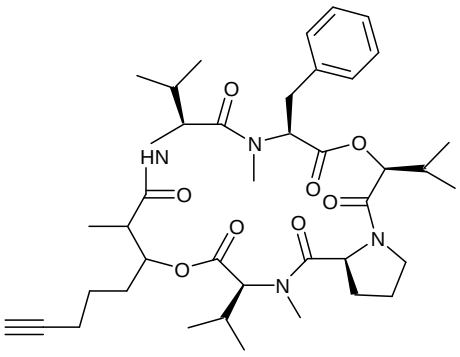

10

Cyclodepsipeptides, or peptide lactones (cyclodepsipeptides possess at least one ester linkage in their mostly peptide backbone), are a diverse group of cyclic lipopeptides derived from mixed peptide and polyketide biosynthesis and have been found to exhibit immunosuppressant, antiviral, insecticidal and antibacterial activities in addition to showing cytotoxicity toward leukemia cells.[16-18] Throughout this range of biological activities it would appear that cyclodepsipeptides display a highly specific affinity for either sodium or potassium ions.[19] In common with other lipopeptides, cyclodepsipeptides also have been found to have an affinity for liposomes and cell membranes.[20] The relatively low molecular weight of many cyclodepsipeptides enables them to pass through the blood/tissue and blood/brain barriers implying that they could be applied directly as drugs.[20]

1.3 A review of cyclodepsipeptides isolated from the marine cyanobacterium *Lyngbya majuscula*

In this thesis the isolation and identification of two cyclodepsipeptides from a Kenyan *L. majuscula* is described. To provide some background to the research discussed in this thesis, the isolation and identification of twenty seven cyclodepsipeptides isolated from *L. majuscula* is discussed here. Gerwick *et al.* have recently comprehensively reviewed the alkaloid (nitrogen containing) metabolites from marine cyanobacteria and other microorganisms, which also included some cyclodepsipeptides from *L. majuscula*.[4] The review presented here focuses in greater detail on the isolation and identification of cyclodepsipeptides from *L. majuscula*, and includes sixteen compounds not covered in Gerwick *et al.'s* review. In our review, we have followed Gerwick *et al.*'s general method of subdividing the nitrogen containing metabolites of marine cyanobacteria according to the presence of two unusual, yet common, structural moieties namely β-amino acids and β-hydroxy acids. Where both β-amino acids and β-hydroxy acids occur in the same cyclodepsipeptide, precedence, in terms of the classification system adopted here, is given to the β-amino acids. A number of *L. majuscula* cyclodepsipeptides, which deviate from this general classification, are also reviewed.

1.3.1 Cyclodepsipeptides containing β-amino acids

The structures of the cyclodepsipeptides containing β-amino acid moieties are presented here in the order of increasing complexity of these β-amino acids. An arrow pointing to the carbonyl carbon (C-1) of the β-amino acid has been used to clearly indicate the position of this moiety in the cyclodepsipeptide structures. Common abbreviations for amino acid and polyketide substructures within the cyclodepsipeptide molecule are given alongside each structure to further simplify the structures of these complex compounds.

1.3.1.1 Cyclodepsipeptides containing a 3-aminopropanoic acid (β-alanine) moiety

Yanucamide A (**11**) and yanucamide B (**12**) were isolated by Gerwick and co-workers from Yanuca island, Fiji out of a mixed assemblage of the marine cyanobacteria *Schizothrix* sp. and *L. majuscula*.[21] The two cyclodepsipeptides were found to be moderately toxic to brine shrimp.

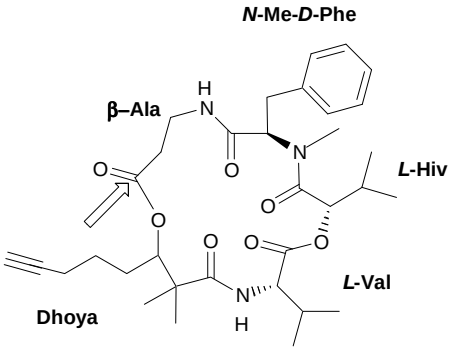

11

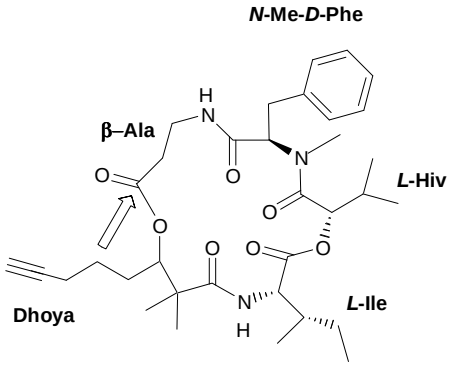

12

Normal and reversed phase vacuum liquid chromatography (VLC) followed by reversed phase high performance liquid chromatography (HPLC) were used to purify the two cyclodepsipeptides.

Fast atom bombardment mass spectrometry (FABMS) data afforded a molecular formula of $C_{33}H_{48}N_3O_7$ for **11** and $C_{34}H_{50}N_3O_7$ for **12** suggesting that **12** possessed one methylene group more than **11**. Nuclear magnetic resonance (NMR) spectroscopic data revealed five partial structures for both yanucamide A and yanucamide B. The five partial structures in **11** were *L*-valine (Val), *N*-methyl-*D*-phenylalanine (*N*-Me-*D*-Phe), β-alanine (β-Ala), 2-hydroxy-*L*-isovaleric acid (*L*-Hiv) and the unusual amino acid residue 2,2-dimethyl-3-hydroxy-7-octynoic acid (Dhoya). The partial structures established for **11** were replicated in **12** except that an *L*-isoleucine (*L*-Ile) residue replaced the *L*-valine residue found in **11**. The heteronuclear multiple bond coherence (HMBC) NMR data was used to connect the unusual 2,2-dimethyl-3-hydroxy-7-octynoic acid fragment to β-alanine and to afford the 2,2-dimethyl-3-hydroxy-7-octynoic acid / *L*-valine / 2-hydroxy-*L*-isovaleric acid / *N*-methyl-*D*-phenylanine sequence of the two yanucamides. Marfey's analysis was used to establish the *L*- and *D*- configurations of the valine and *N*-methylphenylalanine residues respectively whereas the *S*(*L*)-stereochemistry of the 2-hydroxyisovaleric acid moiety was determined by chiral gas chromatography-mass spectrometry (GC-MS) comparison of the methyl ester of **11** with *R* and *S* methyl-2-hydroxyisovalerate. Both Marfey's analysis and the chiral GC method for the determination of amino acid and polyketide fragment stereochemistry are discussed in more detail in Section 1.4. The stereochemistry of the polyketide derived β-hydroxy acid, 2,2-dimethyl-3-hydroxy-7-octynoic acid residue (Dhoya) previously reported in the kulolides and kulokainalide isolated from the mollusc ***Philinopsis speciosa***[22, 23] was undetermined. However, a study by Scheuer and co-workers showed that *P. speciosa* preys on another mollusc *Stylocheillus longicaudus*, which in turn sequesters secondary metabolites from mat-forming cyanobacteria e.g. *L. majuscula*. The isolation of the 2,2-dimethyl-3-hydroxy-7-octynoic acid residue (Dhoya) possessing yanucamides from *L. majuscula* (cyanobacteria) and the findings of the study carried out by Scheuer and co-workers (which revealed that the origin of the kulolides and their related metabolites associated with *P. speciosa* was of a dietary origin) led to the speculation that the stereochemistry of the Dhoya fragment was 3*S* as in kulolide 1.

1.3.1.2 Cyclodepsipeptides containing a 3-amino-2-methylpentanoic acid moiety

Absorption, gel filtration and reversed phase chromatography of an *L. majuscula* collection from Enewetak Atoll in the Marshall Islands by Moore and co-workers, led to the isolation of majusculamide C (**13**) in moderate yield (0.05-0.1% of dry sample).[24] The molecular formula $C_{50}H_{80}N_8O_{12}$ of **13** was obtained by FABMS studies. A combination of infrared spectroscopy, one-dimensional (1D) and two-dimensional (2D) NMR spectroscopy unequivocally supported the molecular formula.

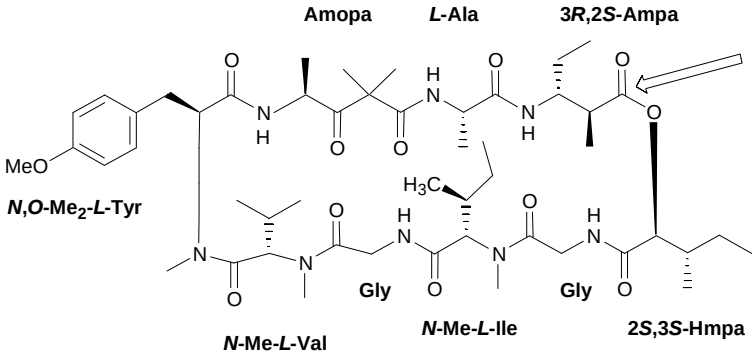

13

Acid hydrolysis of **13** gave eight degradation products of which five were known amino acids. The structures of these amino acids; *L*-alanine (*L*-Ala), 2x glycine (Gly), *N*-methyl-*L*-valine (*N*-Me-*L*-Val), *N,O*-dimethyl-*L*-tyrosine (*N,O*-Me_2-*L*-Tyr) and *N*-methyl-*L*-isoleucine (*N*-Me-*L*-Ile) were established by comparison of the spectroscopic data of the cyclodepsipeptide degradation derived amino acids with authentic samples. The structure of the cyclodepsipeptide was assembled from the partial structures by proton-proton nuclear Overhausser enhancement (nOe) studies. The *L*-stereochemistry of alanine, *N*-methylvaline and *N*-methylisoleucine was established by qualitative optical rotatory dispersion (ORD) studies in which positive Cotton effects were observed at about 225 nm for acidic solutions of these compounds. The *L*-stereochemistry of *N,O*-dimethyltyrosine was confirmed from its dextrorotatory optical rotation. NMR was used to determine the structures of the remaining three degradation

products namely; 3-amino-2-methylpentanoic acid (Ampa), 4-amino-2,2-dimethyl-3-oxo-pentanoic acid (Amopa) and 2*S*-hydroxy-3*S*-methylpentanoic acid (2*S*,3*S*-Hmpa). Moore and co-workers were only able to establish the relative 2*S*,3*S* stereochemistry of the latter degradation product. However, the reisolation of (**13**) from the sponge *Ptilocaulis trachys*,[25] also collected from Enewetak Atoll, enabled confirmation of the absolute stereochemistry of the unusual 3*R*-amino-2*S*-methyl pentanoic acid (3*R*,2*S*-Ampa) fragment through a combination of the synthesis of all possible stereoisomers of the fragment and Marfey's HPLC method. The stereochemical assignment of **13** was later confirmed independently by Bates *et al.*[26] and Williams *et al.*.[25] Majusculamide C was found to be active against the fungal pathogens *Phytophthora infestans* and *Plasmopora viticela*.[24] *Phytophthora infestans* and *P. viticela* are the causative organs of tomato late blight and grape downy mildew respectively. 57-Normajusculamide C (**14**) was isolated by Mynderse *et al.* from a similar Enewetak Atoll collection of *L. majuscula* to the collection which yielded **13**.[27] FABMS data afforded a molecular formula of $C_{49}H_{78}N_8O_{12}$ for **14**, which differed by one methylene group from that of **13**, implying that **14** was a lower homologue of **13**.

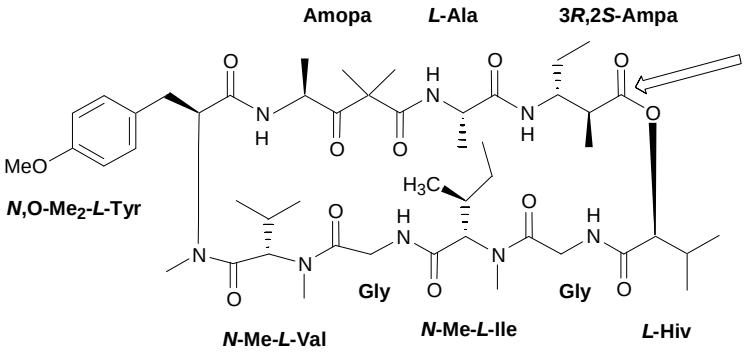

14

One-dimensional (1D) and two-dimensional (2D) NMR spectroscopy were used for the structure elucidation of **14**. The partial structures of **14** identified by NMR were *L*-alanine (*L*-Ala), glycine x2 (Gly x2), *N*-methyl-*L*-valine (*N*-Me-*L*-Val), *N*,*O*-dimethyl-*L*-tyrosine (*N*,*O*-Me_2-*L*-Tyr), *N*-methyl-*L*-isoleucine (*N*-Me-*L*-Ile) and an *L*- α-hydroxy

isovaleric acid (*L*-Hiv) residue in place of the 2*S*-hydroxy-3*S*-methylpentanoic acid residue found in **13**. Acid hydrolysis of the cyclodepsipeptide also resulted in eight degradation products whose structures were confirmed by comparison of spectroscopic data of the cyclodepsipeptide degradation derived amino acids with those of authentic standards. The *L*-stereochemistry observed for the aliphatic amino acids alanine, *N*-methylvaline, *N*,*O*-dimethyltyrosine, *N*-methylisoleucine was determined from ORD data in which Cotton effects were observed at 225 nm for acidic solutions of the respective residues as observed originally for majusculamide C. The amino acid sequence and the substitution of the 2-hydroxyisovaline moiety for the isoleucic acid was established from nOe data and confirmed by studies of the electron impact mass spectrometry (EIMS) fragment ions. 57-normajusculamide was found to be an antimycotic agent against *Saccharomyces pastorianus*.[27]

Lyngbyastatin 1 (**15**) and epilyngbyastatin 1 (**16**) were isolated by Harrigan *et al*.[28] as an inseparable mixture from extracts of firstly an assemblage of *L. majuscula* and *Schizothrix calcicola* and secondly *L. majuscula* strains collected near Guam. ^{1}H and ^{13}C NMR spectral data suggested that the two epimeric complexes contained *N*-methylated depsipeptides and that they differed only in the stereochemistry at a single carbon atom (C-15). Unfortunately, given the epimeric nature of the mixture of **15** and **16**, NMR spectroscopy could not be used as a tool in the structure elucidation of **15** and **16** because of NMR signal doubling and line broadening. The high resolution FABMS data of the epimeric mixture yielded an *m/z* value which afforded the molecular formula $C_{51}H_{82}N_8O_{12}$ for both compounds. Comparison of the high resolution FABMS *m/z* values of the individual base hydrolysis degradation products of the epimeric mixture of **15** and **16** with those of majusculamide C demonstrated that **15** and **16** were the *N*-methylated analogues of **12**. Marfey's HPLC method established that **15** and **16** possessed an *N*-methyl-*L*-alanine residue (*N*-Me-*L*-Ala) instead of the *L*-alanine (*L*-Ala) residue found in **12**. In addition, **16** and **17** also contained an *N*-methyl-*L*-leucine (*N*-Me-*L*-Leu) instead of the *N*-methylisoleucine (*N*-Me-*L*-Ile) found in **12** making them structurally closer to dolastatins 11 and 12 than to majusculamide C.

Dolastatins 11 and 12 are cyclodepsipeptides which were isolated from the Indian Ocean sea hare *Dolabella auricularia*.[29]

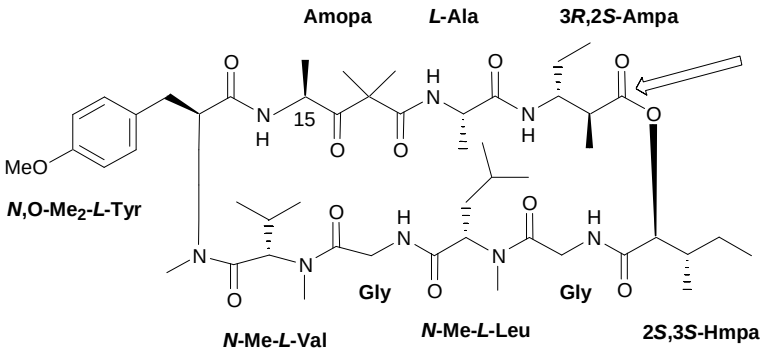

15

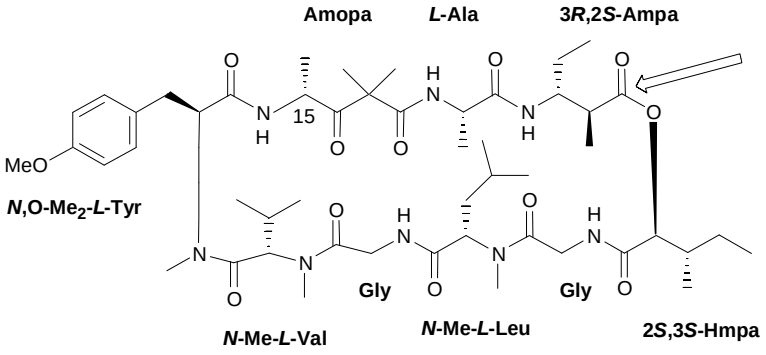

16

As a result of the complexity of the NMR spectra of the two epimeric compounds **15** and **16**, samples of these two cyclodepsipeptides were completely hydrolysed in 6N HCl after which the individual components were isolated by semi-preparative C_{18} reversed phase HPLC. The isolated hydroxy acid component was deduced to be 2*S*-hydroxy-3*S*-methylpentanoic acid by circular dichroism (CD) techniques and ^{1}H NMR spectral comparison with a synthetic standard. The complete structures, amino acid residue sequence and absolute stereochemistry of lyngbyastatin 1 and epilyngbyastatin1

were to a greater extent deduced from a comparative analysis of data published previously for majusculamide C and dolastatin 11.[29] The C-15 epimeric nature of **15** and **16** was confirmed using Marfey's method. Peaks corresponding to derivatised racemic 2-amino-4-methyl-3-pentanone (derived from the 4-amino-2,2-dimethyl-3-oxopentanoic acid residue) were observed in HPLC chromatogram. The 2-amino-4-methyl-3-pentanone was formed during the hydrolysis of the cyclodepsipeptide through a standard acid catalysed decarboxylation of the β-keto acid fragment, 4-amino-2,2-dimethyl-3-oxopentanoic acid (Amopa). Lyngbyastatin 1 and epilyngbyastatin 1 were found to have no exploitable antitumour activity despite their initially observed KB cell cytotoxicity. Both compounds exhibited general cytotoxicity. The cytotoxicity of cyclodepsipeptides **15** and **16** was attributed to their ability to disrupt cellular microfilament networks.[28]

1.3.1.3 Cyclodepsipeptides containing a 3-amino-2-methylhexanoic acid moiety

More recently, Moore and co-workers have isolated ulongamides A-F (**17**-**22**)[30] from the apratoxin-producing cyanobacteria *Lyngbya* sp. NIH309.[31] The *Lyngbya* sp. NIH309 is a strain of *L. majuscula*.[31] The ulongamides are a series of cyclodepsipeptides containing the unusual 3-amino-2-methylhexanoic acid moiety previously associated with malevamide B.[32] Ulongamides A-F were isolated through a combination of solvent partitioning, normal phase or reversed phase column chromatography followed by reversed phase HPLC. FABMS data afforded the molecular formulae $C_{32}H_{45}N_5O_6S$ for ulongamide A (**17**); $C_{32}H_{45}N_5O_7S$ for ulongamide B (**18**); $C_{36}H_{45}N_5O_7S$ for ulongamide C (**19**); $C_{34}H_{49}N_5O_7S$ for ulongamide D (**20**); and $C_{35}H_{51}N_5O_7S$ and $C_{30}H_{49}N_5O_6S$ for ulongamide E (**21**) and F (**22**) respectively. The ulongamides E-F differ from the cyclodepsipeptides discussed previously in that they possess an *L*-alanine derived thiazole carboxylic acid. The sequence of the structural components *L*-lactic acid / *N*-methyl-*L*-phenylalanine / *N*-methyl-*L*-valine / *L*-alanine-thiazole-carboxylic acid / 3*R*-amino-2*R*-methylhexanoic acid (*L*-Lac / *N*-Me-*L*-Phe / *N*-Me-*L*-Val / *L*-Ala_d-thz-ca / 3*R*,2*R*-Amha) was obtained from HMBC and rotating-frame Overhausser enhancement spectroscopy (ROESY) data.

Similar HMBC and ROESY data interpretations afforded the *L*-lactic acid / *N*-methyl-*L*-tyrosine / *N*-methyl-*L*-valine / *L*-alanine-thiazole carboxylic acid / 3*R*-amino-2*R*-hydroxyhexanoic acid (*L*-Lac / *N*-Me-*L*-Tyr / *N*-Me-*L*-Val / *L*-Ala_d-thz-ca / 3*R*,2*R*-Amha) sequence for **18**; *L*-lactic acid / *N*-methyl-*L*-tyrosine / *N*-methyl-*L*-phenylalanine / *L*-alanine-thiazole carboxylic acid / 3*R*-amino-2*R*-hydroxyhexanoic acid (*L*-Lac / *N*-Me-*L*-Tyr / *N*-Me-*L*-Phe / *L*-Ala_d-thz-ca / 3*R*,2*R*-Amha) for **19**; 2*S*-hydroxyisovaleric acid / *N*-methyl-*L*-tyrosine / *N*-methyl-*L*-phenylalanine / *L*-alanine-thiazole carboxylic acid / 3*R*-amino-2*S*-hydroxyhexanoic acid (*S*-Hiva / *N*-Me-*L*-Tyr / *N*-Me-*L*-Phe / *L*-Ala_d-thz-ca / 3*R*,2*S*-Amha) for **20**; 3*S*-hydroxy-2*S*-methylpentanoic acid / *N*-methyl-*L*-tyrosine / *N*-methyl-*L*-phenylalanine / *L*-alanine-thiazole-carboxylic acid / 3*R*-amino-2*S*-hydroxyhexanoic acid (3*S*,2*S*-Hmpa / *N*-Me-*L*-Tyr / *N*-Me-*L*-Phe / *L*-Ala_d-thz-ca / 3*R*,2*S*-Amha) for **21** and 3*S*-hydroxy-2*S*-methylpentanoic acid / *L*-valine / *N*-methyl-*L*-valine / *L*-alanine-thiazole carboxylic acid / 3*R*-amino-2*S*-hydroxyhexanoic acid (3*S*,2*S*-Hmpa / *L*- Val / *N*-Me-*L*-Val / *L*-Ala_d-thz-ca / 3*R*,2*S*-Amha) sequence for **22**. Ozonolysis, followed by acid hydrolysis and chiral HPLC analysis of the residues obtained from ulongamide A revealed that all the aliphatic amino acids in **17** were of the *L* configuration. This *L* configuration of the amino acid residues in **17** was also observed in all the other ulongamides. The stereochemistry at C-2 and C-3 in the 3-amino-2-hydroxyhexanoic acid moiety was established by comparing the HPLC retention times of the Marfey's hydrolysates with those of synthetic standards. The *N*-methyl-*L*-phenylaniline (*N*-Me-*L*-Phe) peptide residue in **17** was replaced by an *N*-methyl-*L*-tyrosine (*N*-Me-*L*-Tyr) group in **18**. Luesch ***et al.*** established the structure of the tyrosine residue from the signal multiplicity (double doublets) in the aromatic ring region of the ^{1}H nuclear magnetic resonance that suggested a ***para*** di-substituted functionality.[31] The difference of sixteen atomic mass units in the FABMS confirmed the presence of this phenol moiety. While compounds **17** and **18** only differ by a single OH group, compounds **18** and **19** differ in the replacement of an *N*-Me-*L*-valine residue with an *N*-methyl-*L*-phenylalanine moiety. In compound **20** an *S*(*L*)-hydroxyisovaleric acid (*S*-Hiva) replaces the *L*-lactic acid (*L*-Lac) moiety observed in **18**.

The configuration at C-2 in the unusual β-amino acid moiety changes from 3*R*-amino-2*R*-methylhexanoic acid (3*R*,2*R*-Amha) in **18** to 3*R*-amino-2*S*-methylhexanoic acid (3*R*,2*S*-Amha) in **20**. Compound **21** differs from **20** in the structure of the 2*S*-hydroxy-3*S*-methylpentanoic acid (2*S*,3*S*-Hmpa) which replaces the *L*-lactic acid moiety.

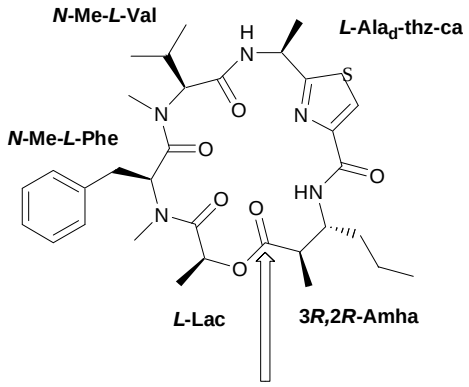

17

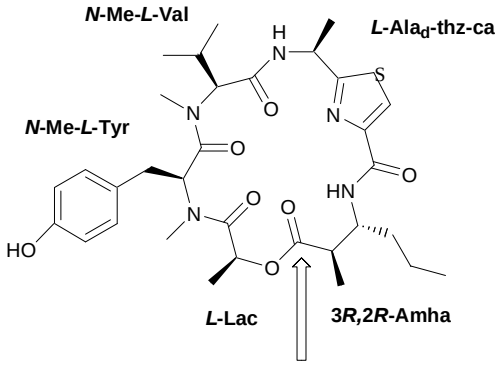

18

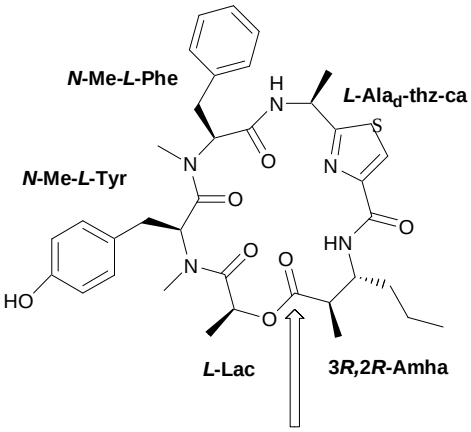

19

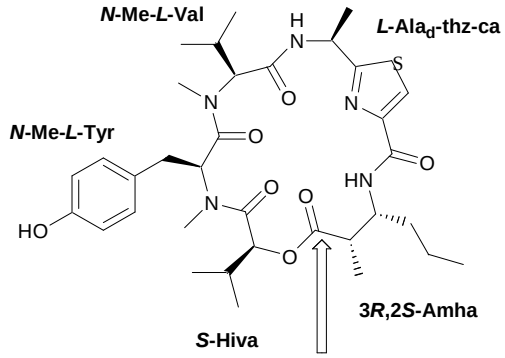

20

The replacement of the *N*-methyl-*L*-tyrosine in **21** with an *L*-valine residue in **22** constitutes the only difference between these two compounds. Despite C-2 epimerisation, the unusual β-amino acid residue 3-amino-2-methylhexanoic acid (Amha) features in all the ulongamides.

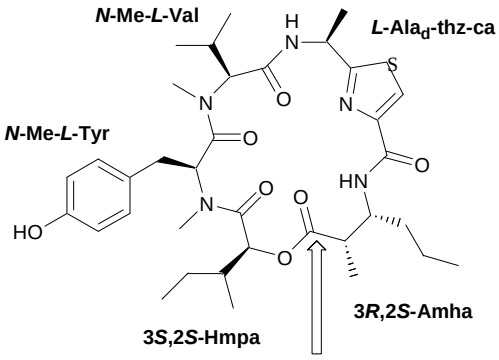

21

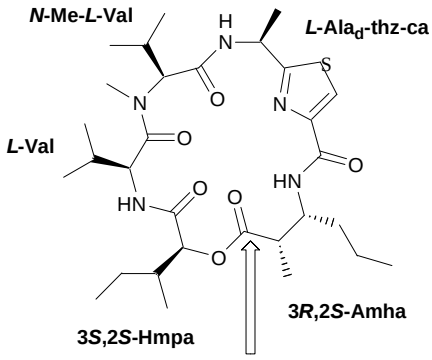

22

Interestingly, the *L*-alanine-thiazole-carboxylic acid moiety was also observed in the ulongamides A-F. Apart from ulongamide F that was inactive (supposedly because of the lack of an aromatic amino acid moiety) **17**-**21** exhibited low cytotoxic activity *in vitro* against KB and LoVo cancer cell lines at median inhibition concentrations of 1-5 μM.[30]

1.3.2 Cyclodepsipeptides containing β-hydroxy acids

The β-hydroxy acids found in cyclodepsipeptides are of polyketide origin and are usually unsaturated and occasionally halogenated. Arrows, as used previously for the β-amino acid moieties, will be used to show the position of the β-hydroxy acid group in each cyclodepsipeptide reviewed here.

1.3.2.1 Cyclodepsipeptides containing either a saturated or an unsaturated 2-methyl-3-hydroxy-7-octanoic acid moiety

In the brief introduction describing some of the general natural product chemistry of the marine cyanobacterium *L. majuscula* (Section 1.2), mention was made on some of the most recent examples of cyclodepsipeptides from *L. majuscula* among which are the antanapeptins A-D (**7**-**10**).[15]

Antanapeptin A (**7**) is one of the two cyclodepsipeptides isolated from the Kenyan circumtropical marine cyanobacterium *L. majuscula* described in this thesis. Details of the isolation, structure elucidation, amino acid sequence and stereochemistry determination of **7** isolated from the Kenyan *L. majuscula* will be discussed in Chapter 2.

Antanapeptins A-D were isolated by Nogle and Gerwick from Madagascan, collections of the cyanobacterium *L. majuscula*.[15] Compounds **7**-**10** were obtained through a combination of solvent partitioning, silica VLC and C_{18} solid-phase extraction followed by reversed phase HPLC. FABMS data yielded the molecular formula $C_{41}H_{60}N_4O_8$ for **7** while NMR data and Marfey's analysis provided the structures and stereochemistry of five amino acids *N*-methyl-*L*-isoleucine (*N*-Me-*L*-Ile), *N*-methyl-*L*-phenylalanine (*N*-Me-*L*-Phe), *L*-proline (*L*-Pro) and *L*-valine (*L*-Val). NMR data also provided the structures of the non-amino acid polyketide derived residues 2*S*-hydroxyisovaleric acid (*L*-Hiv) and the unusual β-hydroxy amino acid 3-hydroxy-2-methyloctynoic acid (Hmoya). Although this latter unusual cyclodepsipeptide residue has been observed in the molluscan secondary metabolites kulomo'opunalides[22] and onchidin B;[33] and also from the yanucamides[21] and apramides[34] isolated recently from marine cyanobacteria, the configuration at C-2 and C-3 was unassigned by Nogle and Gerwick. The 2*S* stereochemistry for hydroxyisovaleric acid (*L*-Hiv) followed from chiral GC studies. The molecular formulae afforded by the FABMS data for **8** and **9** were $C_{41}H_{63}N_4O_8$ and $C_{41}H_{65}N_4O_8$ respectively. Compounds **8** and **9** were accordingly deduced to be the alkene and saturated analogues of **7** respectively, from their ^1H and ^{13}C NMR data which was mostly compatible with those of **7**. The stereochemistries of the amino acid and polyketide derived residues in antanapeptins B-C were established in a similar manner to those for **7**. The *N*-methyl-*L*-isoleucine / 3-hdroxy-2-methyl-7-octynoic acid / *L*-valine / *N*-methyl-*L*-phenylalanine / 2*S*-hydroxyisovaleric acid / *L*-proline (*N*-Me-*L*-Ile / Hmoya / *L*-Val / *N*-Me-*L*-Phe / *L*-Hiv / *L*-Pro) sequence was established from HMBC connectivities.

2D NMR data confirmed that **10** was closely related to **7** except for the substitution of *N*-methyl-*L*-valine (*N*-Me-*L*-Val) for the *N*-methyl-*L*-isoleucine in **7**.

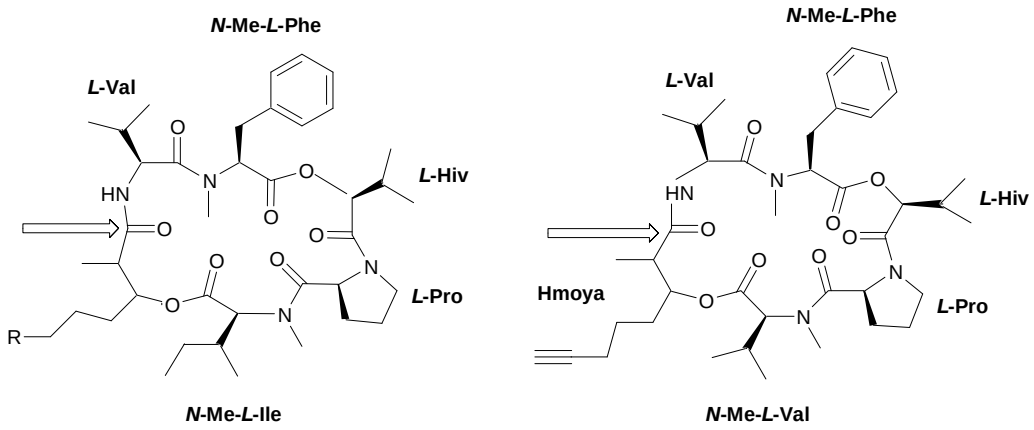

7 R= Hmoya **8** R= Hmoea **10**

9 R= Hmoaa

The molecular formula afforded for **10** from the FABMS data ($C_{40}H_{58}N_4O_8$) confirmed that **10** was a lower analogue of **7** differing only by a single methylene group. The absolute stereochemistries of the analogous amino acid and polyketide derived residues in **10** were identical to those in **7**. The antanapeptins A-D were isolated along with dolastatin 16, a potential antineoplastic agent previously isolated from the Papua New Guinea sea hare *Dolabella auricularia* by Pettit *et al.*[35] Surprisingly, no activity was found for antanapeptins A-D in several biological assays including antimicrobial, brine shrimp and sodium channel modulation assays.

1.3.2.2 Cyclodepsipeptides containing an unsaturated 2,2-dimethyl-3-hydroxy-7-octanoic acid moiety

Pitipeptolides A (**23**) and B (**24**) were isolated from *L. majuscula* collections at Piti Bomb Holes, Guam by Paul and co-workers.[36] Compounds **23** and **24**, which were purified by normal phase HPLC exhibited moderate antimycobacterial activity and were also found to stimulate elastase activity. FABMS established the molecular formulae $C_{44}H_{66}N_5O_9$ and $C_{44}H_{68}N_5O_9$ for **23** and **24** respectively. The seven partial structures found in **23**, *N*-methyl-*L*-phenylalanine (*N*-Me-*L*-Phe), glycine (Gly), *L*-proline (*L*-Pro), *L*-valine (*L*-Val), *L*-isoleucine (*L*-Ile), 2*S*-hydroxy-3*S*-methylpentanoic acid (2*S*,3*S*-Hmp) and 2,2-dimethyl-3*S*-hydroxy-7-octynoic acid (Dhoya) were assembled by analysis of 1D and 2D NMR data. The 2,2-dimethyl-3*S*-hydroxy-7-octynoic acid (Dhoya) fragment in **23** was replaced by a 2,2-dimethyl-3*S*-hydroxy-7-octenoic acid (Dhoea) residue in **24**. All the other amino acid residues of **23** were replicated in **24**. The former β-hydroxy fragment has previously been identified in *L. majuscula* metabolite yanucamide A (**11**).[21]

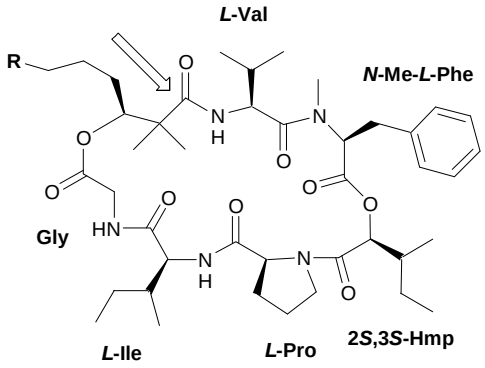

23 R= 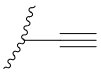 Dhoya **24** R=  Dhoea

With the exception of the connectivity between 2*S*-hydroxy-3*S*-methylpentanoic acid and *L*-proline (established by an evaluation of the one dimensional nOe data, the *L*-isoleucine / glycine / 2,2- dimethyl-3*S*-hydroxy-7-octynoic acid / *L*-valine / *N*-methyl-*L*-phenylalanine connectivity was established from HMBC data and confirmed by analysis of the ROESY data. The *L*- stereochemistry of the various amino acid residues of pitipeptolides A and B was determined from chiral HPLC analysis of the Marfey's hydrolysates. The difference of two mass units between the molecular formulae of **23** and **24** suggested that cyclodepsipeptide **24** was the reduced form of **23**. This suggestion was confirmed from the vinylic signals in both the ^{1}H and ^{13}C NMR spectra.

1.3.2.3 Cyclodepsipeptides containing a 7,7-dichloro-3-hydroxy-2-methyl-7-octanoic acid moiety or a 7,7-dichloro-3-hydroxy-2,2-dimethyloctanoic acid moiety

Lyngbyabellin A (**25**) was isolated from Guam collections of *L. majuscula* whereas lyngbyabellin B (**26**) was simultaneously isolated by Luesch *et al*. from a different collection of cyanobacterium from Guam and the Dry Tortugas in the Carribean.[37,38] The two significantly cytotoxic cyclodepsipeptides were isolated through solvent partitioning, Si gel chromatography and reversed phase HPLC. FABMS established the molecular formula of **25** as $C_{29}H_{40}Cl_2N_4O_7S_2$. The presence of the two chlorine atoms in **25** was consistent with the observed isotope peaks in the FABMS spectra. The six partial structures for **25** established from 1D and 2D NMR data were; glycine (Gly); an isoleucine derived thiazole carboxylic acid (*L*-Ile_d-thz-ca); a 2,3-dihydroxyisovaleric acid derived thiazole carboxylic acid ($Dhiva_d$-thz-ca); and the polyketide derived residue 7,7-dichloro-3-hydroxy-2,2-dimethyloctanoic acid (Dchdmoa). The partial structures were assembled mainly by analysis of the HMBC data. The weak negative Cotton effect which the CD of **25** displayed at 236 nm was interpreted as exciton coupling between the thiazole carboxylate residues. Chiral HPLC of the acid hydrolysed ozonolysis product of **25** was used to establish the absolute stereochemistry of **25**.

The stereochemistry of the β-hydroxy dichloro substituted acid residue in **25** was confirmed as 3*S* from comparison of the specific rotation of the isolated residue with that of an authentic sample of 3*S*-hydroxy-2,2-dimethyloctanoic acid. Compound **25** was cytotoxic to KB cancer cells (median inhibitory concentration of 0.03 μg mL^{-1}.) [38]

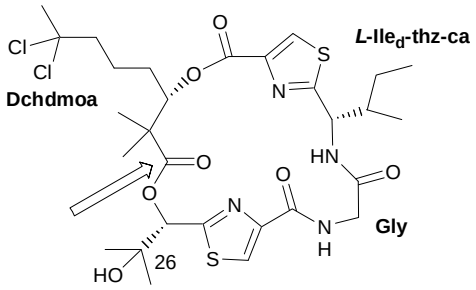

Dhiva$_d$-thz-ca

25

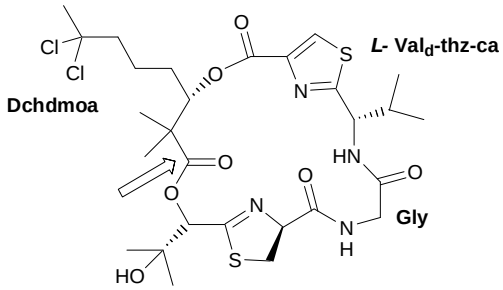

Dhiva$_d$-dhthz-ca

26

Compound **26** differed from **25** by the loss of one methylene group and the presence of a dihydrothiazole ring. These differences were confirmed by the FABMS data which afforded the molecular formula $C_{28}H_{40}Cl_2N_4O_7S_2$ for **26**. A combination of 1D and 2D NMR spectroscopy enabled the structure elucidation of the cyclodepsipeptide. The structural residues of **26**, which were assembled through HMBC, provided the sequence; 2,3-dihydroxyisovaleric derived dihydrothiazole-4-carboxylic acid / glycine / isovaline derived thiazole-4-carboxylic acid / 7,7-dichloro-3-hydroxy-2,2-dimethyloctanoic acid. The same techniques used to determine the stereochemistry of **25**, namely a combination of the chiral HPLC of the acid hydrolysates as well as that of the hydrolysates of the ozonolysis residues, were used to establish the stereochemistry of **26**.

More recently, lyngbyabellin C (**6**), which is a homologue of **25** was isolated from the lipophilic extract of the apratoxin-producing marine cyanobacterium *Lyngbya* sp. NIH309 from Short Dropoff, Palau by Moore and co-workers.[14]

FABMS with support from the 1D and 2D NMR data afforded the molecular formula $C_{24}H_{30}Cl_2N_2O_8S_2$ for **6**. The $[M+Na]^+$ isotopic cluster of peaks in the FABMS spectra of **6** were consistent with the presence of two chlorine atoms. The presence of the 7,7-dichloro-3-hydroxy-2-methyloctanoic (Dchmoa) acid residue in **6** implied that this residue in **6** differed from the similar moiety in **25** by the loss of one methyl group. The presence of the two chlorine atoms and the two disubstituted thiazole rings in **6** was established by extensive use of HSQC NMR data in combination with ^1H, ^{13}C, ^1H-^1H COSY and HMBC NMR analyses.

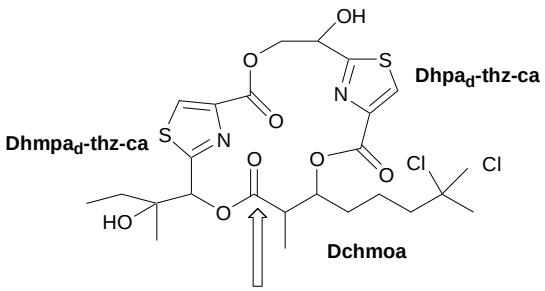

6

The 2,3-dihydroxy-3-methylpentanoic acid derived thiazole carboxylic acid (Dhmpa$_d$-thz-ca) and the 2,3-dihydroxypropanoic acid derived thiazole carboxylic acid (Dhpa$_d$-thz-ca) in **6** were connected to the 7,7-dichloro-3-hydroxy-2-methyl-octanoic acid fragment by HMBC NMR correlations. In contrast to **25** and **26**, **6** was observed to contain no amino acid residues. A paucity of **6** (100 μg) prevented a stereochemical assignment of this compound. Lyngbyabellin C was found to be weakly cytotoxic at median inhibitory concentrations of 2.1 μM against KB cells and 5.3 μM against LoVo cells. Compounds **6**, **25** and **26** were found to be closely related to the acyclic dolabellin which was isolated from the sea hare *Dolabella auricularia* but with a likelihood of a cyanobacterial dietary origin.[39] Once again, the isolation of the lyngbyabellins from *L. majuscula* and their very closely related structures to those of dolabellin strongly suggest that the metabolites isolated from the sea hare *D. auricularia* are of cyanobacterial origin.

1.3.2.4 Cyclodepsipeptides containing a 3,7-dihydroxy-2-methylnonanoic acid moiety

L. majuscula is known to produce a wide range of compounds of diverse structural complexity. The long chain β-hydroxy metabolite 3,7-dihydroxy-2-methylnonanoic acid moiety has been observed in lyngbyastatin 2 (**27**), norlyngbyastatin 2 (**28**)[40] and the molluscan sea hare cyclodepsipeptides dolastatin G and nordolastatin G.[41] Compounds **27** and **28** were isolated by Luesch ***et al.*** from Guam collections of *L. majuscula* (UOG strains VP417 and VP503) through bioassay guided fractionation and partitioning of the cytotoxic crude extracts.[40] Lyngbyastatin 2 and norlyngbyastatin 2 were finally purified on reversed-phase HPLC. Determination of the structures of these two compounds utilized a combination of standard 1D and 2D NMR spectroscopy and comparison of the NMR data with those of dolastatin G.[41] FABMS data established the molecular formula $C_{56}H_{94}N_6O_{13}$ for **27** and $C_{55}H_{92}N_6O_{13}$ for **28** respectively. COSY and HMBC data identified six amino acid residues, proline (x2), *N*-methylvaline (x2), *N*-methylisoleucine, *N*,*O*-dimethylserine. In addition, the structures of two β-hydroxy amino acid residues of a polyketide origin were also established by the same method. These two acids were 8-hydroxy-3-methoxy-4,7-dimethylnon-2,4-dienoic acid (Nena) and 3,7-dihydroxy-2-methylnonanoic acid (Nana). Initial HMBC experiments were only satisfactory in establishing the sequence *N*-methylvaline-2 / *N*-methylisoleucine / 8-hydroxy-3-methoxy--4,7-dimethylnon-2,4-dienoicacid/3,7-dihydroxy-ethylnonanoic acid (*N*-MeVal-2 / *N*-MeIle / Nena / Nana). ROESY data, not only established the remaining proline / *N*-methylvaline-1 / proline-2 (Pro / *N*-Me-Val-1 / Pro-2) sequence for **27** but also enabled expansion of the structure to accommodate the *N*,*O*-dimethylserine (*N*,*O*-diMe-Ser) residue. Additionally, the ROESY data provided the *E* configuration of the olefinic bonds in the Nena residue of **27**. The determination of the absolute stereochemistry of lyngbyastatin 1, using chiral HPLC of the acid hydrolysate, revealed an *L*- stereochemistry for all the amino acid units. Compound **28**, whose spectra exposed the enol ether relationship with **27**, had similar NMR structural features to **27**. The similarities in structure between **27** and **28** was established by the conversion of **27** into **28** on standing in the NMR solvent ($CDCl_3$).

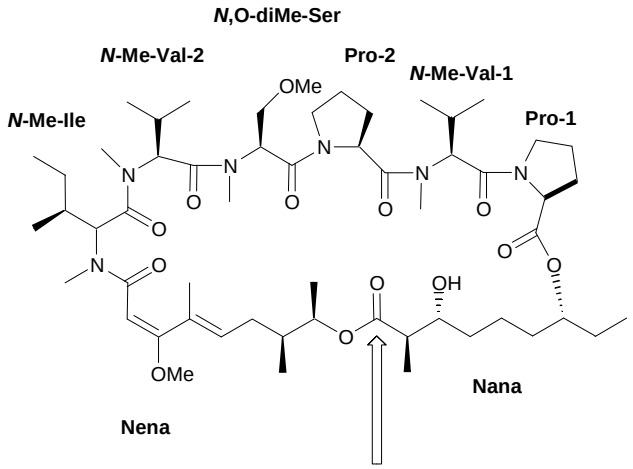

27

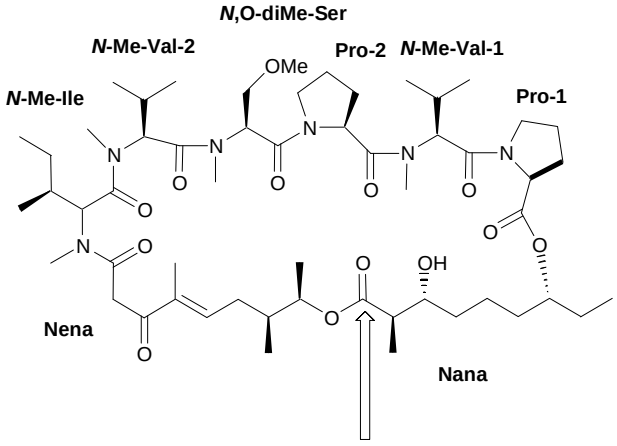

28

The deshielded methyl proton signal correlating to the enolic methoxy group in **27** was missing in **28**. As a consequence of tautomerism, **28** displayed an additional ketone carbonyl carbon signal instead of the enolic quaternary carbon observed in **27**. The close similarity in optical rotation between **27** and **28** and their dolastatin analogues was used to suggest that the configurations at the two chiral centres in the Nana and Nena fragments were the same as those in the dolastatin analogues.

Even though the two compounds **27** and **28** were isolated from bioactive crude extracts, **27**, while showing some cytotoxicity was inactive against C38 murine colon adenocarcinoma *in vivo*.

1.3.3 Cyclodepsipeptides containing more complex residues

The cytotoxic cyclodepsipeptide apratoxin **29** was isolated from Apra Harbor collections of the marine cyanobacterium *L. majuscula*. [31] The FABMS for apratoxin afforded a molecular formula $C_{45}H_{69}N_5O_8S$ while six partial fragments were established from 1D and 2D NMR data. The six identifiable spin systems included *O*-methyltyrosine, *N*-methylalanine, *N*-methylisoleucine, proline, an α,β-unsaturated modified cysteine moiety (containing a trisubstituted olefin) and a highly methylated residue of polyketide origin; 3,7-dihydroxy-2,5,8,8-tetramethylnonanoic acid incorporated in a thiazoline ring. The amino acid residue sequence *N*-methylisoleucine / *N*-methylalanine / *O*-methyltyrosine / α,β-unsaturated modified cysteine residue / 3,7-dihydroxy-2,5,8,8-tetramethylnonanoic acid / proline (*N*-Me-Ile / *N*-Me-Ala / *O*-Me-Tyr-moCys / Dtena / Pro) was determined using HMBC data and confirmed by a ROESY experiment. Marfey's hydrolysis of the hydrolysate of **29** followed by reversed phase HPLC established the *L*- stereochemistry of the *O*-methyltyrosine, *N*-methylalanine, *N*-methylisoleucine and proline. Ozonolysis of **29** released *D*- cysteic acid and established an *R*- configuration at C-30. The *J*-based advanced Karplus calculations, originally developed for stereochemical analysis in simple aliphatic organic compounds, were interestingly used to establish the relative stereochemistry of the unusual 3,7-dihydroxy-2,5,8,8-tetramethylnonanoic acid residue.[31,42,43] This technique which is also finding application in larger cyclic compounds like apratoxin utilises $^{3}J_{H,H}$ and $^{2,3}J_{C,H}$ values. The $^{3}J_{H,H}$ values were determined using 1D total correlation spectroscopy (TOCSY) and homonuclear decoupling experiments whereas the $^{2,3}J_{C,H}$ values were measured using sensitivity and gradient enhanced half-filtered TOCSY or 2D gradient selected heteronuclear single quantum multiple bond correlation (HSQMBC).[31]

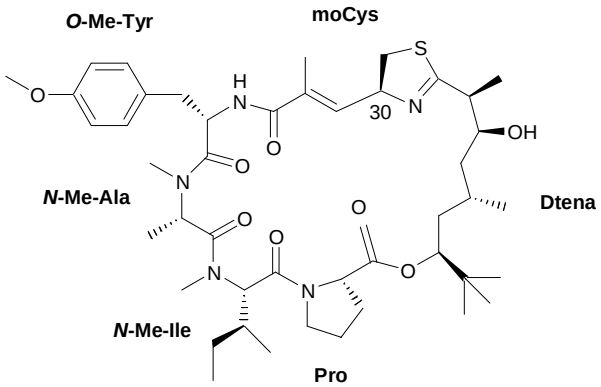

29

Consequently, the relative stereochemistry of the unusual fatty acid residue was found to be 3*S**,7*S**-dihydroxy-2,5*S**,8*S**,8*S**-tetramethylnonanoic acid. Cyclodepsipeptide **29** showed potent cytotoxicity at a medium inhibition concentration of 0.52 nM against KB and 0.36 nM against LoVo cancer cells but was otherwise inactive in vivo against mammary tumors.[42]

Curacao collections of *L. majuscula* led to the isolation of antillatoxin (**30**) as a highly ichthyotoxic compound.[44] An ichthyotoxic compound kills experimental gold fish at a fairly low median lethal dose. Compound **30** was isolated by Orjala *et al*. in small yields from the ichthyotoxic crude extract using exhaustive chromatography on silica and RP-18 gels. Final purification using reversed phase C_{18} HPLC afforded **30** as an armorphous powder. The FABMS data for **30**, yielded the molecular formula $C_{28}H_{45}N_3O_5$ which suggested eight degrees of unsaturation consistent with the single ring, four carbonyls and three olefinic bonds, (two of which were conjugated) as evidenced from the NMR data. Some specimens of *L. majuscula* are prolific producers of numerous diverse compounds as demonstrated by the co-isolation of **30**, curacins, barbamides, carmabins and two other quinoline alkaloids from the same collection of *L. majuscula*.[44] The six peptide fragments of **30** which included *N*-methylvaline (*N*-MeVal), glycine (Gly) and alanine (Ala) were assembled by 2D NMR

spectrometry. The stereochemistry of the two chiral amino acids was found to be *L*- from chiral TLC comparison of the hydrolysates with authentic samples to these two amino acids. The linear sequence glycine / *N*-methylvaline / alanine (Gly / *N*-MeVal / Ala) as well as the incorporation of the conjugated diene and the *tert*-butyl group into the macrostructure in **30** was established from HMBC and NOESY data.

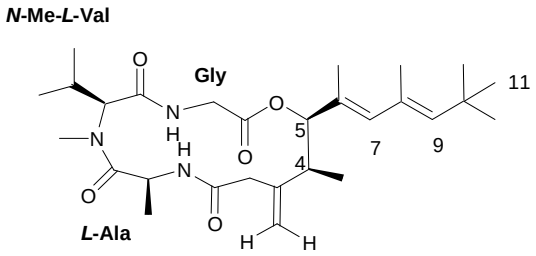

30

Molecular modelling, NOESY data, *J* values and CD spectroscopy were used to establish a 4*S**,5*R** relative stereochemistry at the two stereocenters in the complex polyketide derived residue. The 4*S**,5*R** stereochemistry was later disputed and revised to a 4*R*, 5*R* absolute configuration following synthetic studies by the Shioiri group[45,46] and by White *et al*. [47]

Somamide A (**31**) and somamide B (**32**) were isolated by Nogle *et al*. from a Fiji collection of an assemblage of *L. majuscula* and *Schizothrix* sp.[48] The cyclodepsipeptides **31** and **32** possesed an extended fatty acid residue similar to that previously reported in symplostatin 2 and dolastatin 13.[49] Symplostatin 2 is a secondary metabolite isolated from the marine cyanobacterium *Symploca hydnoides* whereas dolastatin 13 was originally isolated from *Dolabella auricularia*. This extended fatty acid residue has been shown to be responsible for the exceptional cytotoxicity and antineoplastic activities associated with the dolastatins.[50] Somamide A was obtained as a clear oil from C_{18} solid phase extraction (SPE) followed by reversed phase HPLC. Initial IR studies showed strong infra-red bands at 1730 and 1641 cm^{-1}, indicative of the amide and ester functional groups found in **31**.

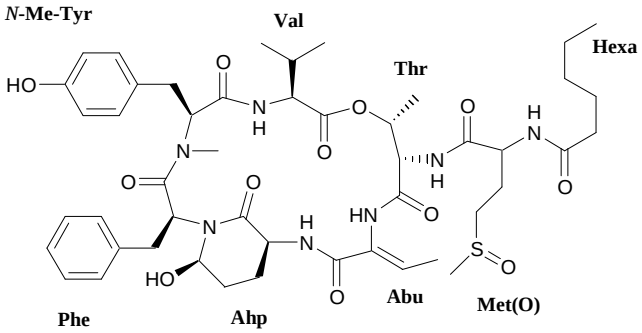

31

FABMS data afforded the molecular formula $C_{48}H_{67}N_7O_{12}S$ for **31**. Evaluation of the HSQC, COSY, HSQC-TOCSY and HMBC spectral data established eight partial structures, four of which were the standard amino acids phenylalanine, *N*-methyltyrosine, threonine and valine. The more unusual 2-amino-2-butenoic acid (Abu) and 3-amino–6-hydroxy-2-piperidone (Ahp) residues, which are usually associated with terrestrial cyclic polypeptides were similarly deduced from the 2D NMR data. Of the remaining two residues, hexanoic acid and methionine sulfoxide, the latter was observed as a racemic mixture of *S* and *R* enantiomers. The valine / *N*-methyltyrosine / phenylalanine / 3-amino–6-hydroxy-2-piperidone (Val / *N*-Me-Tyr / Phe / Ahp) and threonine / methionine sulfoxide / hexanoic acid (Thr / Met(O) / Hexa) sequences were afforded from HMBC data. ROESY correlations linked the 2-amino-2-butenoic acid (Abu) unit to the threonine residue. However, the placement of the 2-amino-2-butenoic acid (Abu) residue between the threonine and the 3-amino–6-hydroxy-2-piperidone (Ahp) was achieved from the FABMS fragmentation ions corresponding to *N*-methyltyrosine / phenylalanine / 3-amino–6-hydroxy-2-piperidone and threonine / methionine sulfoxide / hexanoic acid respectively. The relative configuration of the more unusual 2-amino-2-butenoic acid and the 3-amino–6-hydroxy-2-piperidone were established from an evaluation of HSQMBC and ROESY NMR data and comparison of chemical shift data with those of symplostatin 2 and dolastatin 13. The stereochemistry of the valine, *N*-methyltyrosine, phenylalanine, threonine and methionine amino acids in **31**, as determined by Marfey's analysis of the acid hydrolysate, were all established

to be *L*-. Compound **32**, which had a molecular formula of $C_{46}H_{62}N_8O_{12}$ from HRFABMS data, was isolated as a minor metabolite in much the same way as **31**.

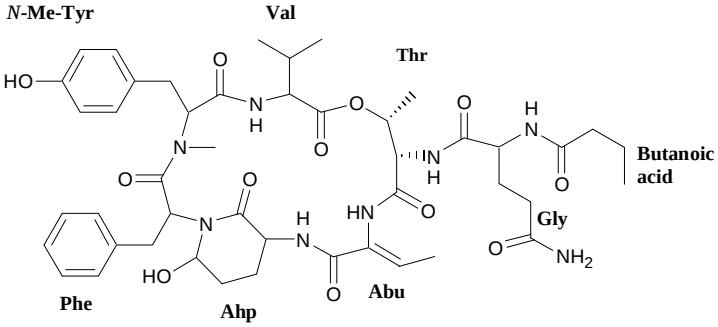

32

HMBC, HMQC and ROESY data assembled the eight partial structures of **32** in addition to establishing the sequence of valine / *N*-methyltyrosine / phenylalanine / 3-amino–6-hydroxy-2-piperidone / 2-amino-2-butenoic acid / threonine / glycine / butanoic acid. Insufficient amounts of **32** were isolated to determine its stereochemistry. The structural similarities between dolastatin 13 and the somamides once again demonstrate the fact that the dolastatins isolated from the sea hare *D. auricularia* are probably of dietary origin with their source in the cyanobacteria eaten by the sea hare.

1.4 Methods used to analyse the α-amino acid residues in *L. majuscula* cyclodepsipeptides

Cyclodepsipeptides are largely made up of chiral α-amino acids with at least one ester linkage. The methods used for the stereochemical determination of α-amino acids in cyanobacteria cyclodepsipeptides are varied. Of these methods, Marfey's method, chiral HPLC and chiral GC will be discussed here. Although the latter has not been used to determine the α-amino acid configuration in the α-amino acids from *L. majuscula* cyclodepsipeptides, this method has been used to determine the absolute stereochemistry of α-amino acids from *L. majuscula* cyclic peptides.[51]

1.4.1 Marfey's method for α-amino acid analysis

Marfey's method of stereochemistry determination of α-amino acids was developed by Marfey in 1984.[52] Prior to this, methods for the stereochemical determination of *D*- and *L*-amino acids included those developed by Manning and Moore which relied on ion-exchange chromatography of the *L*-*D* and *L*-*L* dipeptides.[53]

The initial step in Marfey's method is to liberate the individual amino acid residues by refluxing the cyclodepsipeptide with 6N hydrochloric acid for twelve hours or more. Marfey's method was also found to have the extra advantage of producing a highly absorbing chromophore which permited the determination of diastereomers at low concentrations (in the nanomole range) using HPLC with standard UV detection. In Marfey's method, commercially available 1-fluoro-2,4-dinitrophenyl-5-*L*-alanine amide (FDAA) (**33**) is used to form diastereomers with either enantiomerically pure *L*- or *D*-amino acids or a racemic mixture. The resulting diastereomers can consequently be quantitatively separated by reversed phase HPLC.

Compound **33** is used as a derivatizing agent of *L*- and *D*- α-amino acids because it contains an activated fluorine atom which can be easily displaced by the α-amino acid

moiety of *L*- and *D*- α-amino acids in a standard nucleophilc aromatic substitution reaction.

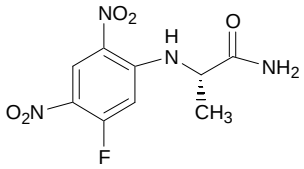

33

1-Fluoro-2,4-dinitrophenyl-5-*L*-alanine was also found to be a highly stable compound that is not easily racemised. Marfey's method is also very flexible because any optically active amino acid can be used in place of the *L*-alanine. The sequence used for the synthesis of 1-fluoro-2,4-dinitrophenyl-5-*L*-alanine amide commonly known as Marfey's reagent, and for the derivatization of *L*-and *D*-isomers of amino acids is illustrated in Scheme 1.

In the event that *D*- stereoisomers of the standard α-amino acids are unavailable, the *D*-Marfey's reagent 1-fluoro-2,4-dinitrophenyl-5-*D*-alanine amide can be synthesised from the reaction between 1,5-difluoro-2,4-dinitrobenzene (FFDNB) and a solution of *D*-Ala-NH_2.HCl in acetone.[52] The *D*- Marfey's reagent can then be used as a derivatization reagent in the same manner as the *L*- Marfey's reagent described earlier with quantitative separation of the resulting diastereomers afforded by reversed phase HPLC. The *D*- Marfey's diastereomers have been found to elute from the column after the *L*- Marfey's diastereomers because of their longer retention on the column probably due to stronger intramolecular hydrogen bonding.[52]

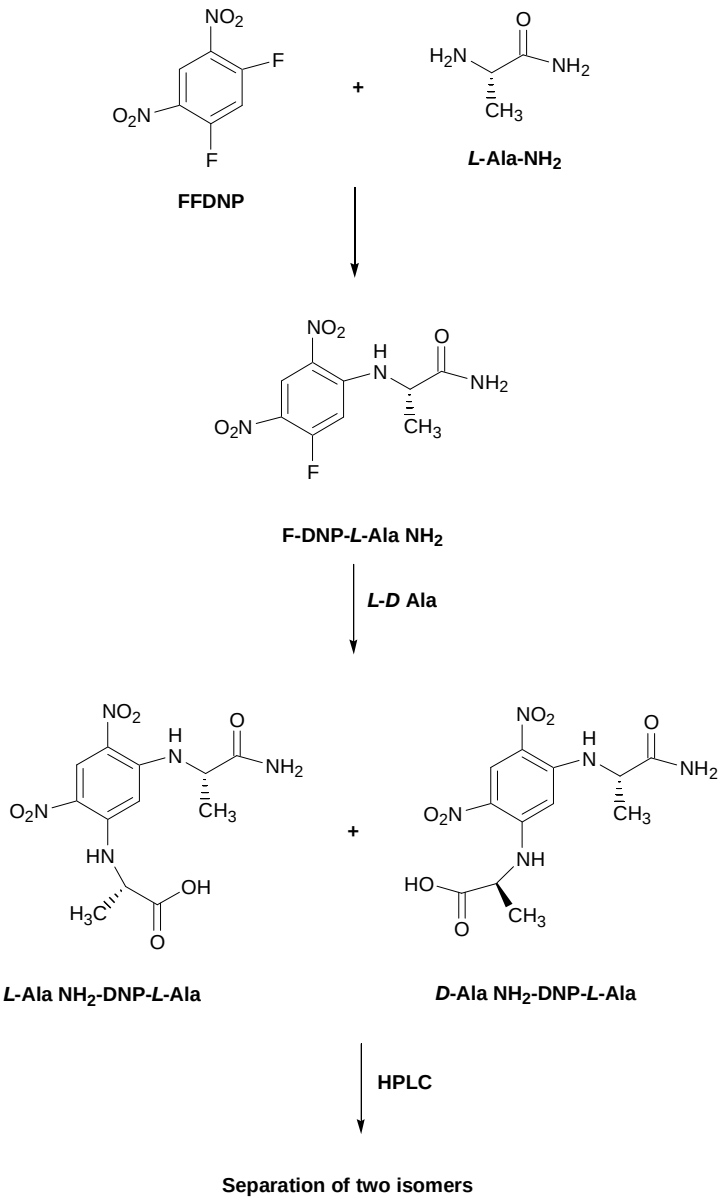

Scheme 1. Outline of the reaction sequence for the synthesis of 1-fluoro-2,4-dinitrophenyl-5-*L*-alanine amide (FDAA) and for the derivatization of *L*- and *D*-isomers of α-amino acids.[52]

Marfey's analysis of the amino acid hydrolysates of the cyclodepsipeptides described in the previous section all used C_{18} column separation of the Marfey's diastereomers. A C_{18} HPLC column has a chemically-bonded stationary phase on a silica gel support. Most bonded-phase materials are derived from the reaction of the surface silanol groups on the silica support material with organochlorosilanes.[54] This reaction results in the linkage of the stationary phase to the support via a siloxane (Si-O-Si) bond. Octadecylsilane (ODS, or C_{18}) has $C_{18}H_{37}$ alkyl groups bonded to the silica via a siloxane bond. Bonded-phase C_{18} chromatography allows the separation of polar, ionic, non-ionic and ionisable molecules with a variety of eluents including methanol, water, acetonitrile and either buffered, acidic or basic solutions of these solvents. In addition, bonded-phase chromatography can be used with gradient elution techniques without the danger of stripping the stationery phase. Gradient elution is the technique that was used for the separation of the Marfey's derivatives of amino acids from the two cyclodepsipeptides (antanapeptin A and homodolastatin 16) isolated from the Kenyan marine cyanobacterium *L. majuscula* (Section 2).

1.4.2 Chiral HPLC

The resolution of enantiomers as diastereomeric derivatives by HPLC discussed in the preceding section (Section 1.4.1) is highly dependent on the purity of the derivatizing agents. Sometimes when the rates of reaction of the enantiomers with the chiral derivatizing reagents are different, diastereoisomers in differing proportions to the enantiomers present in the racemate are formed. The chiral stationary phase HPLC method is an alternative technique for the direct resolution of enantiomers by HPLC. This technique relies on the formation of temporary diastereoisomers between the sample containing enantiomers and the chiral stationary phase. The retention times of the individual enantiomers are therefore a measure of the degree of stability between the transient diastereoisomers. The chiral phase *R*-*N*-3,5-dinitrobenzoylphenylglycine (**34**) originally developed by Pirkle[55] has been successfully employed in several commercially available HPLC columns including the Chirex® column used for the

stereochemistry determination of the amino acids and polyketide residues in **23-26** and **27** as described in Section 1.3. [36-38,40]

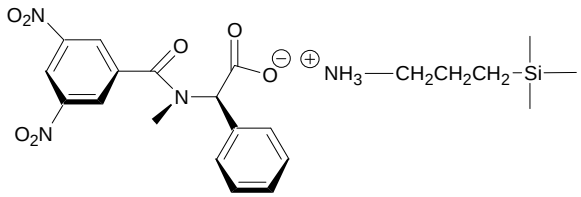

34

1.4.3 Chiral GC

Although chiral GC has not been used to determine the absolute configuration of α-amino acids from *L. majuscula* cyclodepsipeptides, it has been used to determine stereochemical assignments of α-amino acids derived from several cyclic peptides from *L. majuscula*. Cyclic peptides are lipopeptides which do not have an ester linkage within their macrocyclic ring structure. These cyclic peptides include homodolastatin 3 (**35**) and kororamide (**36**), which were isolated along with the known metabolites dolastatin 3, aplysiatoxin, debromoaplysiatoxin and oscillotoxin from Palauian collections of *L. majuscula* by Faulkner and co-workers.[51]

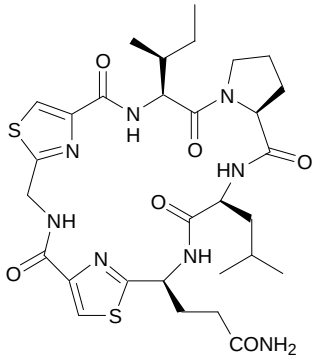

35

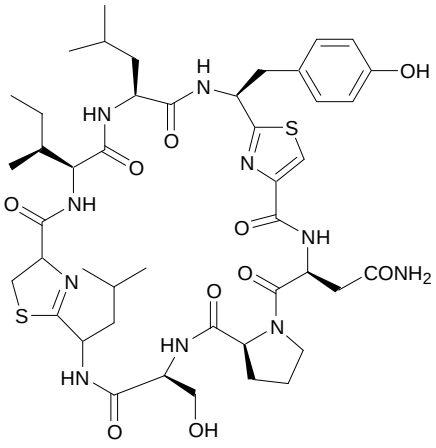

36

As we have used this technique to attempt to determine the absolute stereochemistry of *N*-methylisoleucine (Section 2.4), the general method is described here. Amino acids are non-volatile and in their underivatized form are therefore not suitable for gas chromatographic analysis. Derivatization with fluorinated derivatizing agents is one way in which the volatilization of amino acids can be improved. A standard derivatization scheme using the commercially available Alltech® derivatization kit available commercially is shown in Scheme 2.

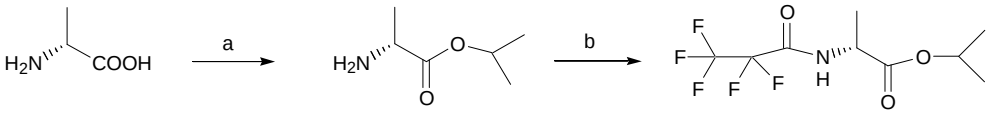

L-alanine ***L***-alanine isopropionate amide

37

Scheme 2. *Reagents and conditions*: (a) 0.2M HCl, heat to 110 ^{o}C, 5 min, isopropanol (*i*-PrOH), acetyl chloride (CH_3COCl), heat to 100 ^{o}C, 45 min ; (b) CH_2Cl_2, pentafluoropropanoic acid anhydride (PFPA), heat to 100 ^{o}C, 15 min. The resulting amide is then dissolved in suitable solvents like EtOAc for GC analysis.[56]

The most common chiral GC column used to separate the derivatized *D*- and *L*- α-amino acids is the ChirasilVal® column supplied by Alltech®. Unfortunately, no details are available about the chemical composition of the stationary phase used in these columns. An example of a typical separation of pentafluoropropanoic acid anhydride derivatized *D*- and *L*- valine is shown in Figure 1, in which the retention times for the *D*- valine and *L*- valine enantiomers are 5.86 minutes and 6.24 minutes respectively.

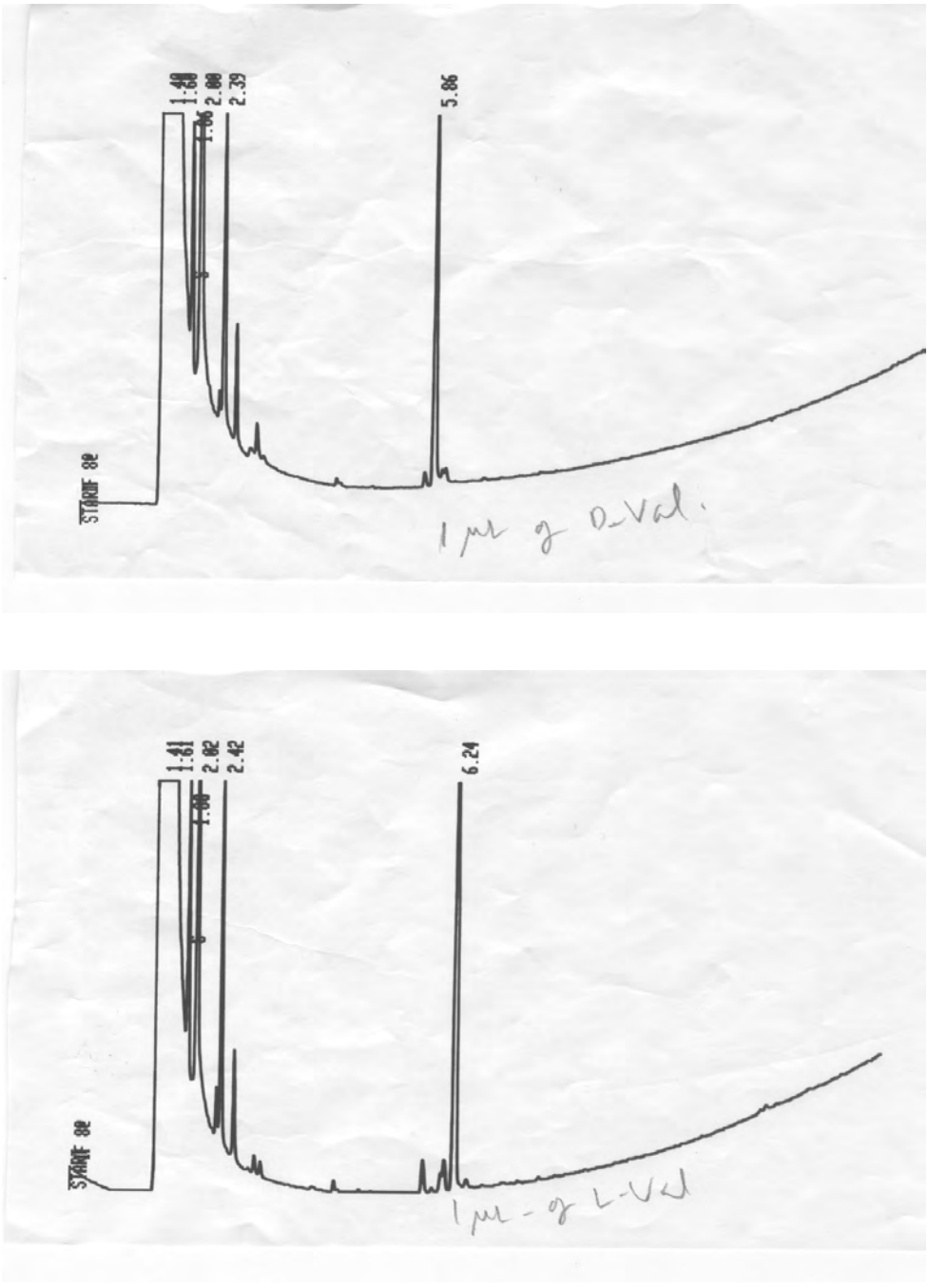

Figure 1. Chiral GC chromatograms showing the separation of a pentafluoropropanoic acid anhydride derivatized *D*- valine (above) and *L*- valine (below). Column temp. 30-120 ^{o}C at 4 ^{o}C min $^{-1}$. Helium flow 32.6 mL min $^{-1}$.

1.4.4 Summary of α-amino acids found in *L. majuscula* cyclodepsipeptides

A summary of the *D*- and *L*- α-amino acids identified in *L. majuscula* cyclodepsipeptides is presented in Figure 2. Interestingly the only *D*- amino acid identified was *D*-methylphenylalanine.[21] As expected, naturally occuring *L*- α-amino acids predominate. The three most common α-amino acids occuring in *L. majuscula* cyclodepsipeptides are *N*-methyl-*L*-valine; glycine and *L*-proline respectively.

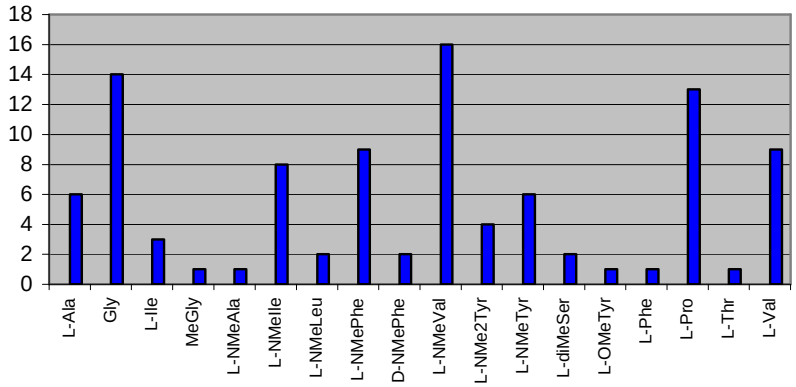

Figure 2. The occurance of *D*- and *L*- α-amino acids in *L. majuscula* cyclodepsi-peptides (the abbreviations used here are the standard abbreviations used in Section 1.3)

1.5 Chiral GC methods used to analyse α-hydroxy and β-hydroxy acid residues in *L. majuscula* cyclodepsipeptides

Initial hydrolysis of the cyclodepsipeptide with 6 N HCl (110 ^{o}C, >12 h) breaks down the molecule to its constituent α-amino acids, α-hydroxy and β-hydroxy acid residues.[52] Derivatization followed by GC, GC-MS or HPLC analysis on a chiral column usually reveals the presence of these α-amino acids, α-hydroxy and β-hydroxy acid residues which can then be compared with similarly derivatized standards as has been described in Section 1.4.

Treatment of the α- and β- hydroxy acid residues from the hydrolysis with diazomethane affords the respective methyl esters. Diazomethane is generated from Diazald® (**38**) (methyl-*N*-nitroso-*p*-toluenesulfonamide) and diethylene glycol monoethyl ether (ethyl digol or carbitol) in base according to Scheme 3 shown below.[57] The volatile diazomethane distills over as a yellow liquid which is trapped in ice cold diethylether prior to use.

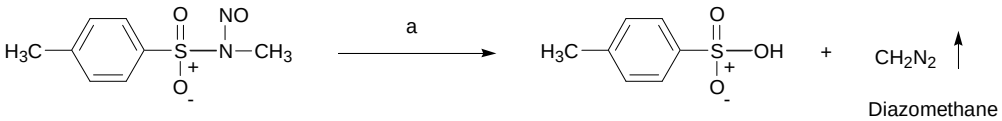

diazald (**38**)

Scheme 3. *Reagents and conditions*: (a) Ethyl digol, KOH, distill at 70-75 ^{o}C.

1.5.1 Chiral GC

Methyl esters of the α- and β- hydroxy acids can then be identified by comparison of their retention times with authentic samples or with synthetic standards using chiral GC or GC-MS. The chiral GC method has been widely used for the stereochemistry determination of α-hydroxy and β-hydroxy acid residues in *L. majuscula* cyclodepsipeptides (Section 1.3). The commercially available ChirasilVal® column is favoured for GC or GCMS. The following example serves to illustrate the stereochemistry determination of hydroxyisovaleric acid (Hiv) which is an α-hydroxy acid residue in yanucamide A (**11**) and yanucamide B (**12**).[21] Methylation of the hydroxyisovaleric acid residue with diazomethane affords the following methyl ester derived product methyl 2*S*-hydroxy-3-methyl-butanoate (**39**).

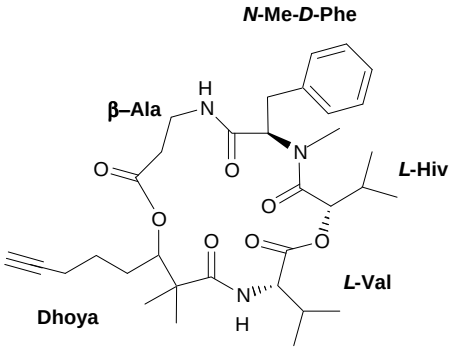

11

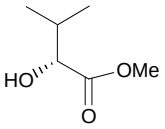

39

Another example of the use of chiral GC for the stereochemistry determination of a polyketide derived α-hydroxy acid residue is the lactic acid (*L*-Lac) moiety in dolastatin 16 (**40**).[35] The free lactic acid afforded after the 6 N HCl acid hydrolysis of **40** (110 ^{o}C, >12 h) forms the volatile lactate enantiomer (**41**) upon treatment with diazomethane, whose retention time compared favourably with a similarly derivatized sample of *L*-methyl lactate on chiral GC.

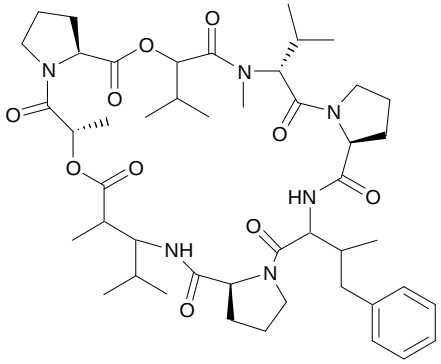

40

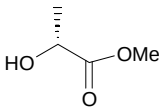

41

We have used this technique to separate a derivatized racemic mixture (50% *D*- and 50% *L*-) of methyl *S, R*-(±) – lactate using a ChirasilVal® column in our stereochemistry determination of homodolastatin 16 (**42**) described in Section 2.6.The chromatogram obtained for the separation of the derivatized racemic *S,R* lactate (the peak at t_R 5.95 minutes represents the *R* isomer and the peak at t_R 6.29 minutes

represents the *S* isomer) is presented in Figure 3.

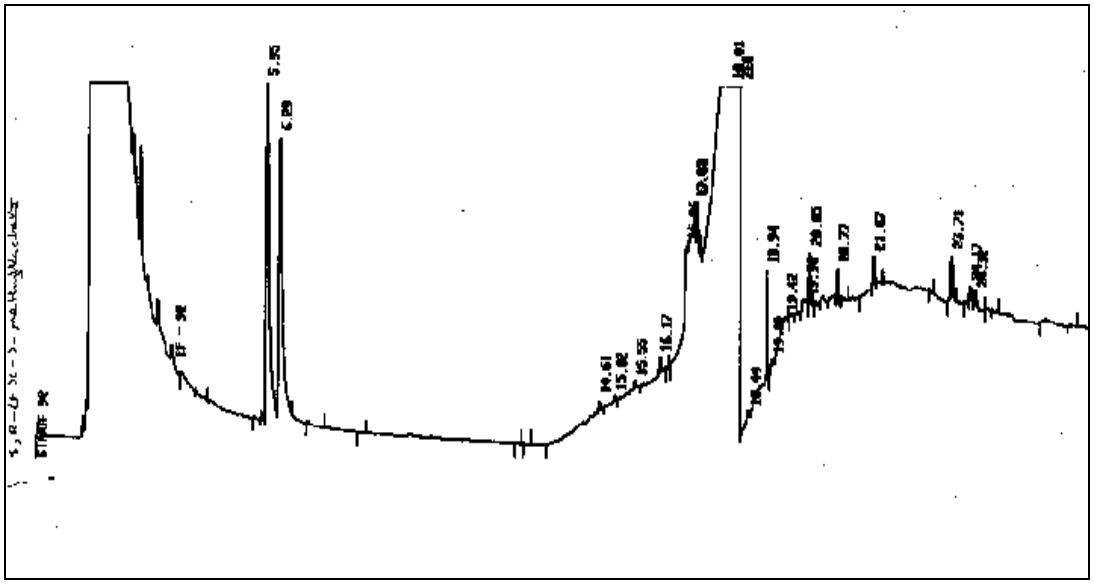

Figure 3. Chiral GC chromatogram showing the separation of the *S* and *R* diastereomers in a racemic methyl *S*, *R*-(±)–lactate mixture on a ChirasilVal® column. Column temp. gradient 30-40 ^{o}C at 1 ^{o}C min $^{-1}$, delay time 3 min; then ramped to 200 ^{o}C at 30 ^{o}C min $^{-1}$. Helium flow 32.6 mL min $^{-1}$.

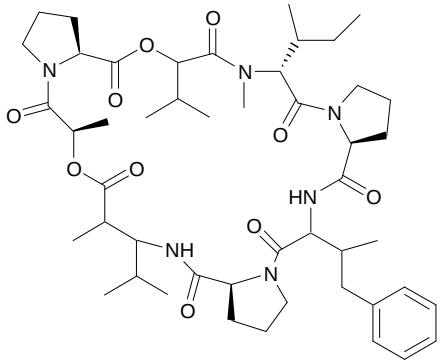

42

1.5.2 Summary of β-amino, α-hydroxy and β-hydroxy acids residues in *L. majuscula* cyclodepsipeptides

The following pie chart and bar graphs (Figures 4-7) summarize the relative abundance of β-amino, α-hydroxy and β-hydroxy acids in *L. majuscula* cyclodepsipeptides. In addition to these three groups of residues, a fourth group *viz.* 'complex residues' can be added. Complex residues are those residues which cannot be classified as α- or β-amino acids or α- or β- hydroxy acids. Of a total of twenty one complex residues observed in the twenty seven *L. majuscula* cyclodepsipeptides, 4-amino-2,2-dimethyl-3-oxo-pentanoic acid (Amopa) was found to be the most common. The complex 4-amino-2,2-dimethyl-3-oxo-pentanoic acid residue was observed in majusculamide C (**13**), 57-normajusculamide C (**14**), lyngbyastatin 1 (**15**) and epilyngbyastatin 1 (**16**). Of the five residues considered, namely α and β-amino acids; α and β-hydroxy acids and complex residues in *L. majuscula* cyclodepsipeptides, the α-amino acids were the most commonly observed entities followed by the complex residues. [12,24,30,44]

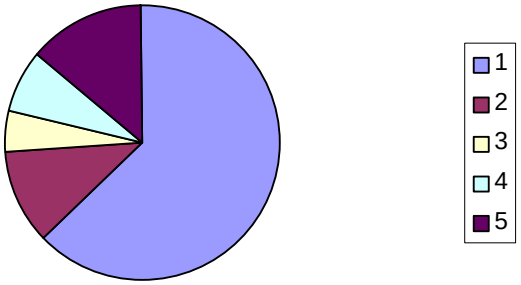

Legend: (1) α-amino acids-62.3% (2) α-hydroxy acids-11.3%; (3) β- hydroxy acids-5.0% (4) β-amino acids-7.5%; and (5) complex residues-13.8%

Figure 4. Pie-chart showing the relative abundance of the residue classes commonly found in *L. majuscula* cyclodepsipeptides.

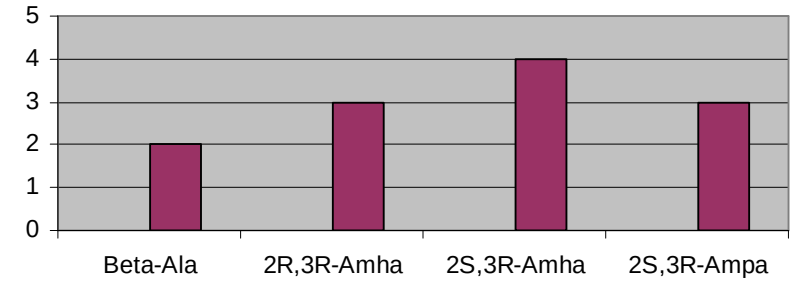

Figure 5. The more common β-amino acids found in *L. majuscula* cyclodepsipeptides (only β-amino acids that occur more than once are reflected here) .

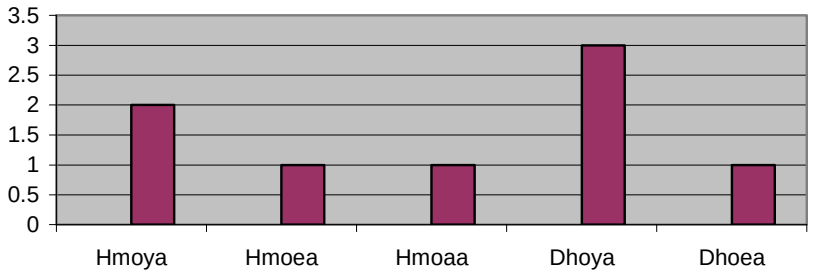

Figure 6. The more common β-hydroxy acids found in *L. majuscula* cyclodepsipeptides.

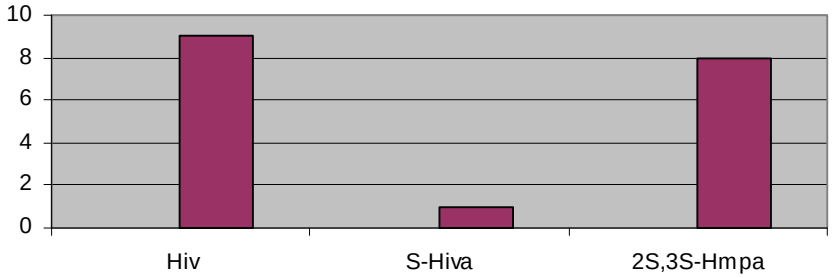

Figure 7. The more common α-hydroxy acids found in *L. majuscula* cyclodepsipeptides.

Figure 5 shows that the 3*R*-amino-2*S*-methylhexanoic acid (2*S*,3*R*-Amha) residue is the most common β-amino acid found in *L. majuscula* cyclodepsipeptides and was isolated from the ulongamides A-F (**17**-**22**).

Figure 6 shows that the 2,2-dimethyl-3-hydroxy-7-octynoic acid residue (Dhoya) is the most common β-hydroxy acid residue found in the twenty seven known *L. majuscula* cyclodepsipeptides. The 2,2-dimethyl-3-hydroxy-7-octynoic acid residue was isolated from yanucamide A and B (**11** and **12**) and pitipeptolide A (**23**). From Figure 7, the 2-hydroxyisovaleric acid (Hiv) residue was more common than the other α-hydroxy acids. 2-Hydroxyisovaleric acid featured in yanucamides A and B (**11** and **12**), 57-normajusculamide C (**14**) and in antanapeptins A-D (**7**-**10**).

1.6 Sample collection and preservation

Two samples of *L. majuscula* were collected by snorkeling in December 2000 (Figure 8), one from near the mainland coastal town of Shimoni and the other from the adjacent shore of the Wasini island (see Map in Figure 9, Section 1.6.1). The specimens collected were stored in isopropanol prior to freezing and transportation to South Africa for isolation and identification of their secondary metabolite contents. An electron micrograph of the Kenyan *L. majuscula* from Wasini island is reproduced in Figure 9. The identity of the *L. majuscula* was confirmed by Dr. Mirjan Girt at Oregon State University.

Figure 8. Author collecting *Lyngbya majuscula* at the Wasini collecting site.

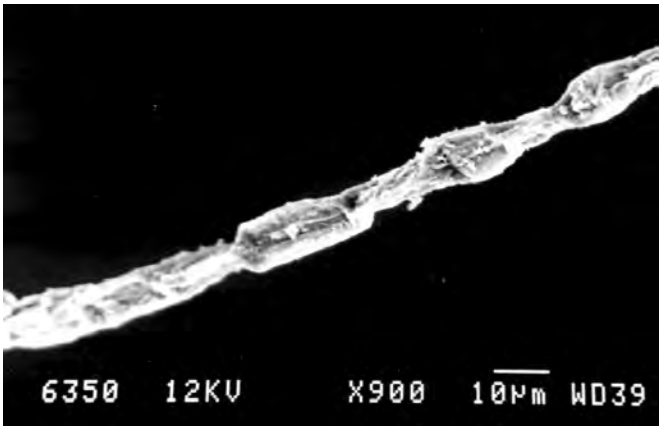

Figure 9. Electron micrograph of the Wasini island collection of *L. majuscula*.

1.6.1 A description of the collection Sites

Kenya's coastline is about 500 km long and lies between latitudes 1 and 5^{o} S. The Kenyan coast generally enjoys warm tropical conditions from the influence of the East African Coastal Current in the south and the upwelling cold waters of the Somali current in the north. This coast also experiences two periodic monsoonal winds, namely the Northeast monsoon and the Southeast monsoon which occur between December and March and from May to October respectively with a 1-2 months transition period in between the two monsoons. There is consistencies in the water column salinity variation as well as in other physicochemical parameters. Surface water temperatures range from 25^{o}C to 31 ^{o}C but could otherwise reach a high mid day peak of 36 ^{o}C in shallow estuaries.[58] Nutrients studies have shown that phosphate concentrations of reef and offshore creek waters along the Kenyan coast are highest during the Southeast monsoon and lowest during the Northeast monsoon. By contrast chlorophyll-a values showed minimal seasonal variability.[58] In general nitrogen concentrations in the form of nitrate and ammonia were only elevated due to the influence of localized urban inputs and / or river run off.[58,59]

The Shimoni channel which lies between the mainland and the Wasini (Vumba) island experiences very little influence from river run off or ground water seepage as this part of the coast is surrounded by coastal hills. As in other other parts of the coast, the Shimoni, Wasini and Kisite/Mpunguti areas are influenced by seasonality of the Northeast and Southeast monsoon winds.

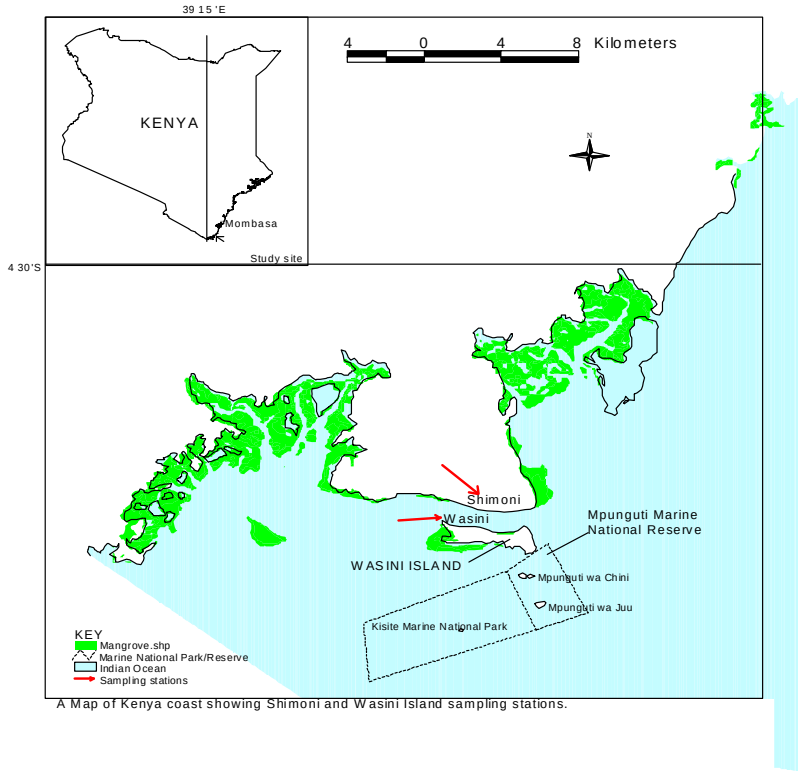

Figure 10. A map of Kenya showing the sampling sites at Shimoni and Wasini island.

The Kenyan *L. majuscula*, occurs in the sub-littoral zone of the Kenyan coast.[60] The area from which the Kenyan *L. majuscula* specimen was collected (Figure 10) is characterized by fringing reefs forming platforms that serve as automatic barriers to oceanic winds and strong currents. These platforms have a periodical semi-diurnal tidal

regime that varies between 2.5m and 3m and reaching a 4m maximum. This scenario has resulted into the strong zonation of intertidal communities into the littoral fringe, eulittoral and the sub littoral zone.[61] Coral communities flourish on the outer edge of the offshore reef which also has substantial sea grass beds and mangroves.

CHAPTER TWO

RESULTS AND DISCUSSION

2.1 Initial Laboratory Workup and Screening of Collected Material

It has been stated earlier in Section 1.6 that after the algal specimen was collected, it was stored in isopropanol and transported to South Africa where it was kept in cold storage. After retrieval from cold storage, the algal sample was filtered through cheese cloth and the aqueous isopropanol filtrate concentrated on a rotary evaporator (30 ^{o}C). The alga was further soaked for approximately 15 minutes in 2:1 dichloromethane/methanol with gentle heating on a water bath prior to cooling and filtration. The filtered dichloromethane/methanol extract was concentrated as *per* the original isopropanol extract. Fifteen subsequent soakings of the alga in warm dichloromethane/methanol were deemed sufficient to exhaustively extract the alga. The concentrated isopropanol and dichloromethane/methanol extracts were combined and partitioned with water. A ^{1}H NMR examination (Figures 11-14) of the organic partition layer resulting from extraction of the Shimoni (TD1SH1-007) and Wasini island (TD1WA1-008) collections showed similar interesting signals (*viz*. two small multiplets at δ 0.2 and δ 0.44 and several small singlets between between δ 2.6 and δ 3.7).

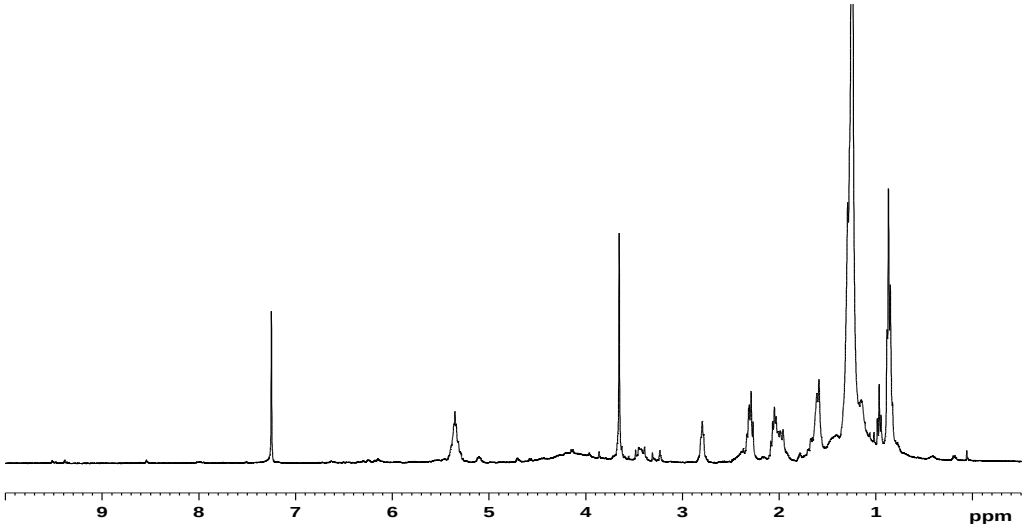

Figure 11. ^{1}H NMR spectrum ($CDCl_3$, 400 MHz) of TD1SH1-007

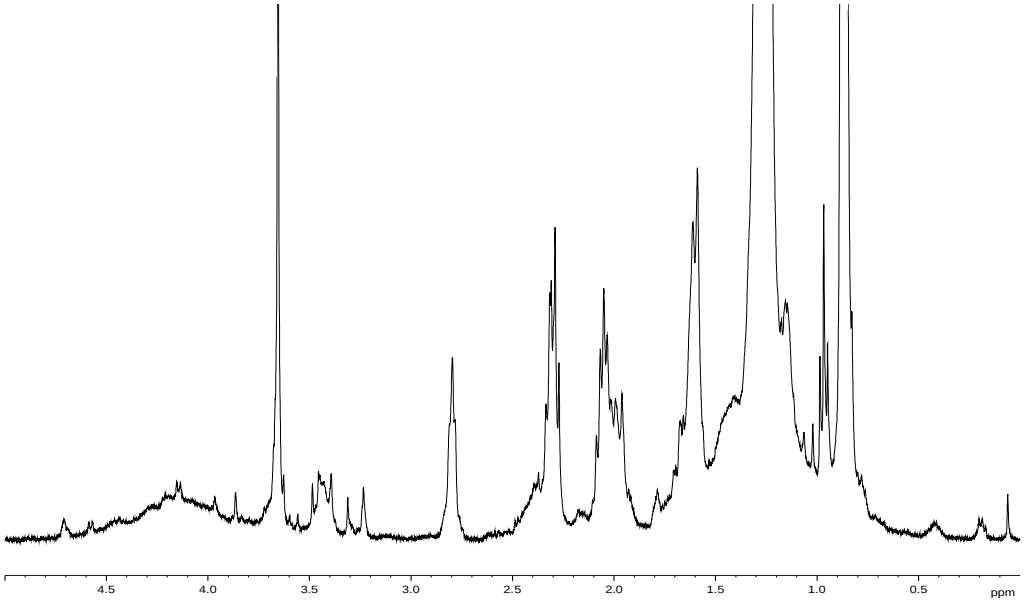

Figure 12. An expansion of the ^{1}H NMR spectrum ($CDCl_3$, 400 MHz) of TD1SH1-007 showing the signals of interest (δ 0.20, 0.44 and δ 3.0-5.0)

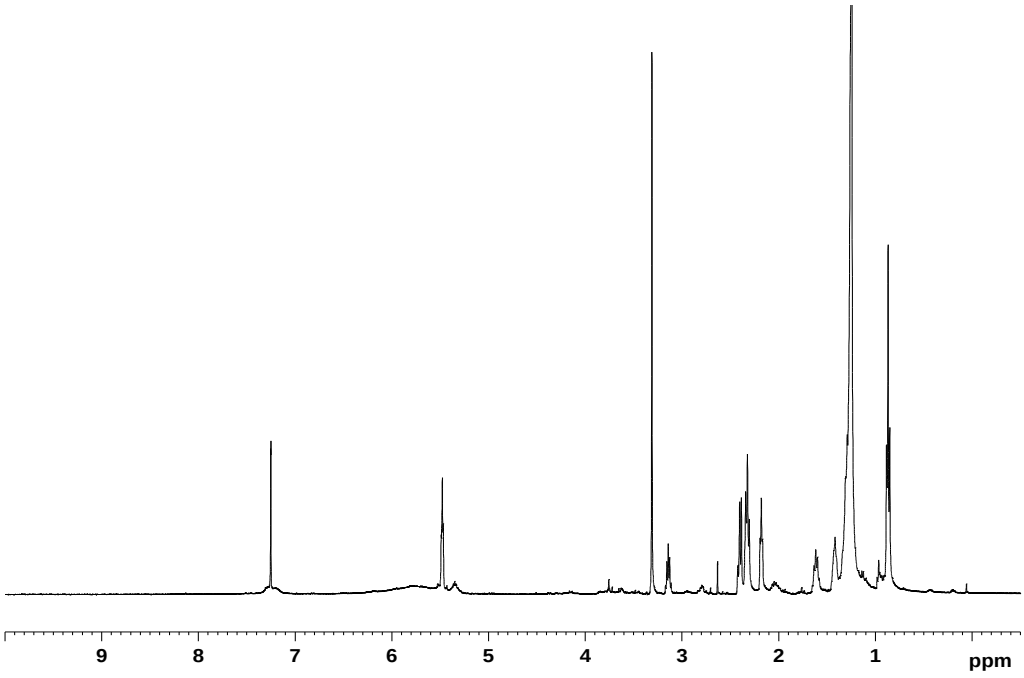

Figure 13. ^{1}H NMR spectrum ($CDCl_3$, 400 MHz) of TD1WA1-008

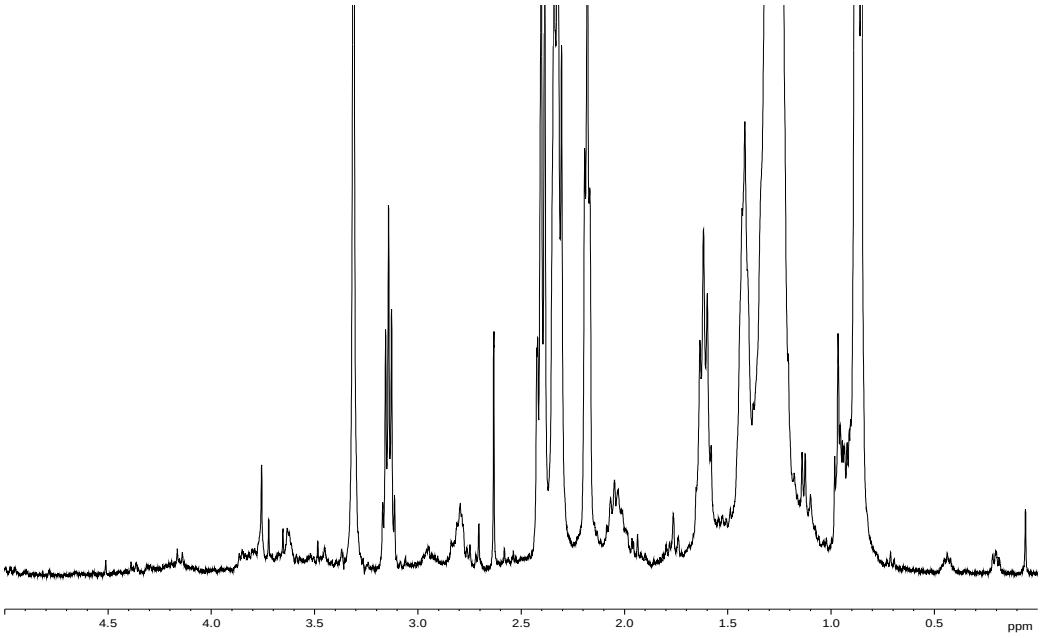

Figure 14. An expansion of the ^{1}H NMR spectrum ($CDCl_3$, 400 MHz) of TD1WA1-008 showing the signals of interest (δ 0.20, 0.44 and δ 3.0-5.0)

2.2 Brine shrimp toxicity screening of crude extracts and partition fractions

A spatula of brine shrimp eggs were hatched in well illuminated and aerated sea water (24 hours). About 20 of the newly hatched brine shrimp larvae (*Artemia salina*) in approximately 0.5 mL seawater were added to each well of a 96 cell plate. Each well contained varying concentrations of the Kenyan *L. majuscula* extracts made up in 50 µL dichloromethane and 4.5 mL sea water. The assay was run in triplicate with suitable controls (50 µL dichloromethane and 4.5 mL sea water). The two crude extracts TD1SH1-007 and TD1WA1-008 and their dichloromethane/methanol partition fractions were tested in the assay at concentrations of 25 µg mL^{-1}, 50 µg mL^{-1} and 100 µg mL^{-1} respectively. After 24 hours at 25 ^{o}C, the dead brine shrimp were counted using a dissecting light microscope, after which a drop of methanol was added to each well. The purpose of adding the methanol at the end of the assay is to facilitate the counting of the total number of brine shrimp in each well by killing the very fast swimming and

difficult to count living brine shrimps. A statistical comparison of the number of living versus dead brine shrimp at the various concentrations provides the median lethal dose (LD_{50}) value for a bioactive extract.[62] Unfortunately, although the *L. majuscula* extracts were inactive at concentrations of 100 μg mL^{-1} we continued our investigations of these extracts based on their interesting ^1H NMR spectra.

2.3 Isolation of cyclodepsipeptides from the Kenyan *L. majuscula*

The isolation of cyclodepsipeptides from *L. majuscula* collected circumtropically, together with their structural elucidation and stereochemical determination has been reviewed in Chapter One. The isolation protocol followed for the isolation of antanapeptin A (**7**) and homodolastatin 16 (**42**) is consistent with protocols used previously and is summarized in Scheme 4. Sephadex LH-20 size exclusion chromatography of the CH_2Cl_2/MeOH partition fractions (700 mg) resulted in several fractions which were combined to give three fractions Fn 1 - Fn 3 based on their TLC and ^1H NMR spectra. Fraction 2 which contained the minor signals of interest was chromatographed again on Sephadex LH-20 (1:1 EtOAc/ MeOH) to give three further fractions (Fn 2/1 - Fn 2/3). Si gel flash chromatograph of Fn 2/2 with gradient elution ($CHCl_3$ – MeOH) yielded Fn 2/2/1 - Fn 2/2/4. Fortuitously, Si gel chromatography also removed the chlorophyll clearly evident in Fn 2/2/2, as Fn 2/2/1- Fn 2/2/4 were pale yellow in colour and not dark green. An examination of the ^1H NMR spectra of these four fractions revealed that Fn 2/2/3 contained the minor metabolites which we were interested in isolating. Further purification of Fn 2/2/3 by C_{18} reversed phase semi-preparative HPLC (7:3 CH_3CN/H_2O) produced **7** (3.7 mg, 0.0035 % dry wt) and **42** (3.4 mg, 0.0035%) as white amorphous powders. The choice of the solvent system for the semi-preparative HPLC of Fn 2/2/3 was established using a compatible reversed phase C_{18} analytical column using different combinations of CH_3CN/H_2O. The ^1H NMR spectra reproduced in Figures 14-16 illustrate the sequential (progressive) purification of the crude extract TD1WA1-008 to give compounds **7** and **42**.

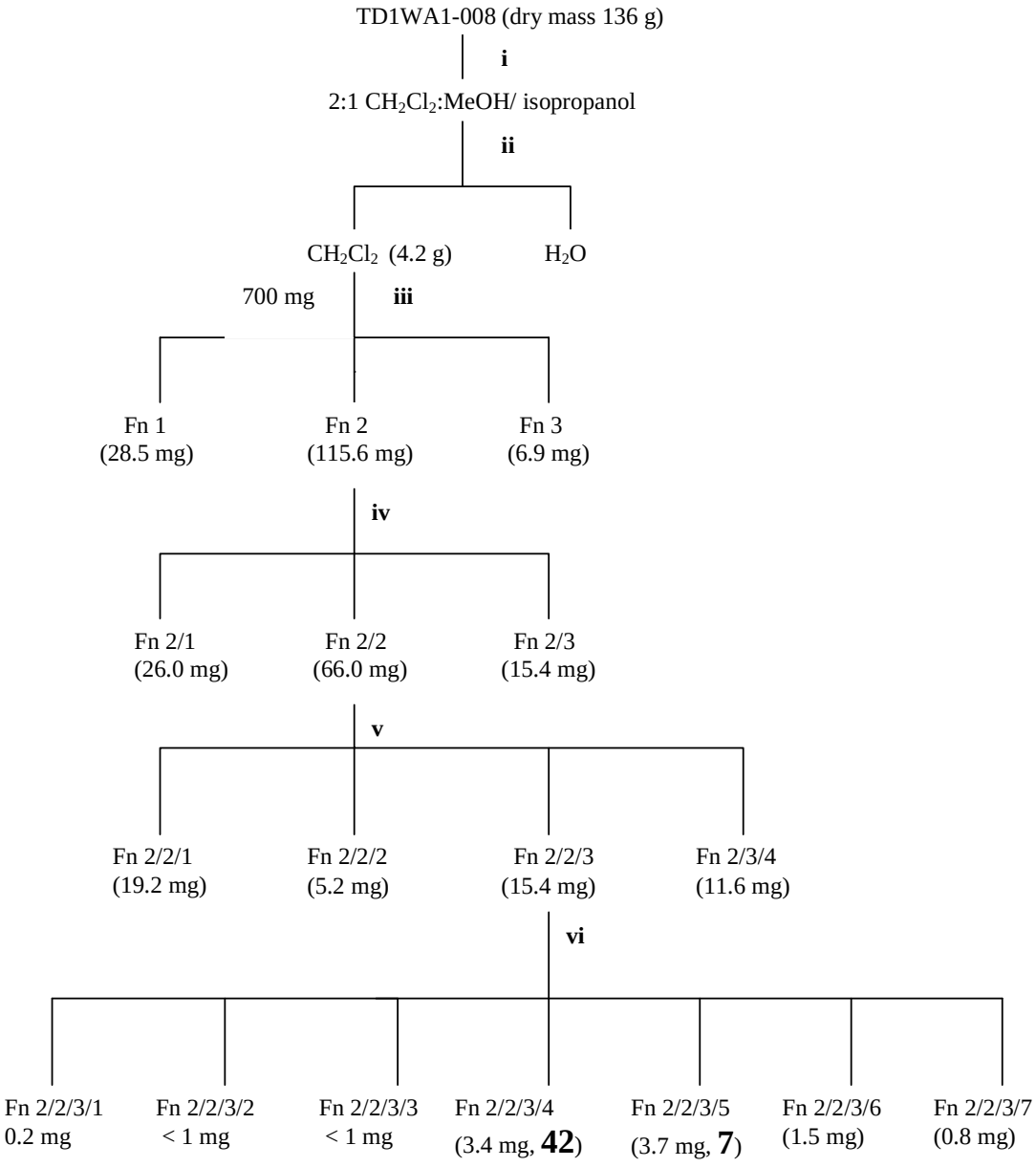

Scheme 4. Isolation of antanapeptin A (**7**) and homodolastatin 16 (**42**). (**i**) Extraction of *L. majuscula* with i-PrOH + CH_2Cl_2/MeOH (2:1) (**ii**) partitioning of i-PrOH and CH_2Cl_2 combined extracts with H_2O (**iii**) Sephadex LH-20 size exclusion chromatography, (5:2:1 CH_2Cl_2:hexane:MeOH) (**iv**) Sephadex LH-20 size exclusion chromatography, (1:1 EtOAc:MeOH) (**v**) Si Gel flash chromatography ($CHCl_3$-EtOAc-MeOH) (vi) Reversed phase semi-preparative HPLC ODS-C18 column, (7:3 CH_3CN:H_2O).

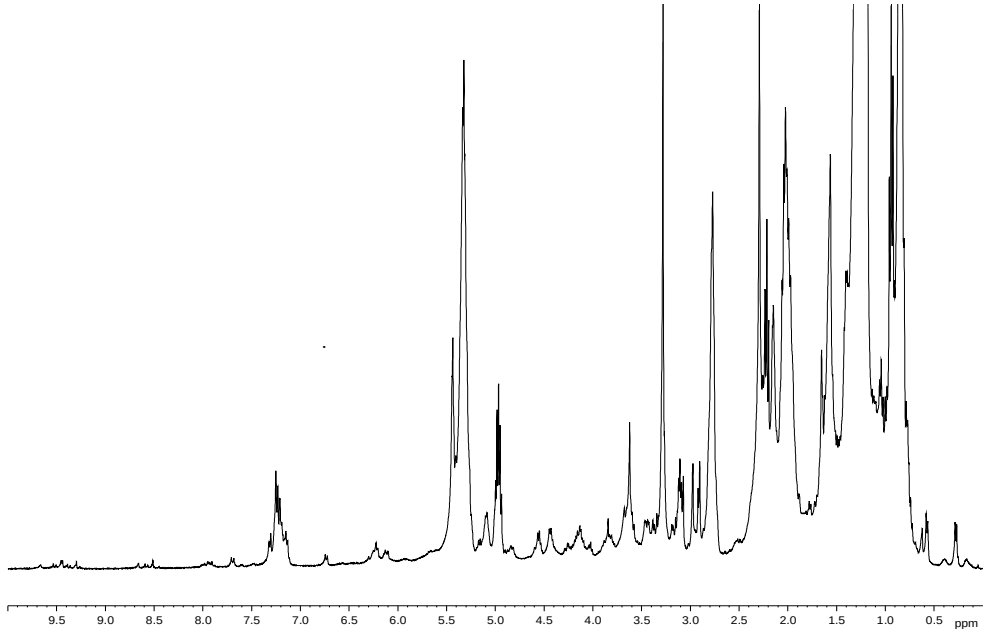

Figure 15. ^{1}H NMR spectrum ($CDCl_3$, 400 MHz) of Fn 2 (refer to Scheme 4)

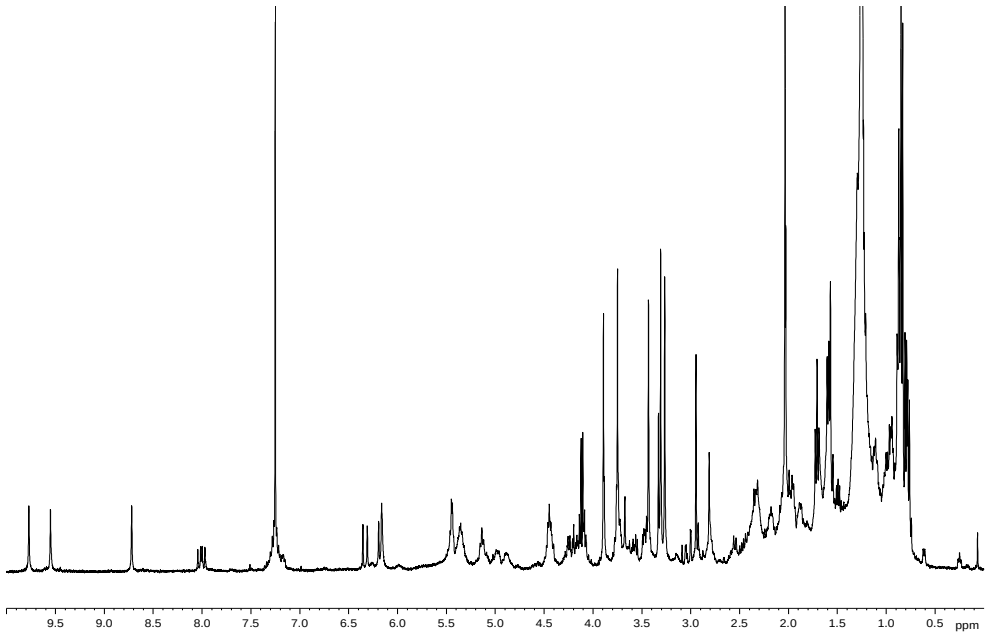

Figure 16. ^{1}H NMR spectrum ($CDCl_3$, 400 MHz) of Fn 2/2 (refer to Scheme 4)

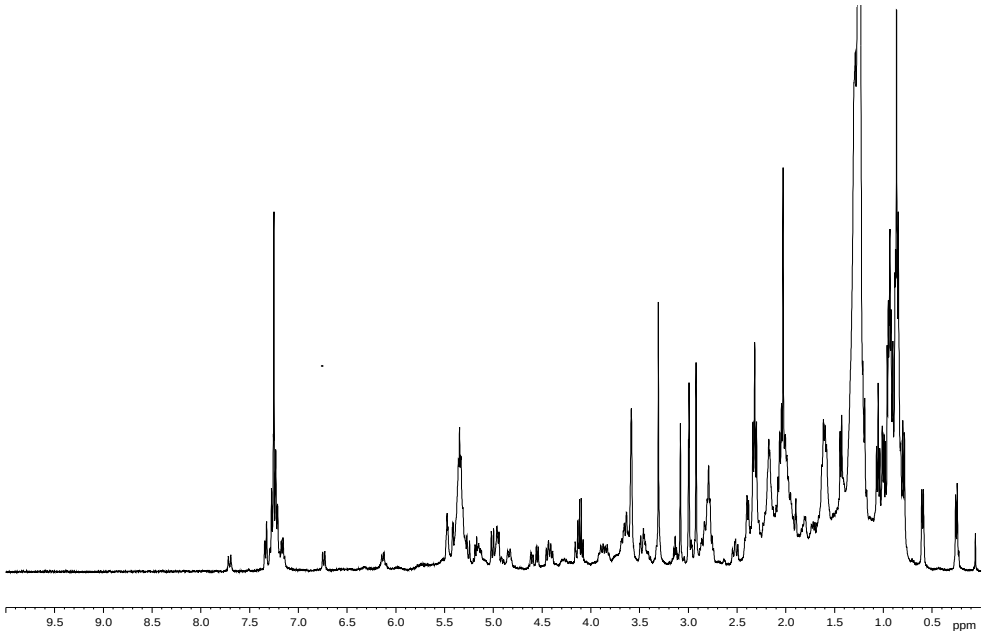

Figure 17. ^{1}H NMR spectrum ($CDCl_3$, 400 MHz) of Fn 2/2/3 (refer to Scheme 4)

2.4 Structure elucidation of antanapeptin A (7)

While we were busy with the structure determination of **7** the structure of antanapeptin A was published by Nogle and Gerwick in the January 2002 edition of the Journal of Natural Products.[15] The NMR and other spectroscopic data as well as $[\alpha]_D$ for **7** from

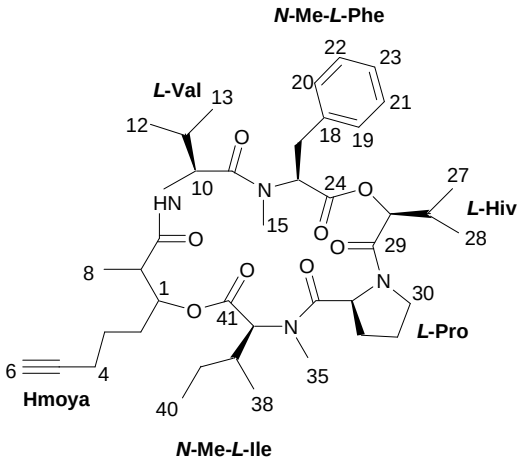

7

the Madagascan *L. majuscula* was consistent with the data which we had in hand for the compound we had isolated from the Kenyan *L. majuscula*. Our structural determination process however differed from that used by Nogle ***et al.*** and is presented as follows.

Antanapeptin A (**7**) was isolated from the TDWA1-008 extract as described in Scheme 4. The yield of this cyclodepsipeptide was 3.7 mg (0.0035% yield calculated ***per*** dry weight of *L. majuscula*). FABMS data established the molecular formula $C_{41}H_{60}N_4O_8$ for **7** ($[M+H]^+$; 737.4460 Δmmu = -2.9 mmu), which was consistent with the ^{13}C NMR data (Figure 18) that showed forty one carbon resonances. The molecular formula suggested that **7** had fourteen degrees of unsaturation six of which were accounted for by the carbonyl carbons (δ 165-176).

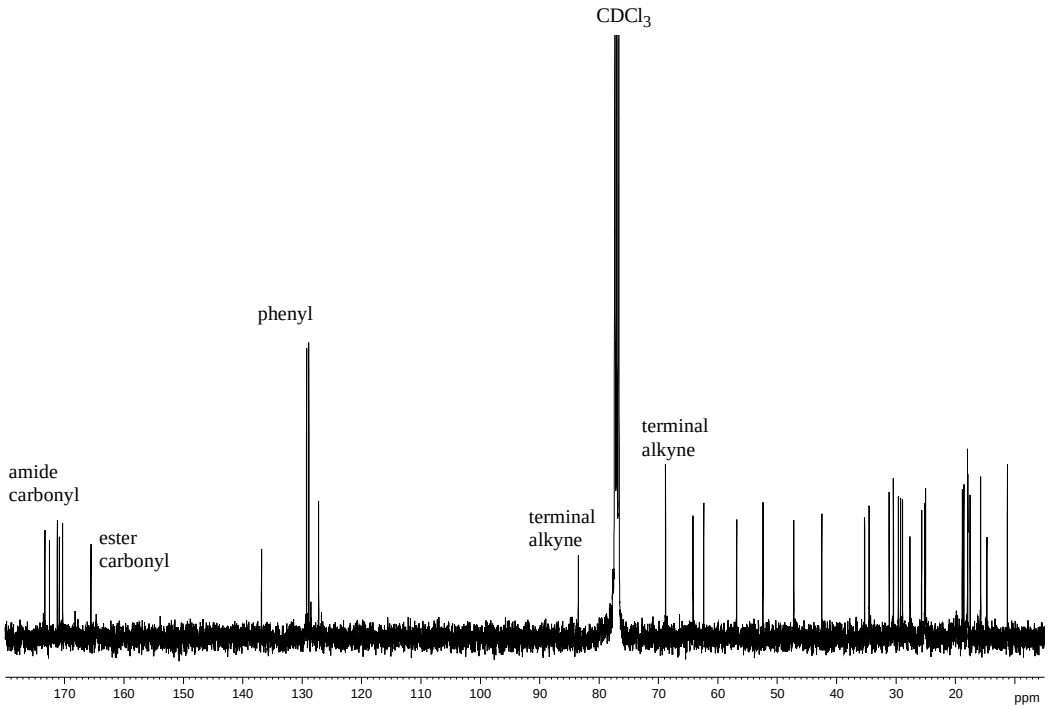

Figure 18. ^{13}C NMR ($CDCl_3$, 100MHz) spectrum of antanapeptin A (**7**)

Five of the six quarternary carbonyl carbons (δ 170.3, 170.9 171.2, 172.6, 173.3) were assigned to peptide carbonyls whereas the sixth signal at δ 165.6 was assigned to an ester carbonyl carbon (Figure 18). Evidence for the peptide nature of **7** was provided by the exchangeable amide proton doublet at δ 6.00 and the two amide *N*-Me singlets at δ 2.93 and 2.98 in the ^{1}H NMR spectrum of **7** (Figure 19). Both the ^{13}C and ^{1}H NMR spectra (Figure 18 and 19) revealed the presence of a mono-substituted phenyl group (δ_H 7.2; δ_C 127.2, 128.9, 129.3) and a terminal alkyne functionality (δ 68.8 and 83.5). In addition, the presence of the monosubstituted benzene ring was supported by strong infra red absorption bands at 702 and 750 cm^{-1} consistent with standard aromatic carbon-hydrogen stretching frequencies.

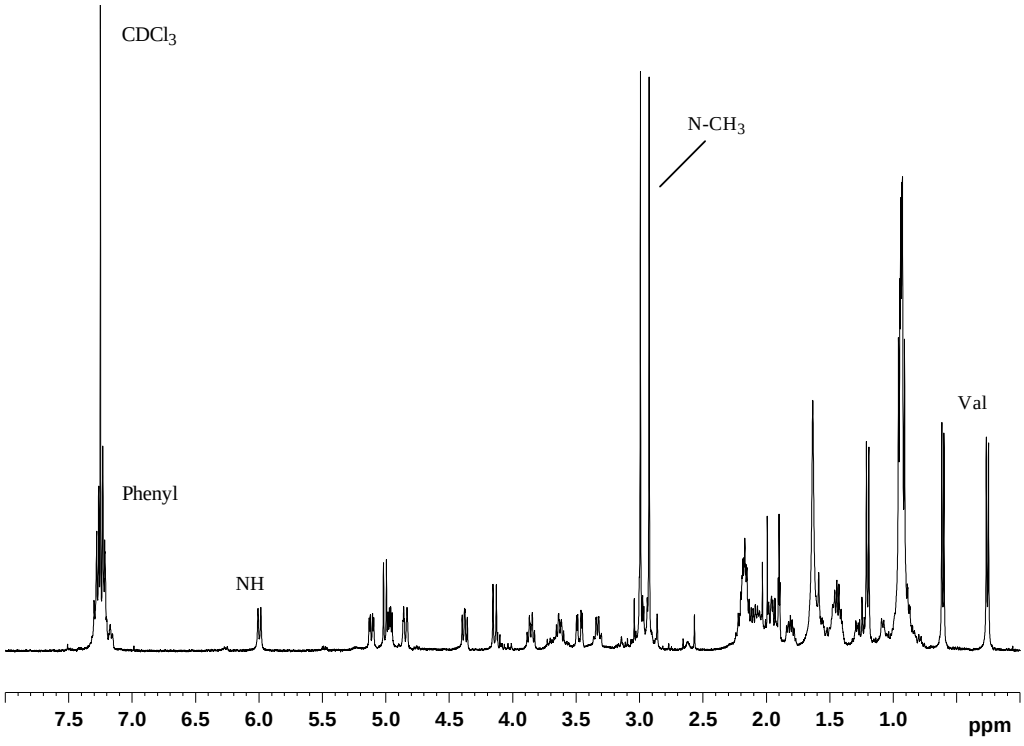

Figure 19. ^{1}H NMR ($CDCl_3$, 400MHz) spectrum of antanapeptin A (**7)**

The degrees of unsaturation accounted for by the terminal alkyne functionality (two), the peptide (five) and ester (one) carbonyl carbons as well as the monosubstituted benzene ring (four) meant that the structure was two double bond equivalents short of the expected fourteen degrees of unsaturation. The macrocyclic ring of the cyclodepsipeptide accounted for one of the two remaining degrees of unsaturation.

Our review of *L. majuscula* cyclodepsipeptides (Chapter 1) has shown that the cyclic amino acid proline, is amongst the most common amino acids reported in these cyclodepsipeptides. In support of our suggested presence of a proline ring moiety in **7**, ^{1}H and ^{13}C NMR data of the proline moiety in norlyngbyastatin 2 (**28**) and pitipeptolide A and B (**23, 24**) are compared with the ^{1}H and ^{13}C NMR data for **7** in Table 1. Norlyngbyastatin 2 possesses two proline rings in its macrostructure and the NMR data for both proline moieties is given in Table 1. The contiguous coupling sequence from H-33 through the three pairs of diastereotopic methylene protons (H_2-30 – H_2-32) is clearly shown in the COSY spectrum of **7** (Figure 20).

Further evaluation and interpretation of the COSY spectrum of **7** revealed the presence of a valine amino acid residue. The two upfield methyl doublets at δ 0.27 and 0.62 which, initially were our signals of interest in studying the chemistry of the cyanobacterium, were attributed to the isopropyl methyl groups of the valine moiety in **7**. The proton spin system NH-9 (δ 6.00) - H-10 (δ 4.38) - H-11 (δ 1.45) - H_3-12 (δ 0.62) - H_3-13(δ 0.27) supporting the presence of the valine moiety of antanapeptin A is clearly discernible in the COSY spectrum shown in Figure 21.

	Antanapeptin A (**7**)		Pitipeptolide A (**23**)[36]		norlyngbyastatin 2 (**28**)[40]	
δ	47.2 t	3.87 q	46.3 t	3.55 d (11.96, 9.6 Hz)	46.3 t	3.13 m
		3.62 q		3.70 m		3.53 m
γ	25.1 t	2.13 m	21.7 t	1.76 m	23.9 t	1.84 m
		1.98 m		1.97 m		2.16 m
β	29.2 t	1.81 m	31.2 t	1.97 m	27.7 t	1.99 m
				2.64 m		2.06 m
α	56.8 t	4.97 dd,	61.1 t	4.62 d (7.1 Hz)	58.2 d	4.71 dd
		(8.1, 4.0 Hz)				(8.6, 1.6 Hz)
CO	172.6 s	-	170.3 s	-	170.8 s	-
	Kulokainalide 1 (**43**)[22]		Pitipeptolide B (**24**) [36]		norlyngbyastatin 2 (**28**)[40]	
δ	47.9	3.58 dd (7.1 Hz)	46.3 t	3.55 dd (11.7, 9.4 Hz)	45.7 t	3.57 m
		2.40 m		3.70 m (7.33)		3.61 m
γ	25.5	1.98 m	21.7 t	1.77 m	21.8 t	1.75 m
		1.79 m		1.96 m		1.93 m
β	28.6	1.81 m	31.2 t	1.96 m	31.5 t	2.15 m
		1.62 m		2.66 m		2.19 m
α	58.9	2.92 t (7.6 Hz)	61.2 d	4.62 d (7.3 Hz)	60.1 d	4.78 (7.2 Hz)
CO	170.3	-	170.2	-	170.7	-

Table 1. Comparative ^{1}H and ^{13}C NMR data ($CDCl_3$) for the proline moiety in compounds **7** (400/100 MHz), **23** (400/100 MHZ), **24** (400/100 MHz), **28** (500/125 MHz) and **43** (500/125 MHz). The latter compound was isolated from a gastropod mollusc ***Philinopsis speciosa*** which feeds on ***L. majuscula*** and its spectra were recorded in CD_2Cl_2.

The presence of the benzene ring suggested that one of the amino acid residues could be phenylalanine. The phenylalanine moiety in **7** was confirmed by interpretation of the HMBC data, which also revealed the methylated nature of the phenylalanine amino acid residue (*N*-methylphenylalanine). Three bond HMBC correlations were observed from H_2 -17/17'(δ 2.98,) to C-19/20 (δ 129.3) and from H-16 (δ 5.13) to C-18 (δ 136.8) whereas two bond correlations were evident from H_2 -17/17'(δ 2.98) to C-18 (Figure 21).

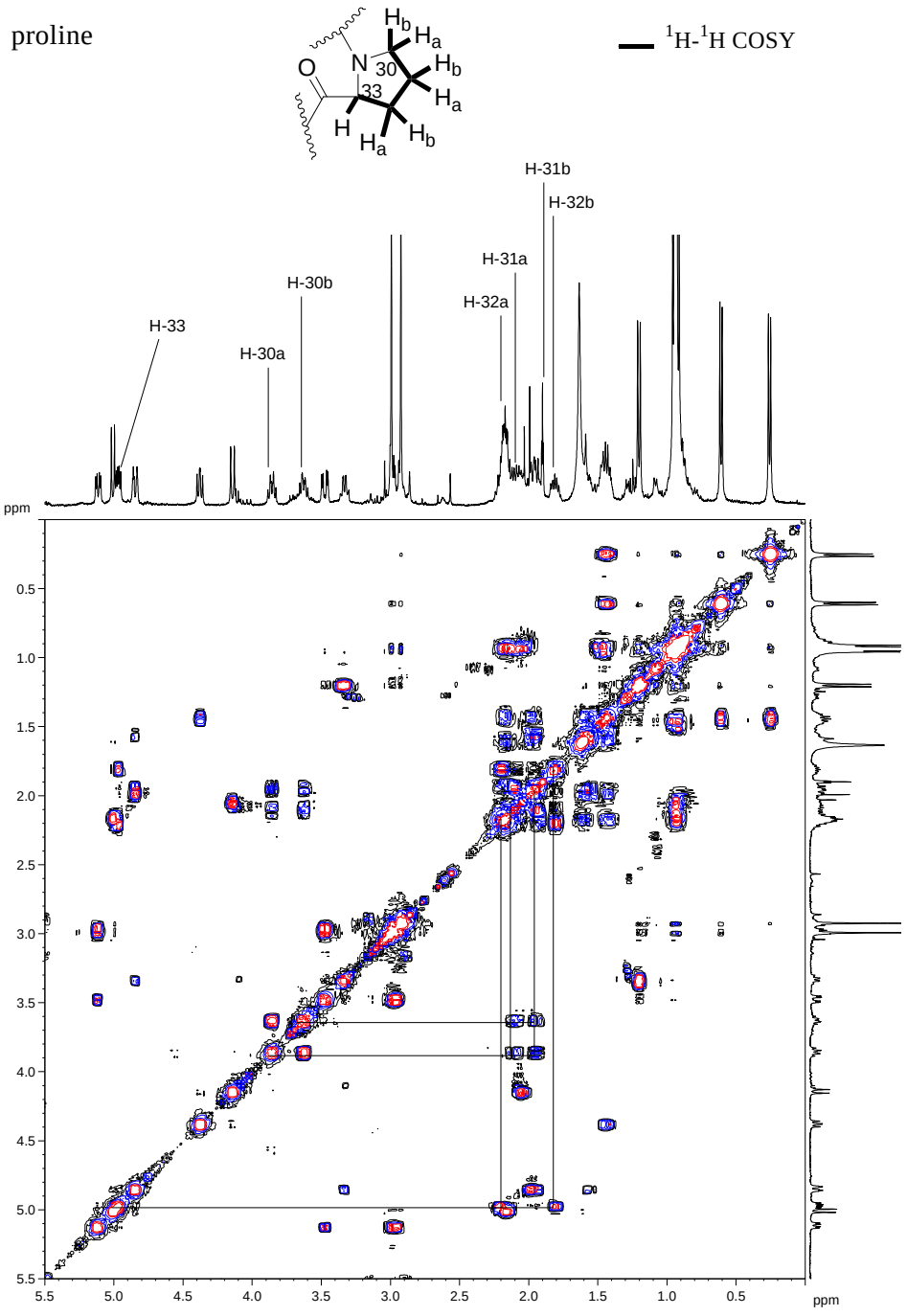

Figure 20. COSY ($CDCl_3$, 400 MHz ; F1=F2, δ_H 0-5.5 ppm) spectrum showing the proline spin systems in antanapeptin A (**7**).

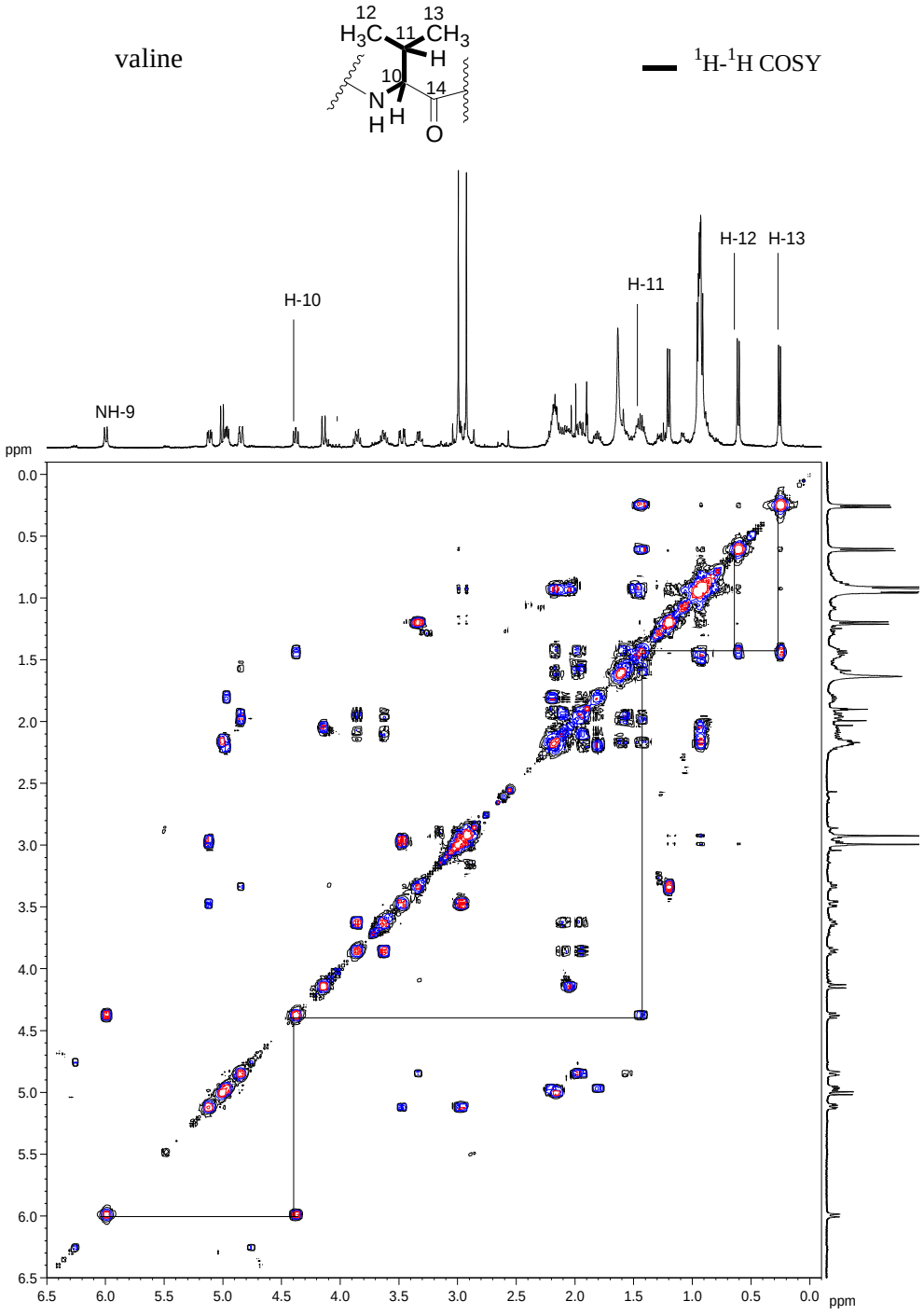

Figure 21. COSY ($CDCl_3$, 400 MHz ; F1=F2, δ_H 0-6.5 ppm) spectrum showing the valine spin system in antanapeptin A (**7**).

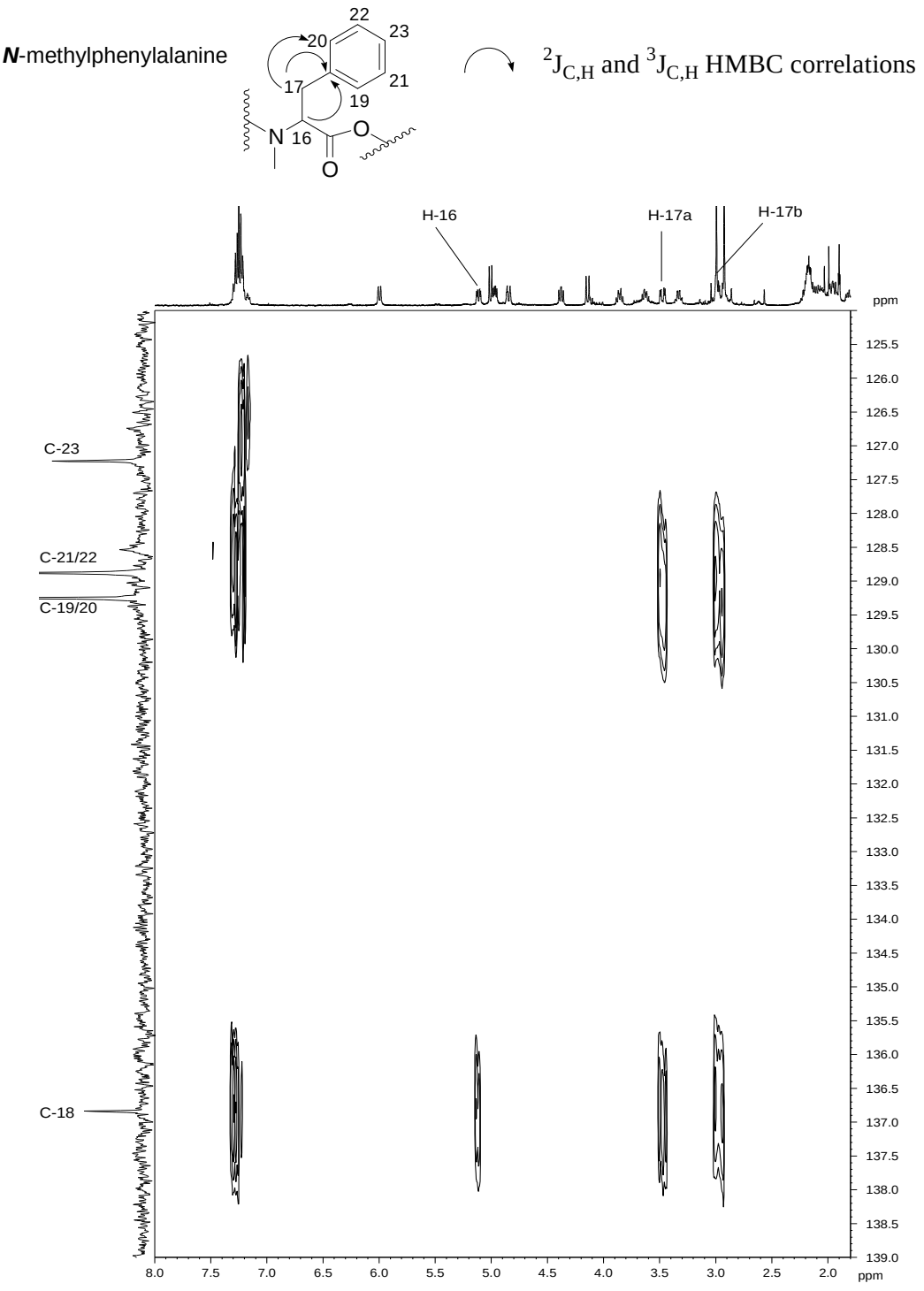

Figure 22. HMBC spectrum ($CDCl_3$, 400 MHz; F1= δ_C 125.0-139.0, F2=δ_H 1.8-8.0) correlations, D6=80 msec) of antanapeptin A.

The other three bond correlation observed was that from the *N*-methyl protons at δ 2.93 to C-16 (δ 62.4). The connectivities between the *N*-methylphenylalanine moiety and the valine and hydroxyisovaleric acid residues were also provided by interpretation of the HMBC data.

Three bond HMBC correlations observed from H-16 – C-14 (δ 173.3) and from the *N*-15-methyl protons (δ 2.93) to C-14 established a connectivity between valine and *N*-methylphenylalanine (Figure 23). Although the presence of the proline moiety in **7** was confirmed by interpretation of the COSY spectral data (Figure 20), there was no evidence to link the proline moiety directly either to the valine or the *N*-methylphenylalanine. Long range HMBC couplings were however observed from the proline methylene protons H_2-30 to C-29 (δ 165.6) and from the oxymethine proton H-25 to carbonyls C-29 and to C-24 (δ 170.3). These HMBC correlations involving an oxymethine carbon, proline and *N*-methylphenylalanine placed an α-hydroxyisovaleric acid (Hiv) moiety between the proline and the *N*-methylphenylalanine, the structure of which was also confirmed by both COSY and HMBC data (Table 2.)

Contiguous COSY correlations from H-36 (δ 4.16) to H-37 (δ 2.05) and H_3-38 (δ 0.94) as well as through H_2-39 (δ 1.63, 1.45) to H_3-40 (δ 0.93) afforded the structure of the *N*-methylisoleucine moiety in **7**, which was also confirmed by the HMBC data (Table 2). The HMBC correlations observed from H-36 (δ 4.16) to C-34 (δ 172.6) linked the *N*-methylisoleucine moiety to the proline moiety, whereas HMBC correlations from H-36 to C-41 (δ 170.9) established the connectivity between the *N*-methylisoleucine and the β-hydroxy acid residues (Figure 23-24).

The octyne moiety 3-hydroxy-2-methyl-octynoic acid moiety was established through HMBC correlations linking the diastereotopic H_2-4 methylene protons (δ 1.09, 1.31) to the terminal methine carbon C-6 (δ 68.8); from H_2-3 (δ 1.42) to C-5 (δ 83.5) and from the methylene protons H_2-2 (δ 1.99) to the methine carbon C-1 (δ 76.7).

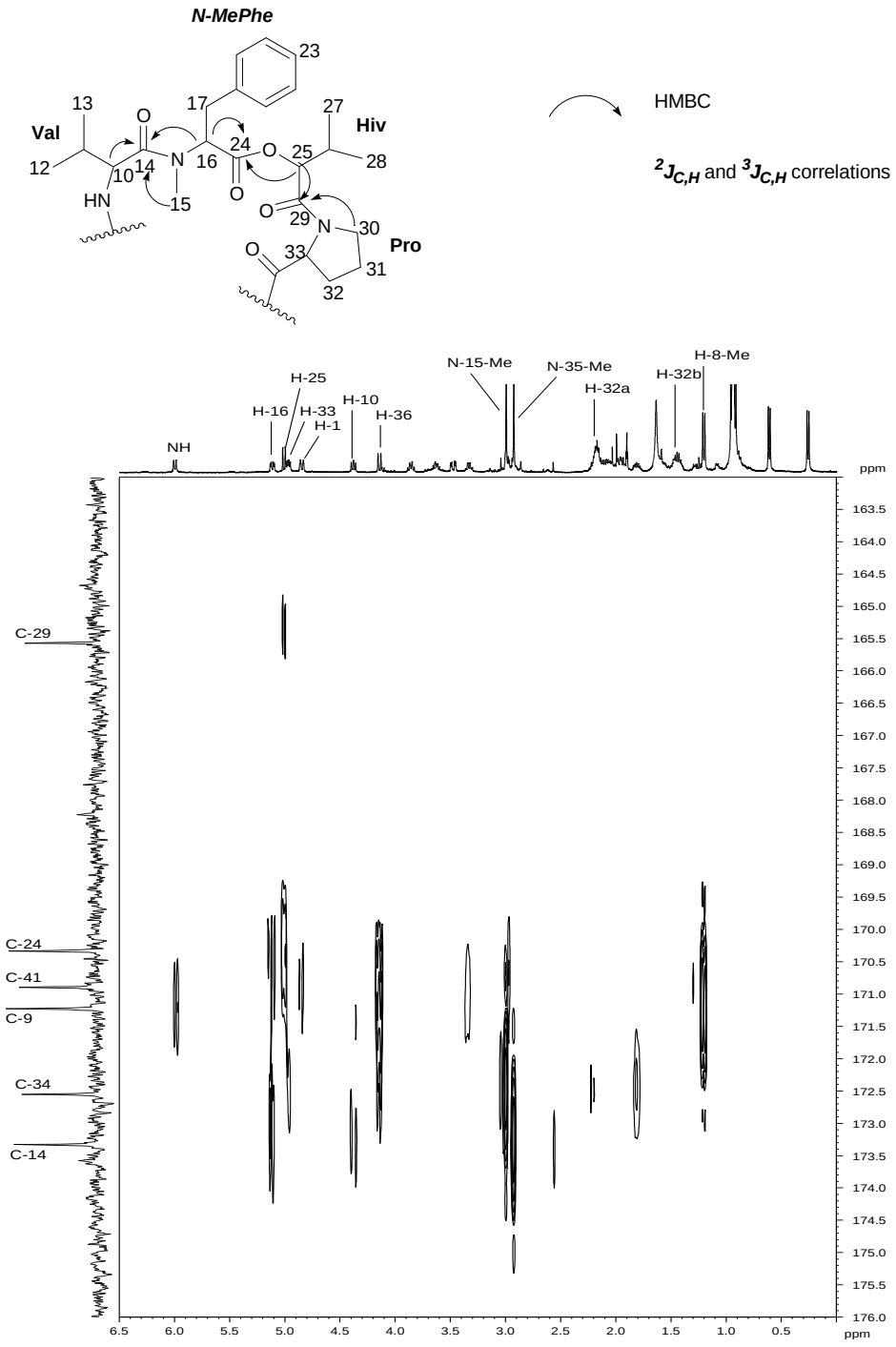

Figure 23. HMBC spectrum (F1 = δ_C 163.0-176.0, F2 = δ_H 0.0 - 6.5) correlations ($CDCl_3$, 400 MHz, D6 = 80 msec) linking the protons of the amino acid and polyketide derived residues and the carbonyl carbons in antanapeptin A.

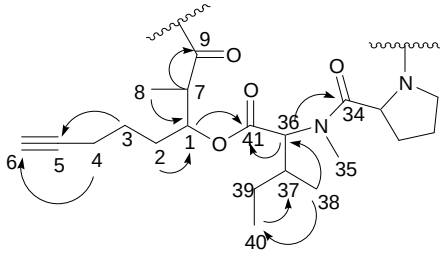

Figure 24. HMBC correlations linking the *N*-methylisoleucine to the alkyne and proline moieties and for establishing the structure of the 3-hydroxy-2-methyl-octynoic acid residue (the numbering of this polyketide residue is as it appears in the overall cyclodepsipeptide numbering system).

HMBC correlations observed from H-1 (δ 4.85) to C-41 connected the 3-hydroxy-2-methyl-octynoic acid to the *N*-methylisoleucine. Carbon 9 (δ 171.2) was the link carbonyl carbon between the octyne and the valine functionalities. Terminal alkyne moieties have been observed in the cyclodepsipeptides onchidin B and kulomo'opunalides, which were previously isolated from the Papua New Guinea gastropod mollusc *Philinopsis speciosa*.[22] Recently, these terminal C_8 alkyne moieties have been reported in *L. majuscula* cyclodepsipeptides yanucamide A and B (**11**, **12**); [21] and pitipeptolides A and B (**23**, **24**).[36] The octyne moieties of the former cyclodepsipeptides possesed a 2,2-dimethyl substitution pattern (Dhoya) whereas in the latter cyclodepsipeptide, the Hmoya residue is monomethylated at C-2. However, as only one methyl group was identified in antanapeptin A as residing on the α-carbonation of the Hmoya residue we suggest that antanapeptin A is more closely related to pitipeptolides A and B than to yanucamides A and B.

Table 3. NMR spectral data ($CDCl_3$, 400 MHz) for antanapeptin A (7)

		^{13}C	^{1}H J (Hz)	COSY	HMBC
Hmoya	1	76.7	4.85 d (10.6 Hz)	2,7	2,3,8,9,41
	2	27.7	1.99 m, 1.60 m	1,3	1,3,4,7
	3	25.0	1.42 m, 1.63 m	4	1,2, 4,5
	4	17.9	2.20 m	3	2,5,6
	5	83.5	-		
	6	68.8	1.90 m		5
	7	42.5	3.33 d (7.6 Hz)	1,8	1,2,8,9
	8	14.7	1.21 d (7.6 Hz)	7	1,7,9
	9	171.2	-		
Val	NH	-	6.00 d (8.8 Hz)	10	9,10,14
	10	52.4	4.38 d (7.6 Hz)	11	9,11,12,13,14
	11	31.1	1.45 m	11,12,13	10,12,13,14
	12	17.5	0.62 d (6.8 Hz)	11	10,11,13
	13	18.8	0.27 d (6.6 Hz)	11	10,11,12
	14	173.3	-		
N-MePhe	15	30.4	2.93 s		10,14,16
	16	62.4	5.13 dd (10.6, 4.0 Hz)	17	14,15,17,18,24
	17	35.3	2.98 dd (14.4, 3.5 Hz) 3.50 dd (14.3, 3.5 Hz)	17	16,18,19/20,24
	18	136.8	-		
	19/20	129.3	7.23 m	21/22	17,21/22,23
	21/22	128.9	7.29 m	19/20, 23	18,19/20
	23	127.2	7.20 m		19/20
	24	170.3	-		16/17
Hiv	25	77.3	5.01 d (9.4 Hz)	26	24,26, 27,28,29
	26	29.6	2.22 m	25,27,28	25,27,29
	27	18.0	0.96	26	25,26,28
	28	18.6	0.95	26	25,26,27
	29	165.6	-		
Pro	30	47.2	3.87 q (7.3 Hz) 3.62 q (7.3 Hz)	31	29,31,32
	31	25.1	2.13 m 1.98 m	30,32	30,32,33
	32	29.2	2.22 m	31,33	30,31,33,34
	33	56.8	4.97 dd (8.1, 4.0 Hz)	32	29,30,32,34
	34	172.6	-		
N-MeIle	35	28.9	2.98 s		33,34,36
	36	64.2	4.16 d (10.6 Hz)	37	34,35,37,38,39,41
	37	34.5	2.05 m	36,38,39	36,38,40
	38	15.7	0.94 m	37	36,37,39
	39	25.7	1.49 m 0.93 m	37,40	36,38,40
	40	11.2	0.93	39	37,39
	41	170.9	-		

Data acquired in $CDCl_3$ (400 and 100 MHz for ^{1}H and ^{13}C respectively) spectra referenced to $CDCl_3$ (^{1}H δ 7.25, ^{13}C δ 77.0). J values given in Hz; chemical shifts in ppm.

2.5 The stereochemistry of antanapeptin A (7)

Prior to the stereochemistry determination studies, antanapeptin A (100 μg) was subjected to acid hydrolysis (6N HCl, 110 ^{o}C, 14 h) according to the procedure described earlier (Sections 1.4.1 and 1.5) to yield the free amino acid and polyketide derived residues.

2.5.1 Marfey's analysis of the α-amino acids in antanapeptin A

The free amino acids arising from hydrolysis of (**7**) were derivatized with 1-fluoro-2,4-dinitrophenyl-5-*L*-alanine amide (*L*- Marfey's reagent) forming their respective diastereomers which were subsequently separated using reversed phase HPLC with gradient elution. The retention times of the derivatized amino acids hydrolysates were compared with similarly derivatized authentic, commercially available standard compounds. Efforts to make synthetic 1-fluoro-2,4-dinitrophenyl-5-*D*-alanine amide (*D*- Marfey's reagent)[52] from 1,5-difluoro-2,4-dinitrobenzene (FFDNB) and a solution of *D*-Ala-NH_2.HCl in acetone were unsuccessful resulting only in unchanged starting material. The reason for attempting to make *D*- Marfey's reagent was that we were only able to procure *L*- *N*-methylphenylalanine and *L*- *N*-methylisoleucine (see Section 1.4.1). Not having access to the *D*- *N*-methylphenylalanine and *D*- *N*-methylisoleucine standards was therefore problematic. Although we were able to detect the *L*- Marfey's derivative of *L*- phenylalanine by HPLC, repeated attempts to prepare the *L*- Marfey's derivative of *N*-methylisoleucine were unsuccessful. The *N*-methylated amino acids clearly appeared to be more difficult to derivatize. Our assignment of an *L*-stereochemistry to the *N*-methylphenylalanine from **7** is tenuous because we did not have an authentic sample of the *D*- isomer to compare its retention time. A chromatogram representing our successful separation of racemic *L*- and *D*- proline using Marfey's HPLC analysis is shown in Figure 25. We used this chromatogram to determine the stereochemistry of the proline moiety in antanapeptin A (Figure 26).

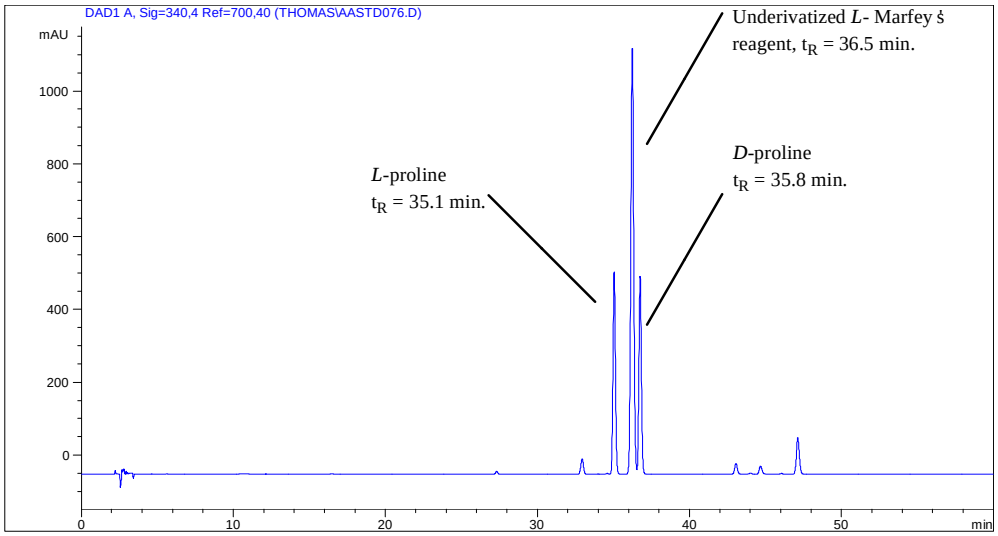

Figure 25. HPLC chromatogram on the separation of Marfey's derivatized racemic *DL*- proline obtained from a Zorbax SB C_{18} (4.6 x 250 mm i.d., 5 µm) column, gradient elution from H_2O/TFA (100: 0.05) to MeCN/H_2O/TFA (10:90:0.05) in 60 minutes, flow rate 1 mL min^{-1}, UV detection at 340 nm.

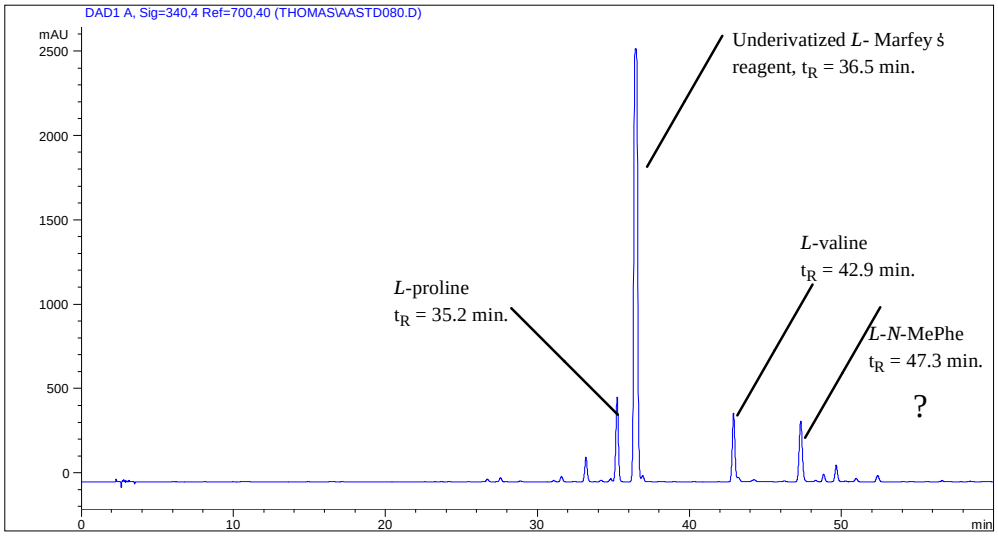

Figure 26. HPLC chromatogram of Marfey's derivatized antanapeptin A obtained from a Zorbax SB C_{18} (4.6 x 250 mm i.d., 5 µm) column, gradient elution from H_2O/TFA (100: 0.05) to MeCN/H_2O/TFA (10:90:0.05) in 60 minutes, flow rate 1 mL min^{-1}, UV detection at 340 nm.

This finding is in agreement with Marfey's postulate that the *D*- enantiomer has a longer retention time on the column because of stronger intramolecular hydrogen bonding.[52] The chromatogram presented in Figure 26 clearly shows that the α-amino acids proline, valine and *N*-methylphenylalanine (*N*-MePhe) established in antanapeptin A were all of the *L*- stereochemistry (see Table 4 for a detailed summary). The chromatogram on Figure 27 represents the underivatized *L*- Marfey's reagent which was present in all our chromatograms.

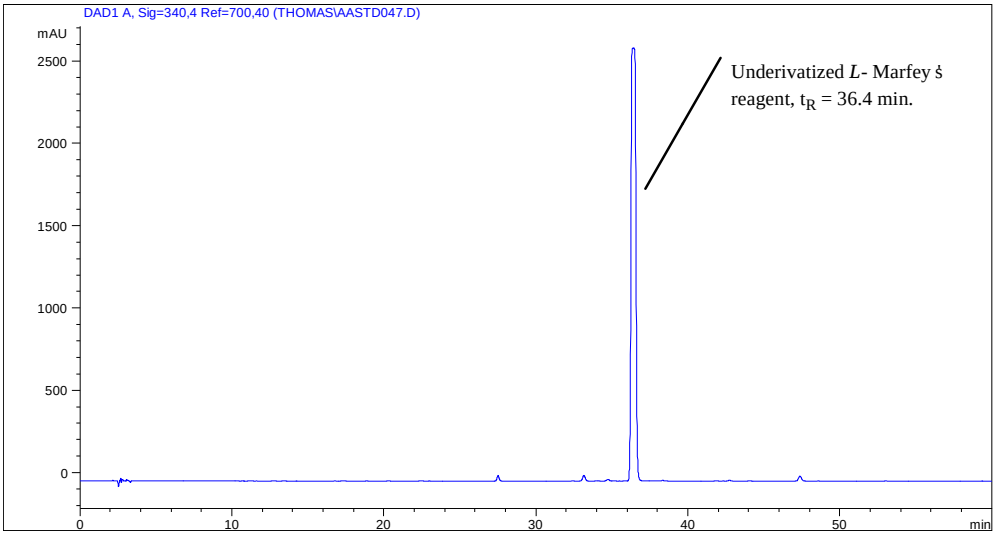

Figure 27. HPLC chromatogram of underivatized *L*- Marfey's reagent obtained from a Zorbax SB C_{18} (4.6 x 250 mm i.d., 5 μm) column, gradient elution from H_2O/TFA (100: 0.05) to MeCN/H_2O/TFA (10:90:0.05) in 60 minutes, flow rate 1 mL min^{-1}, UV detection at 340 nm.

2.5.2 Determination of the stereochemistry of the 2-hydroxy-3-methylbutanoic acid (α-hydroxyisovaleric acid) residue from antanapeptin A using chiral GC analysis

Methylation of the acid hydrolysate of antanapeptin A with diazomethane (Section 1.5) afforded the volatile methyl 2-hydroxy-3-methyl-butanoate derivative from the 2-hydroxy-3-methylbutanoic acid residue.

Elution of this methyl ester derivative from a GC ChirasilVal® column yielded a retention time (t_R = 13.07 min.) that compared favourably with the retention time of an authentic methyl *S*-(-)-2-hydroxy-3-methylbutanoate standard (t_R = 13.08 min.). The chromatogram obtained for the separation of the racemic methyl *S,R*-(±)-2-hydroxy-3-methylbutanoate mixture is shown in Figure 28 in which the peak at t_R 13.08 minutes represents the *S*- isomer and the peak at t_R = 13.67 minutes represents the *R*- isomer. The chromatogram obtained from the methyl 2-hydroxy-3-methyl-butanoate derived from **7** is presented in Figure 29 in which the retention time of 13.07 minutes clearly matched the retention time of the *S*- enantiomer.

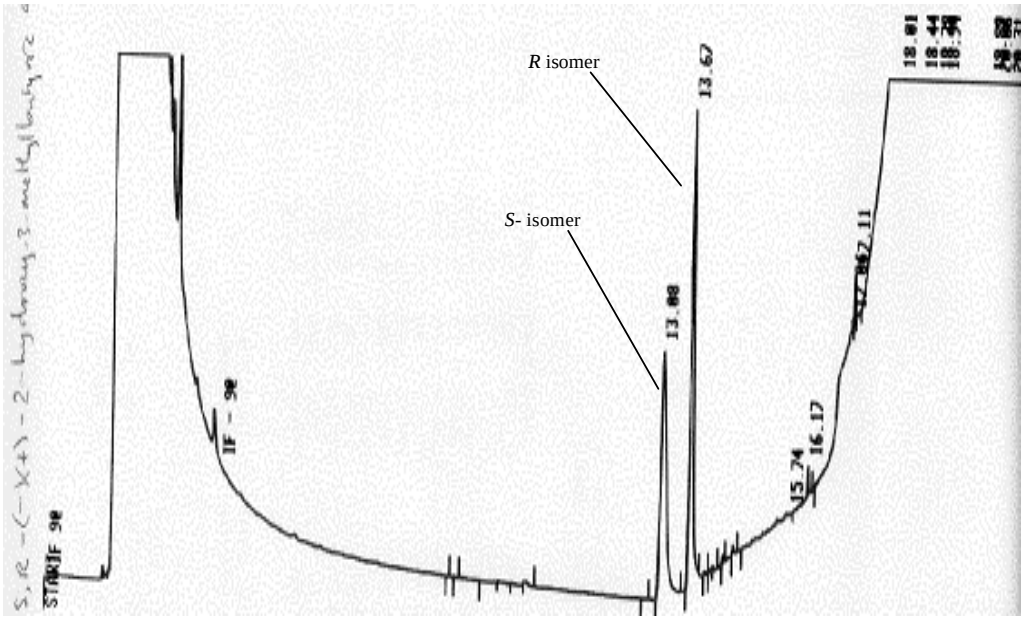

Figure 28. Chiral GC chromatogram showing the separation of the *S* and *R* diastereomers in a racemic methyl *S,R*-(±)-2-hydroxy-3-methyl-butanoate ester afforded from a ChirasilVal® column. Column temp. gradient 30-40 ^{o}C at 1 ^{o}C min $^{-1}$, delay time 3 min; then ramped to 200 ^{o}C at 30 ^{o}C min $^{-1}$. Helium flow 32.6 mL min$^{-1.}$

This finding clearly suggests an *S*(*L*)- stereochemistry of the 2-hydroxy-3-methylbutanoic acid (α-hydroxyisovaleric acid) residue in **7** which confirms the configuration proposed by Nogle and Gerwick for the Hiv derived from antanapeptin A.

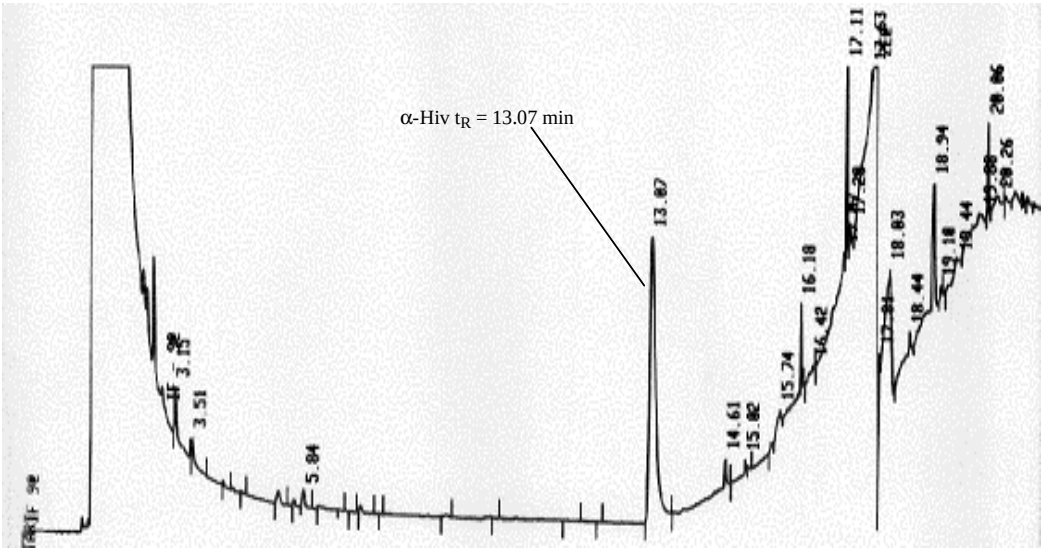

Figure 29. Chiral GC chromatogram of a diazomethane derivatized anatanapeptin A acid hydrolysate afforded from a ChirasilVal® column. Column temp. gradient 30-40 °C at 1 °C min^{-1}, delay time 3 min; then ramped to 200 °C at 30 °C min^{-1}. Helium flow 32.6 mL min^{-1}.

2.5.3 A summary of the stereochemistry of the α-amino acid and β-hydroxy acid residues in antanapeptin A (7)

Table 4. A summary of the observed stereochemistry of the residues in (**7**).

	Mean retention times, t_R (minutes)			
	Standards			
Residue	*L*-	*D*-	Antanapeptin A (**7**)	
Proline[a]	35.1	35.8	35.2	*L*-
N-methylphenylalanine[a*]	47.4	-	47.3	*L*-
Valine[a]	42.4	46.2	42.9	*L*-
α-hydroxyisovaleric acid[b]	13.08	13.67	13.07	*L*- (*S*)

[a] Retention times acquired using Marfey's analysis; [b] Retention times from chiral GC. * The *L*-stereochemistry assignment is tenuous (see Section 2.4.1). Note: The *N*-methylisoleucine residue could not be derivatized for HPLC.

Table 4 lists the observed stereochemistry of the α-amino acids proline, *N*-methylphenylalanine and valine; and the α-hydroxyisovaleric acid residues in (**7**). Our analyses confirmed the stereochemistry of antanapeptin A proposed by Nogle and Gerwick.[15] The stereochemistry of the 3-hydroxy-2-methyloctynoic acid (Hmoya) in antanapeptin A was not determined.

2.6 Structure elucidation of homodolastatin 16 (42)

Homodolastatin 16 was isolated along with antanapeptin A from the TDWA1-008 extract as *per* the procedure outlined in Scheme 4. A yield of 3.4 mg (0.0035% yield calculated *per* dry weight of *L. majuscula*) was obtained for **42**. The molecular formula $C_{48}H_{72}O_{10}N_6$ (*m/z* $[M + Cs]^+$ 1025.4364) was afforded by the FABMS data, which was consistent with the forty eight carbon resonances observed in the ^{13}C NMR spectrum of **42**.

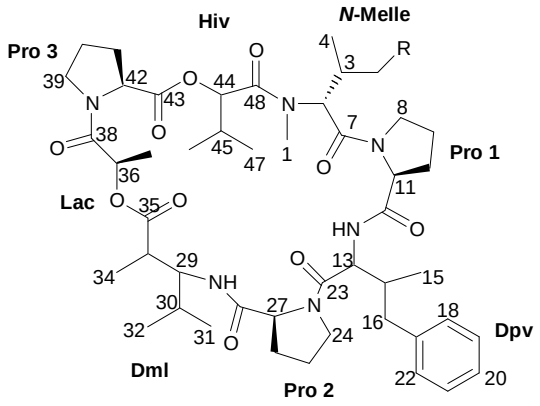

40 R = H, **42** R = CH_3

The molecular formula suggested that **42** possessed sixteen degrees of unsaturation, twelve of which were accounted for by eight carbonyl signals (δ 169-175) and four attributed to a phenyl ring (δ_C 126.1, 128.3, 129.6, 140.6).

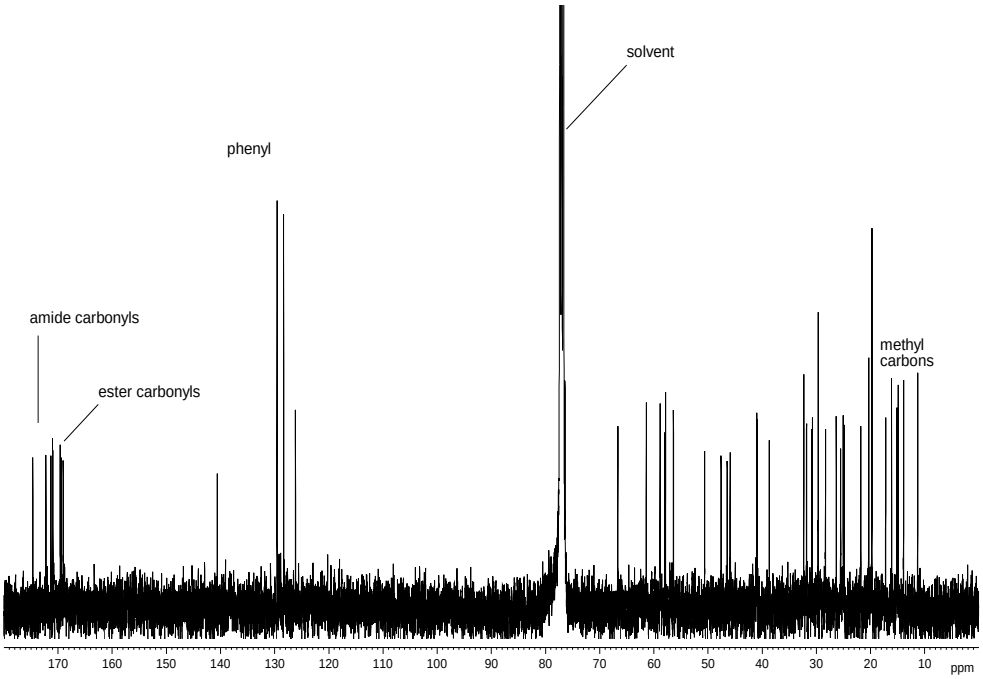

Figure 30. ^{13}C NMR spectrum ($CDCl_3$, 100 MHz) of homodolastatin 16 (**42**).

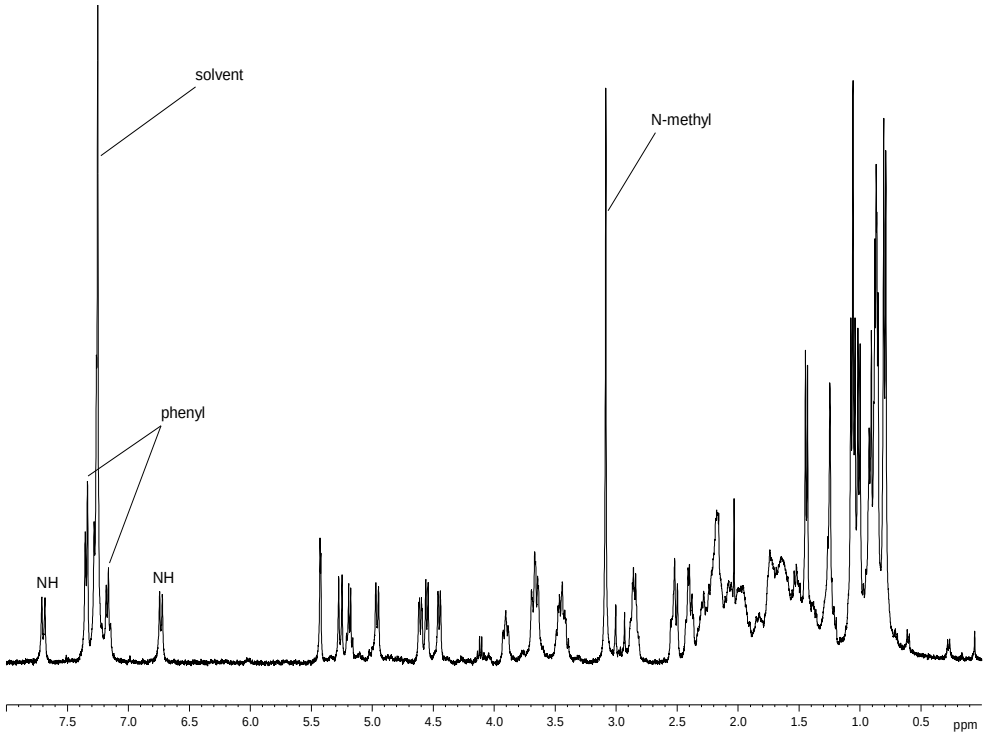

Figure 31. ^{1}H NMR spectrum ($CDCl_3$, 400 MHz) of homodolastatin 16 (**42**).

The peptide nature of homodolastatin 16 was evident from the exchangeable amide N-H and the carbonyl signals in the ^{1}H and ^{13}C NMR (δ_H 6.7, 7.7; δ_C 169.4, 171.0, 171.0, 171.3, 172.2, 174.6) spectra respectively (Figure 30-31) and from the *N*-methyl protons at δ 3.08 in the proton NMR spectra (Figure 31). Both the proton and carbon spectra for **42** were typical of a monosubstituted benzene ring (δ_H 7.15; δ_C 126.1, 128.3, 129.6, 140.6), the presence of which was supported by similar strong infra red carbon-hydrogen stretching bands as those observed for antanapeptin A at 702 and 753 cm^{-1}. One of the remaining four degrees of unsaturation was attributed to the macrocyclic ring of a cyclodepsipeptide. The absence of any evidence for vinylic or alkyne functionalities required the outstanding three double bond equivalents to be rings (possibly three proline moieties). A search of the marine natural products literature data-base MarinLit[63] revealed that a marine compound with a molecular formula of $C_{48}H_{72}O_{10}N_6$ had not been isolated before. Two compounds with molecular formulae close to $C_{48}H_{72}O_{10}N_6$ were dolastatin 16 ($C_{47}H_{70}O_{10}N_6$, **40**)[35] and kulokainalide 1 ($C_{48}H_{70}O_{10}N_6$, **43**).[22]

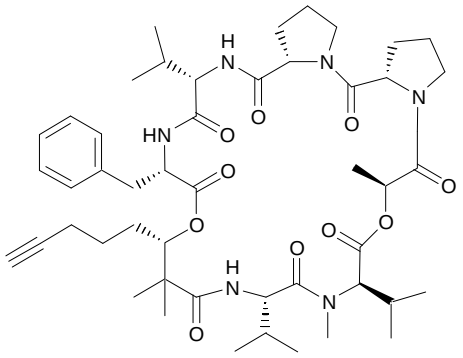

43

The absence of the typical alkyne or alkene signals in the ^{13}C NMR spectrum of **42** eliminated **43** as a possible analogue of **42**. However, the isolation of dolastatin 16 in conjunction with antanapeptins A-D by Nogle and Gerwick from Madagascan *L. majuscula* led us to consider that **42** may be an analogue of dolastatin 16 differing by 14 mass units. A comparison of the ^{13}C NMR data of **42** with those reported for dolastatin

16 supported this idea with the only significant differences in ^{13}C chemical shifts limited to the *N*-methylvaline moiety.

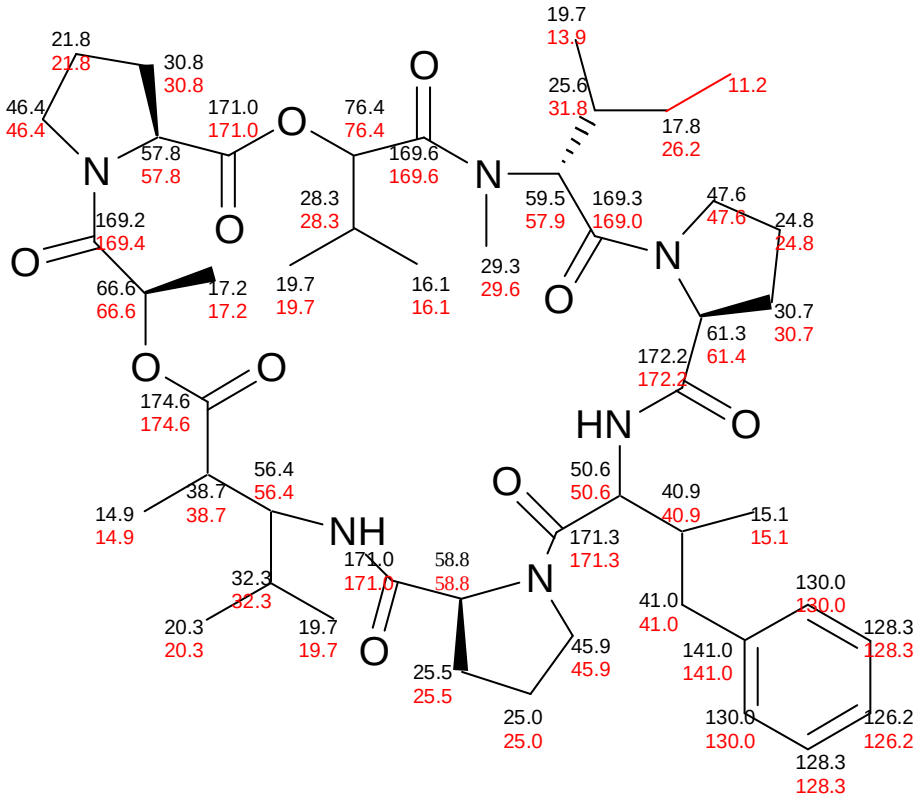

Figure 32. A comparison of the ^{13}C NMR data for **42** ($CDCl_3$, 100 MHz) and dolastatin 16 ($CDCl_3$, 125 MHz). The ^{13}C chemical shifts for **42** are in red. The extended line in red is the point of difference between **40** and **42**.

The difference of fourteen mass units in molecular mass is equivalent to a methylene group. A fairly common homologue of *N*-methylvaline in cyclodepsipeptides is *N*-methylisoleucine (Sections 1.3.1.2, 1.3.2.1, 1.3.2.4 and 1.3.3). The NMR data of **42** supports the presence of an *N*-methylisoleucine moiety through the contiguous COSY couplings observed from H-2 (δ 5.27) – H-3 (δ 2.17)-H_3-4 (δ 0.80), H_2-5 (δ 2.14) and H_3-6 (δ 0.90) (Figure 33). Despite their proximity in the methylene envelope the methine signal H-3 and the methylene protons H_2-5 were clearly coupled to a methyl doublet at δ 0.80 (J 7.1 Hz) and a methyl triplet at δ 0.90 (J 7.3 Hz) respectively.

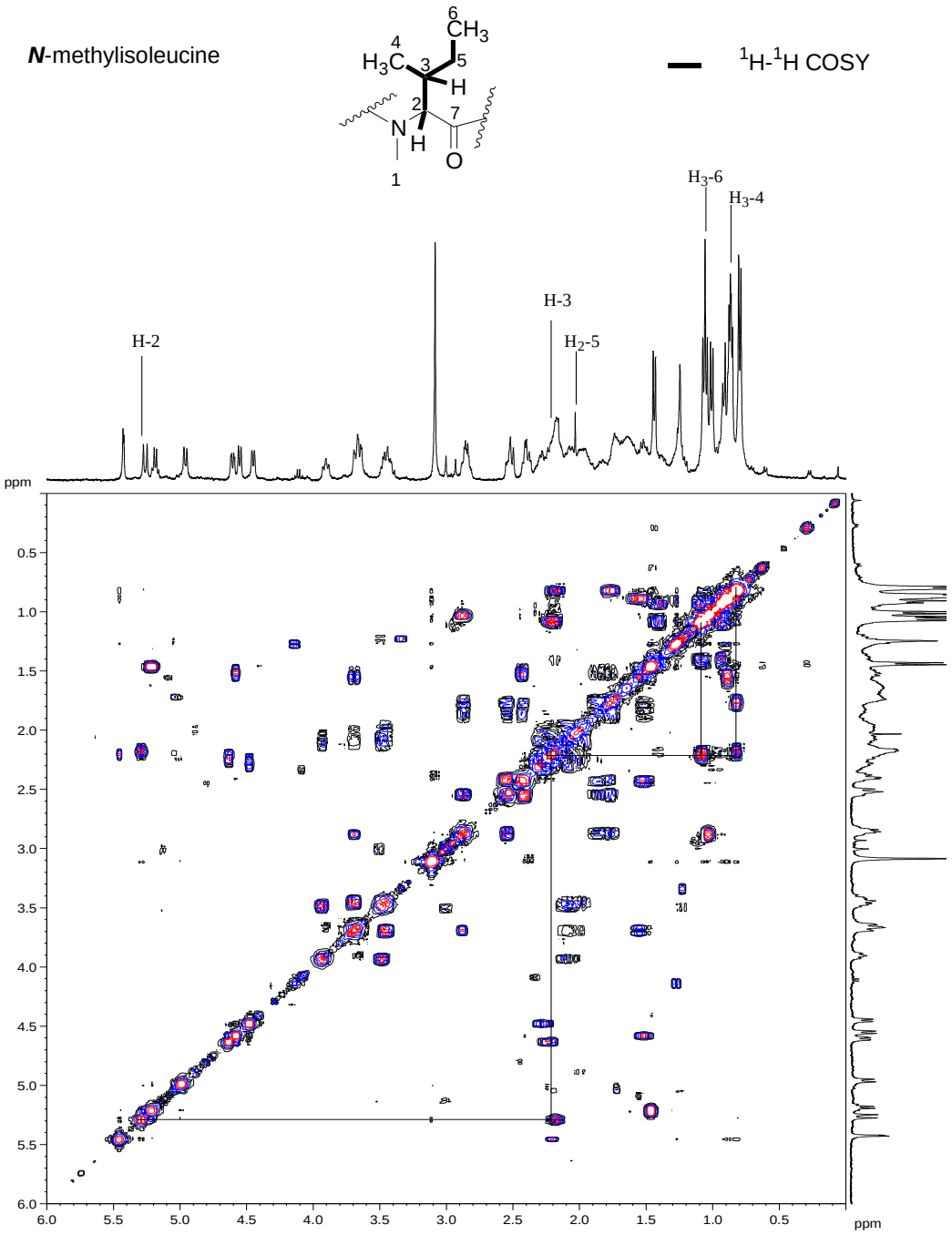

Figure 33. A section of the COSY ($CDCl_3$, 100 MHz; F1 = F2, δ_H 0.0-6.0 ppm) spectrum of **42** showing the contiguous correlations assigned to the *N*-methyl-isoleucine moiety.

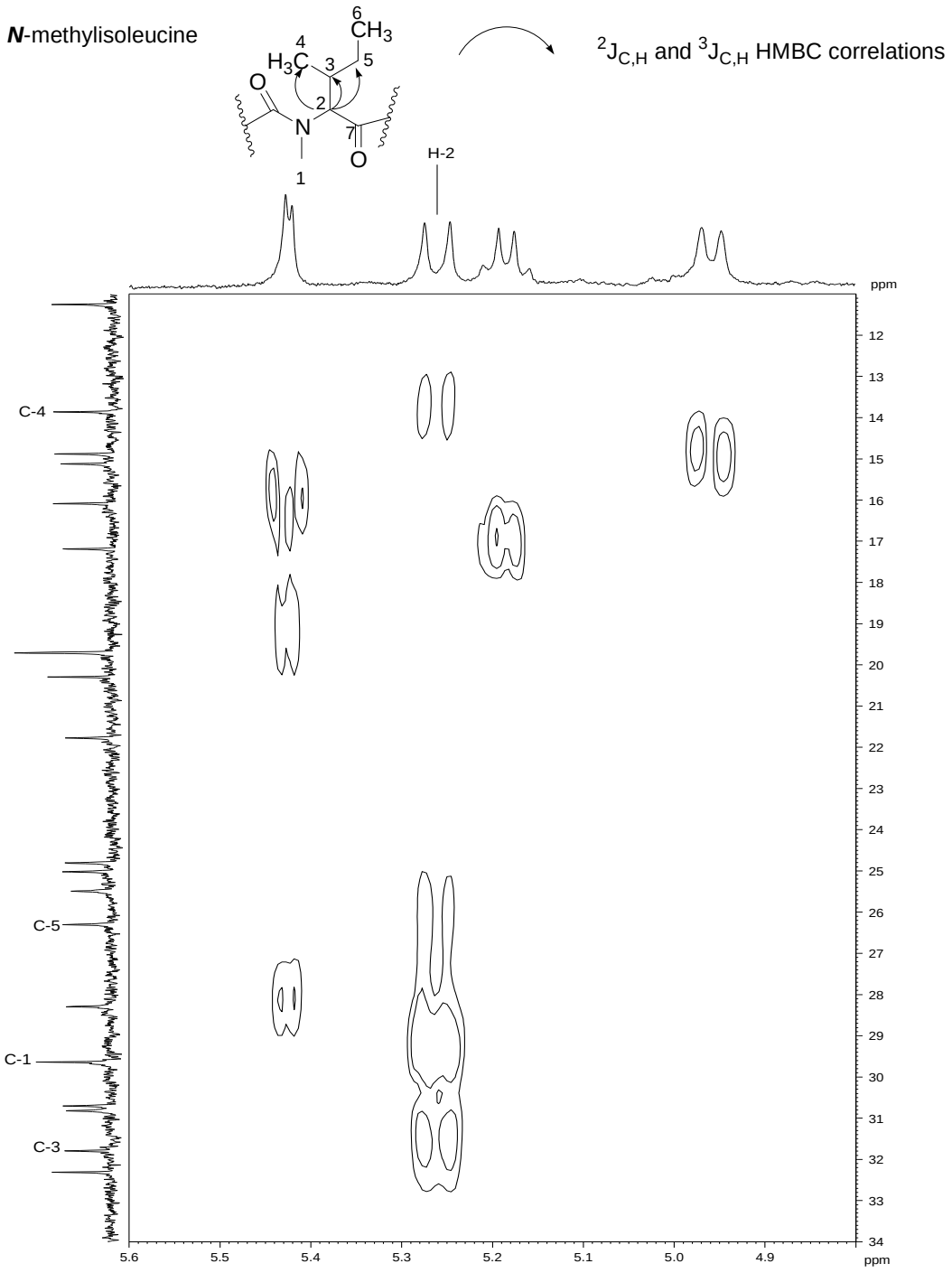

Figure 34. A section of the HMBC spectrum of **42** ($CDCl_3$, 400 MHz; F1 = δ_C 11.0 - 34.0, F2 = δ_H 4.8 -5.6, D6 = 80 msec) showing important correlations for the *N*-methylisoleucine moiety in homodolastatin 16.

Table 4. NMR spectral data of homodolastatin 16 (**42**)

		^{13}C	^{1}H J (Hz)	COSY	HMBC
N-MeIle	1	29.6	3.08 s		
	2	57.9	5.27 d	3	3,4,5,7
	3	31.8	2.17 m	2,4,5	2,4,5,6
	4	13.8	0.80 d (6.6 Hz)	3	2,3,5
	5	26.2	2.14 m	3,6	2,3,4,6
	6	11.2	1.05 t (6.8 Hz)		3,5
	7	169.0	-		
Pro 1	8	47.6	3.92 m, 3.45 m	9	9,10,11
	9	24.8	2.00 m, 1.51 m	8,11	10
	10	30.7	2.16 m	11	9,11,12
	11	61.4	4.61 dd (7.2, 2.0 Hz)	10	8,9,10,12
	12	172.2	-		
Dpv	NH	-	6.72 d (8.1 Hz)	13	
	13	50.6	4.96 d (8.1 Hz)	NH,14	12,14,15,16,23
	14	40.9	1.76 m	15	13,16,17,18
	15	15.1	0.80 d (6.8 Hz)	14	13,14,16
	16	41.0	2.51 m, 2.39 m		13,14,15,17,18/22
	17	140.6	-		
	18/22	129.6	7.35 d (7.1 Hz)		16,20
	19/21	128.3	7.27 d (7.6 Hz)		17
	20	126.1	7.17 dd (7.6, 7.1Hz)		18,22
	23	171.3	-		
Pro 2	24	45.9	2.85 m, 2.52m	25	25
	25	25.0	1.73 m, 1.85 m	24	26
	26	25.5	2.40 m, 1.49 m		24,28
	27	58.8	4.55 d (7.6 Hz)		23,24,25,26
	28	171.0	-		
Dml	NH	-	7.70 d (10.1 Hz)	29	28
	29	56.4	3.66 m	30,33	28,30,33,35
	30	32.3	1.54 m	31,32	29,31,32,33
	31	19.7	1.01 d (7.1 Hz)	30	22,29,30
	32	20.3	0.87 d (7.1 Hz)	30	29,30,31
	33	38.7	2.86 m	29,34	34,35
	34	14.9	0.88 d (7.1 Hz)	33	29,33,35
	35	174.6	-		
Lac	36	66.6	5.19 q (6.8 Hz)	37	35,37,38
	37	17.2	1.44 d (6.6 Hz)	36	36,38
	38	169.4	-		
Pro 3	39	46.4	3.67 m, 3.43 m	40	40
	40	21.8	1.95 m, 2.07 m	39	41
	41	30.8	2.28 m, 2.17 m		39,43
	42	57.8	4.45 dd (7.6, 1.1 Hz)		39,40,41,43
	43	171.0	-		
Hiv	44	76.4	5.42 m		43,45,46,47,48
	45	28.3	2.18 m		46,47
	46	19.7	1.07 d (7.1 Hz)		44,45,47
	47	16.1	1.05 d (7.1 Hz)		44,45,46
	48	169.6	-		

Data acquired in $CDCl_3$; (400 and 100 MHz for ^{1}H and ^{13}C respectively); Proton and carbon spectra referenced to $CDCl_3$ (^{1}H δ 7.25, ^{13}C δ 77.0). J values given in Hz; chemical shifts in ppm.

HMBC correlations from H_2-2 (δ 5.27) to C-3 (δ 31.8), C-4 (δ 13.9) and C-5 (δ 26.2) respectively confirm the observed COSY correlations for the *N*-methylisoleucine moiety in **42** (Figure 34). Unequivocal confirmation of the structure of **42** followed from careful analysis of the HMBC (Figure 35) and NOESY (Figure 36) spectra of this compound.

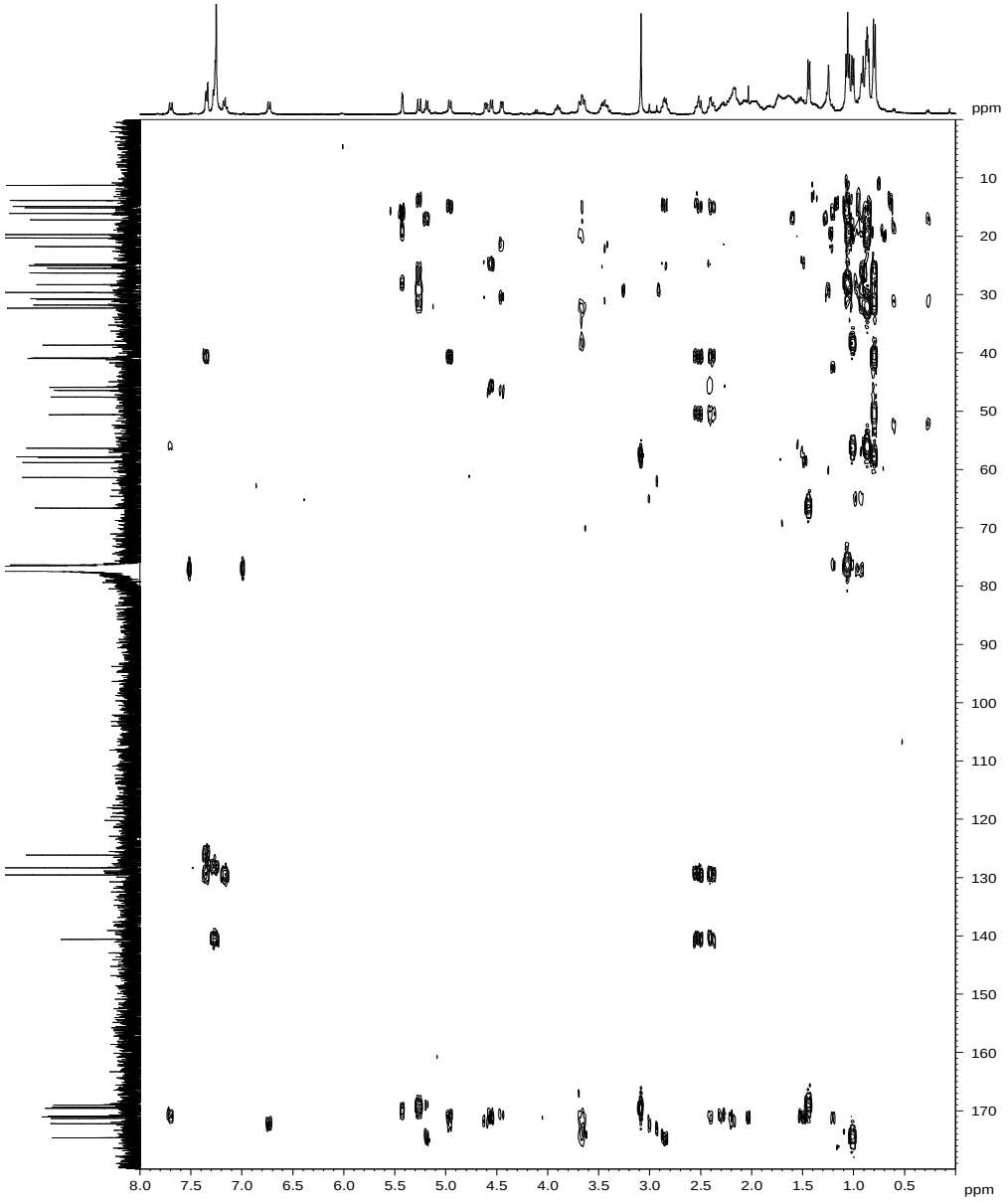

Figure 35. The HMBC ($CDCl_3$, 400/100 MHz) spectrum of **42**.

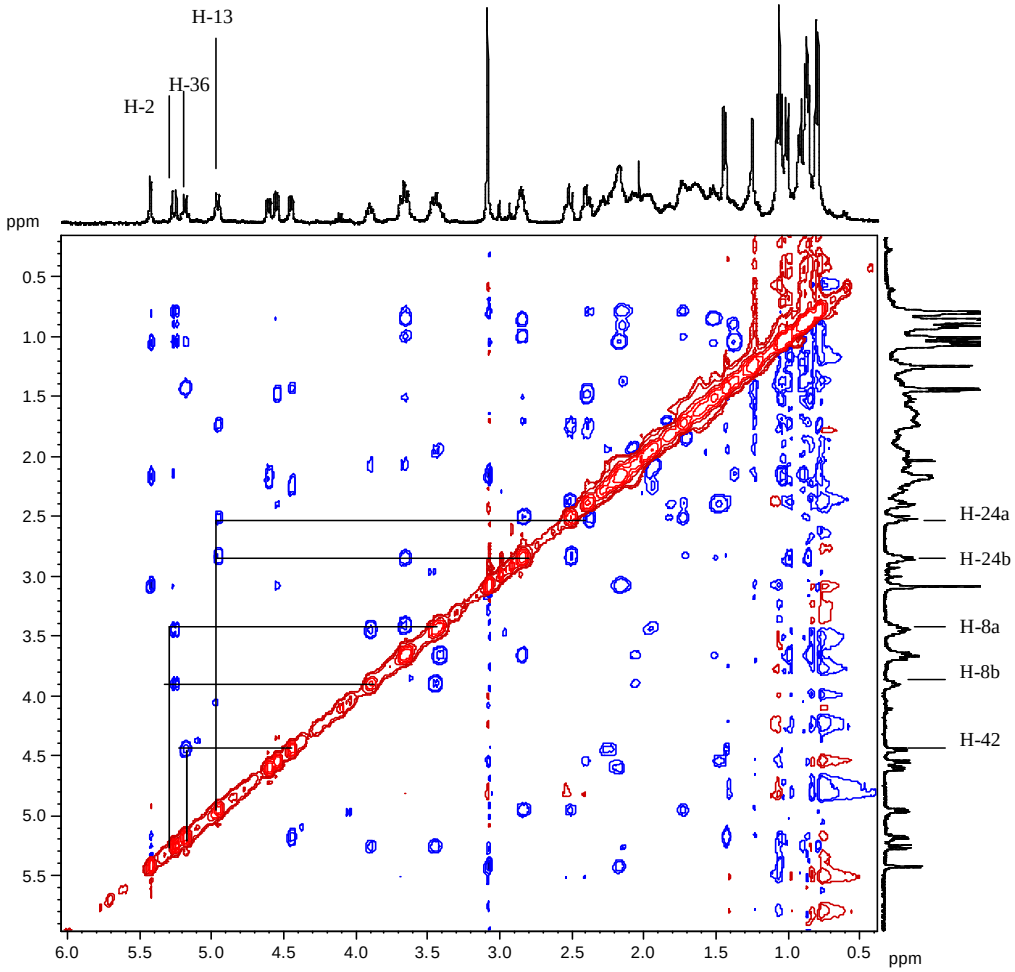

Figure 36. A section of the NOESY spectrum of **42** ($CDCl_3$, 400 MHz, F1 = F2, δ_H = 0.3-6.2 ppm) showing the nOe correlations supporting the linkage of segments A-C (see Figure 37)

In their structure determination of dolastatin 16, Pettit *et al.*[35] identified three substructures (segments A-C, Figure 37) from the NMR data. The sequencing of these segments was achieved mostly from HMBC data. We were also able to support the structure of the three segments from the HMBC data we acquired for homodolastatin 16 (Table 5) thus providing further support for the similarity between the structures of **40** and **42**.

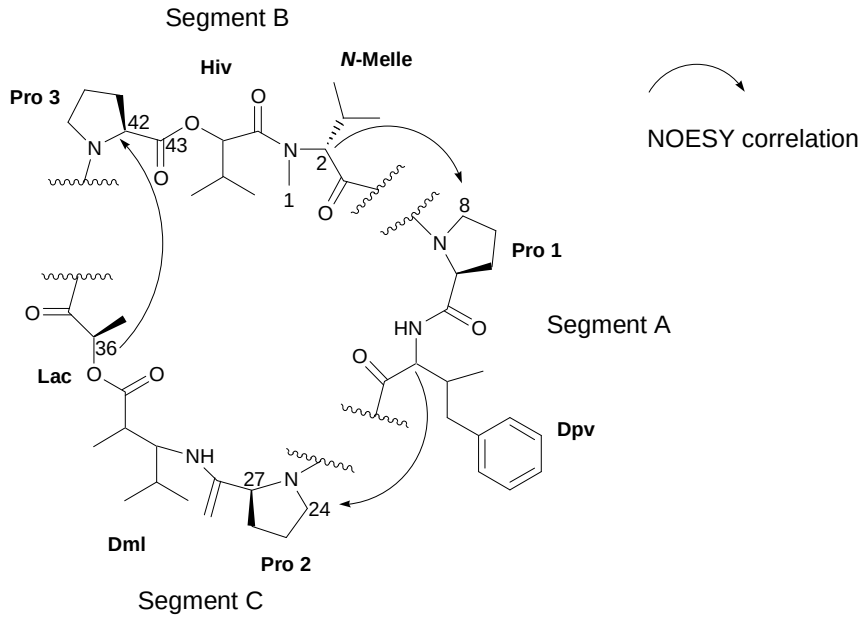

Figure 37. The structures of Pettit *et al.*'s segments A-C for dolastatin 16. Important NOESY correlations which linked these segments together are shown (see Figure 36 for the analogous correlations for **42**).

Although the close correlation between the ^{13}C NMR chemical shifts of dolastatin 16 and homodolastatin 16 would suggest that the linkage of the three segments in **40** is reproduced in **42**, we felt it was necessary to confirm this linkage through NOESY correlations as *per* Pettit *et al.* [35] The NOESY spectrum of **42** reproduced in Figure 36 clearly shows the definitive nOe correlations between H-2 and H_2-8, H-13 and H_2-24, and H-36 and H-42 that link the segments A-C together in the order shown.

2.7 The stereochemistry of homodolastatin 16 (42)

Homodolastatin 16 (100 μg) was hydrolysed (6N HCl, 110 °C, 14 h) as *per* the procedure described in Sections 1.4.1 and 1.5 affording the free amino acid and polyketide hydrolysates. The acid hydrolysates of **42** were derivatized with 1-fluoro-2,4-dinitrophenyl-5-*L*-alanine amide (*L*- Marfey's reagent) to form their respective diastereomers which were separated using gradient elution reversed phase HPLC.

Marfey's derivatization of homodolastatin 16 was only successful in establishing the *L*-stereochemistry of proline following the difficulty encountered in derivatizing *N*-methylisoleucine and in the non availability of standards for the dolamethylleuline (Dml) and dolaphenylvaline (Dpv) moieties. The chromatogram of *L*- Marfey's derivatized **42** (Figure 38) clearly reveals that the retention time, t_R = 35.3 minutes for the proline residues in **42** matched the retention time, t_R = 35.1 minutes of the *L*- proline standard (Figure 25). The retention time of underivatized *L*- Marfey's reagent was 36.5 minutes.

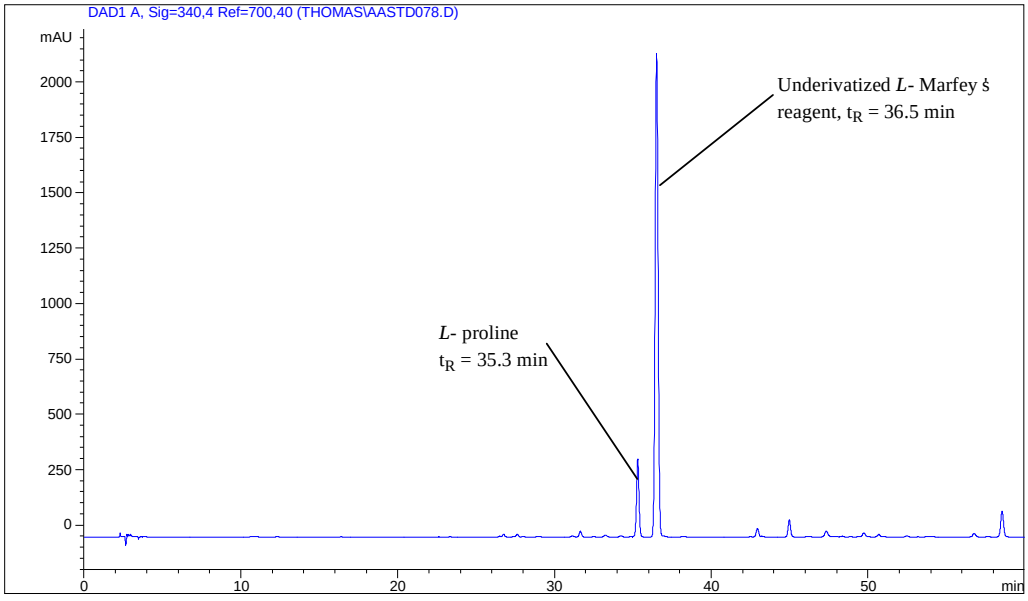

Figure 38. HPLC chromatogram of Marfey's derivatized homodolastatin 16 obtained from a Zorbax SB C_{18} (4.6 x 250 mm i.d., 5 μm) column, gradient elution from H_2O/TFA (100: 0.05) to MeCN/H_2O/TFA (10:90:0.05) in 60 minutes, flow rate 1 mL min^{-1}, UV detection at 340 nm.

As a result of the unsuccessful derivatization of the *N*-methylisoleucine acid hydrolysates with *L*- Marfey's reagent we chose to determine the stereochemistry of the *N*-methylisoleucine α-amino acid residue in homodolastatin 16 using chiral GC. The Chiral GC method was used by Faulkner and co-workers to establish the streochemistry

of α-amino acid residues in the cyclic lipopeptides homodolastatin 3 (**35**) and kororamide (**36**) which were isolated from Palauian collections of *L. majuscula*.[51] Homodolastatin 16 hydrolysates were treated with acetyl chloride prior to derivatization with pentafluoropropionic anhydride (PFPA, 400 μL) in dry CH_2Cl_2 (400 μL) using the commercially available Alltech® derivatization kit (Sections 1.4.3 and 3.4.1). The retention time, t_R = 15.49 minutes of the pentafluoropropionic acid derivative of the *N*-methylisoleucine residue from **42** was found to compare favourably with the retention time of an authentic *S*(*L*-)-*N*-methylisoleucine pentafluoropropionic acid derivatized standard, t_R = 15.44 minutes on analysis by GC (ChirasilVal® column) (Figure 39 and 40).

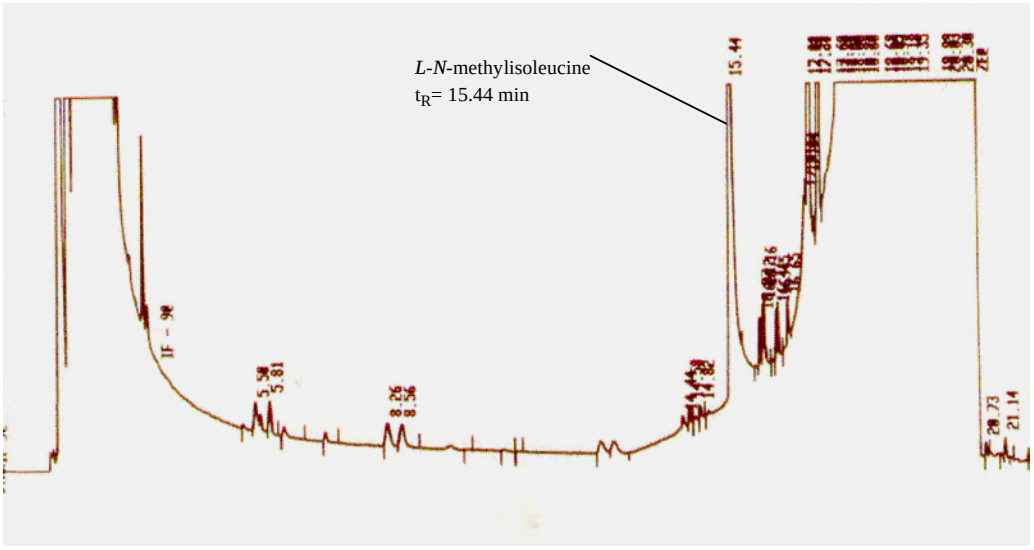

Figure 39. GC chromatogram of a pentafluoropropionic anhydride derivatized acid hydrolysate of *L-N*-methylisoleucine standard on a ChirasilVal® column. Column temp. gradient 30-40 °C at 1 °C min^{-1}, delay time 3 min; then ramped to 200 °C at 30 °C min^{-1}. Helium flow 32.6 mL min^{-1}.

Although we tentatively established an *L*- stereochemistry of the *N*-methylisoleucine amino acid residue in **42**, this assignment was speculative because we were unable to procure the *D,L*- *N*-methylisoleucine amino acid standard to afford a separation of the *D*- and the *L*- stereoisomers.

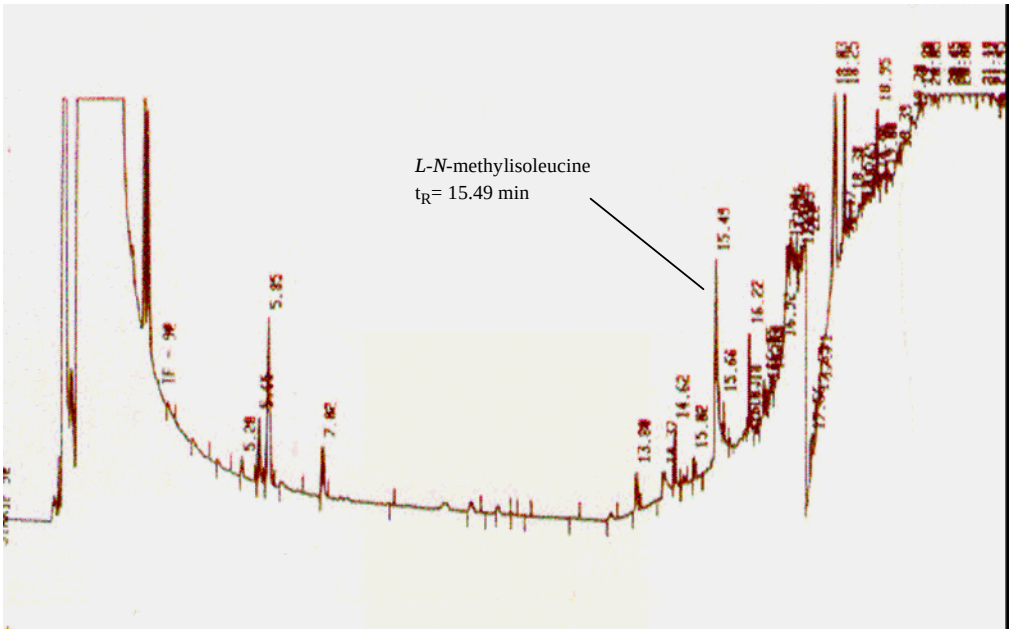

Figure 40. GC chromatogram of a pentafluoropropionic anhydride derivatized acid hydrolysate of homodolastatin 16 on a ChirasilVal® column. Column temp. gradient 30-40 °C at 1 °C min $^{-1}$, delay time 3 min; then ramped to 200 °C at 30 °C min $^{-1}$. Helium flow 32.6 mL min $^{-1}$.

The hydrolysate of **42** was also methylated with diazomethane (Section 1.5 and 3.4.4) to afford the methyl ester derivatives of the lactic and 2-hydroxy-3-methylbutanoic (α-hydroxyisovaleric acid) acids respectively. GC analysis of the methyl ester derivatives with a ChirasilVal® column produced chromatograms whose retention times (t_R = 6.32 minutes for the methyl lactate and t_R = 13.88 minutes for the methyl 2-hydroxy-3-methylbutanoate) were comparable to authentic methyl *R*-(+)-lactate (t_R = 6.29 minutes) and methyl *R*- (+)-2-hydroxy-3-methyl butanoate standard (t_R = 13.67 minutes) (Figure 41). The chromatograms for the separation of the *S* and *R* diastereomers in a racemic methyl *S, R*-(±)-lactate mixture are reproduced in Figure 3 and those for the separation of the *S* and *R* diastereomers in a racemic methyl *S,R*-(±)-2-hydroxy-3-methylbutanoate mixture are shown in Figure 28. Ideally, the identity of the GC peaks should have been confirmed by GCMS but this facility was not available. The absolute stereochemistry of dolaphenylvaline and dolamethylleuline in homodolastatin 16 was not established.

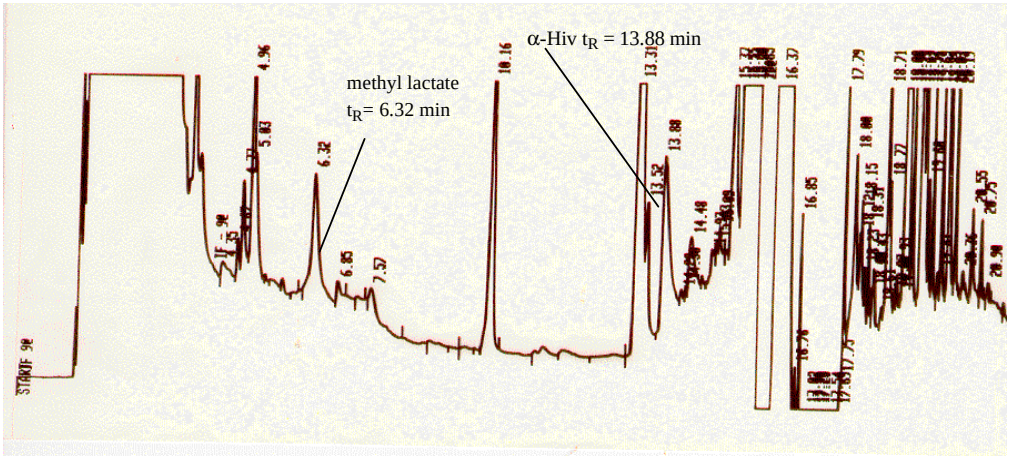

Figure 41. Chiral GC chromatogram of a diazomethane derivatized homodolastatin 16 acid hydrolysate afforded from a chirasilVal column. Column temp. gradient 30-40 °C at 1 °C min $^{-1}$, delay time 3 min; then ramped to 200 °C at 30 °C min $^{-1}$. Helium flow 32.6 mL min $^{-1}$.

2.7.1 A summary of the stereochemistry of the α-amino and β-hydroxy acid residues in homodolastatin 16 (42)

Table 6. A list of the observed stereochemistry of the residues in (**42**).

	Mean retention times, t_R (minutes)			
	Standards			
Residue	*L*-	*D*-	Homodolastatin (**42**)	
Proline[a]	35.1	36.7	35.1	*L*-
N-methylisoleucine[b*]	15.44	-	15.49	*L*-
Lactic acid[b]	5.95	6.29	6.32	*D*- (*R*)
α-hydroxyisovaleric acid[b]	13.08	13.67	13.88	*D*- (*R*)

[a] Retention times acquired using Marfey's analysis; [b] Retention times from chiral GC. * The *L*-stereochemistry assignment is tenuous as the *D*- stereoisomer was not available.

The stereochemical assignment of the *R*- lactic acid residue in **42** is opposite to that in **40** while the asignment of an *R*- configuration to the Hiv moiety in **42** is consistent with that established for **40**.

2.8 Biological activity of homodolastatin 16

In a global context South Africa, especially in the Western and Eastern Cape Provinces, has a particularly high prevalence of oesophageal cancer. The relatively high incidence of this form of cancer is reflected in Figure 42 which relates the number of cancer deaths to the type of cancer in the coastal city of Port Elizabeth (estimated population 1 036 700) during 1998.[65] Woodsmoke inhalation from cooking fires and the effects of inadvertently eating the carcinogenic aflatoxins produced by the *Fusarium* fungus that grows on damp stored grain, are thought to be the two main contributing factors to the high levels of oesophageal cancer in South Africa.[66]

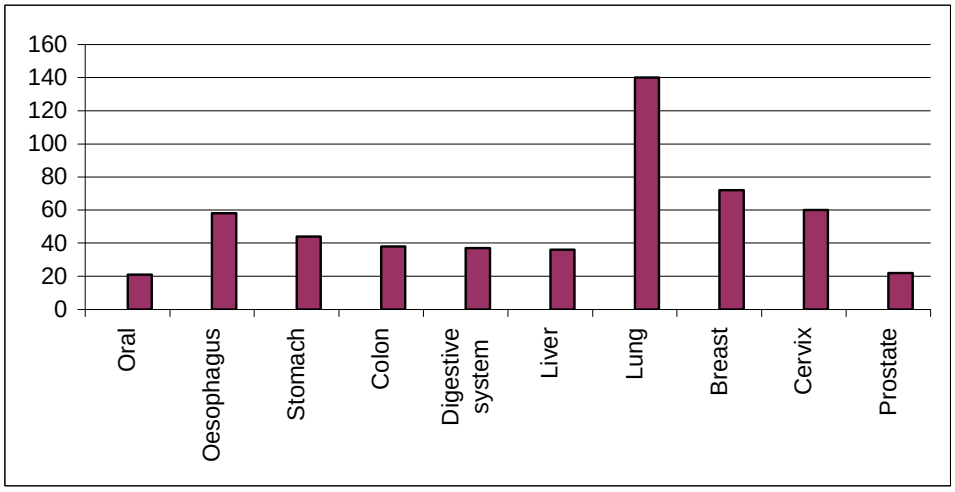

Figure 42. The number of cancer deaths in Port Elizabeth (July 1997- June 1998)[65]

Given the strong activity of dolastatin 16 [35] against lung (NCI-H460: GI_{50} 0.00096 μgmL^{-1}), colon (KM20L2 GI_{50} 0.0012 μgmL^{-1}), brain (SF-295, GI_{50} 0.0052 μgmL^{-1}) and melanoma (SK-MEL5 GI_{50} 0.0033 μgmL^{-1}) cancer cell lines, the homodolastatin 16, isolated in this MSc thesis research, was submitted to the Department of Medical Biochemistry at the University of Cape Town as part of an ongoing collaborative programme for testing marine natural products against two human oesophageal cancer cell lines (WHCO1 and WHCO6). The preliminary results obtained are reproduced in Figures 43.

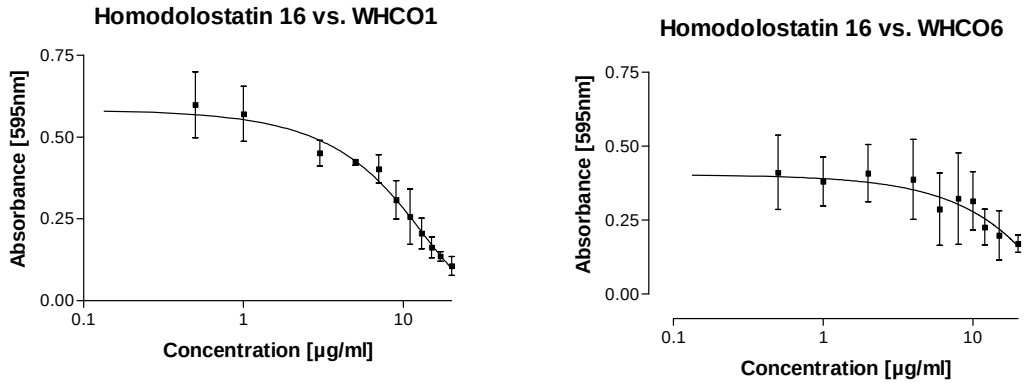

Figure 43. Preliminary dose response curves showing the activity of homodolastatin 16 against two oesophageal cancer cell lines WHCO1 and WHCO6.

The preliminary IC_{50} values for homodolastatin 16 in the WHCO1 and WHCO6 cell lines were 4.31 and 10.05 gmL^{-1} respectively. Surprisingly homodolastatin 16 is clearly not as active against oesophageal cancer as its lower homologue, dolastatin 16 is against a wide variety of cancers.[35]

CHAPTER THREE

EXPERIMENTAL

3.1 General experimental procedures

3.1.1 Analytical

The ^{1}H (400 MHz), ^{13}C (100 MHz), DEPT 135, HMQC, HMBC, COSY-90 and NOESY spectra were recorded on a Bruker AMX 400 spectrometer using standard pulse sequences. The chemical shifts, which were referenced to the residual protonated solvent resonances ($CHCl_3$ δ_H 7.25, δ_C 77.0) and were reported in ppm. Coupling constants were recorded directly in Hz from the ^{1}H NMR spectra and were not matched to corresponding values. High performance liquid chromatographic separations were performed on Whatman Magnum 10 Partisil and Phenomenex Luna RP C_{18} (250 x 10 mm, 9mm i.d., flow rate 4 mL min $^{-}$1) using a Spectra-Physics liquid chromatography pump, Waters R401 differential refractometer and a Rheodyne injector. High resolution fast atom bombardment mass spectra were obtained from the NIDDK Mass Spectrometry Unit at the National Institutes of Health in the United States and were recorded on a JEOL SX102 FAB mass spectrometer using a magic bullet matrix. Optical rotations were measured at the sodium-D line (589 nm) using a Perkin-Elmer 141 polarimeter. The concentration of the solutions used to determine optical rotations followed standard protocol and were expressed in g/100 mL. Infra red spectra of the compounds were recorded as films (neat) on NaCl discs using a Perkin-Elmer Spectrum 2000 FT-IR spectrometer.

3.1.2 Chromatography

All the general laboratory solvents were redistilled from glass before use. Analytical normal phase thin layer chromatography were performed on DC-Plastikfolien Kieselgel 60 F_{254} plates whilst analytical reverse phase thin layer chromatography were performed on DC-Ferigplatten RP18 F_{254} plates. The plates were viewed under UV light (254 nm) and developed by spraying with 10% H_2SO_4 in MeOH followed by heating. Flash chromatography was performed using Kieselgel 60 (230-400 mesh) silica

gel and size exclusion was performed using lipophilic Sephadex LH-20 (25-100 μ) from Sigma, USA.

Where appropriate, solvents and reagents were dried by distillation from the usual drying reagent prior to use following standard procedures. Dichloromethane was dried from calcium hydride whereas tetrahydrofuran and diethyl ether were dried over sodium wire and benzophenone. All reactions were magnetically stirred unless otherwise stated.

3.2 Collection and extraction of *L. majuscula*

L. majuscula specimens were collected by snorkelling from Shimoni and Wasini island (map on Figure 10, Section 1.6.1) in December 2000 and stored in isopropanol prior to transportation to South Africa for isolation and study of the cyanobacterium chemistry. A voucher specimen of *L. majuscula* is deposited at the Rhodes University marine organism collection. The mat forming cyanobacterium *L. majuscula* occurs pan-tropically and is characterised by very long filaments. The inner part of the filament (trichome) is usually 20-40 μ broad[64] (Kenyan *L. majuscula* 33 μ). The cells are enclosed in a lamellated sheath (c.a. 4 μm; Kenyan *L. majuscula* 5.5 μ). The dry mass of the Wasini Island *L. majuscula* was 136 g and the Shimoni *L. majuscula* was 44 g.

The initial isopropanol extract was decanted and the Wasini Island and Shimoni specimens repeatedly extracted with 2:1 CH_2Cl_2/MeOH. The dichloromethane extracts were pooled and partitioned with water. Concentration of the pooled dichloromethane extracts of the Wasini Island collection resulted into a dark sticky gum (4.2 g) which on subjection to Sephadex LH-20 (5:2:1 CH_2Cl_2: hexane: MeOH) chromatography provided fractions Fn 1-Fn 3 based on their TLC and ^{1}H NMR spectra (Scheme 4). Further Sephadex LH-20 (1: 1 EtOAc/MeOH) chromatography of Fn 2 resulted into Fn 2/1- Fn 2/3. Flash Si Gel (silica 50g; column r = 0.6 cm, h = 32 cm) chromatography of Fn 2/2 with gradient elution ($CHCl_3$-EtOAc-MeOH) provided Fn 2/2/1- Fn 2/2/4. The cyclodepsipeptides antanapeptin A (**7**) (3.7 mg) and homodolastatin 16 (**42**) (3.4 mg)

were obtained from Fn 2/2/3 (15.4 mg) as white amorphous powders by C_{18} reversed phase HPLC (7:3 CH_3CN: H_2O).

Antanapeptin A (7): white armophous powder; $[\alpha]^{32}_D$ –25.7 (*c* 0.1, MeOH Lit:[15] $[\alpha]_D$ –50); IR (neat) 3392 br, 2965, 2930, 2870, 1732, 1651, 1645, 1505, 1455, 1385, 1243, 1184, 1086, 750, 702 cm $^{-1}$; 1H and ^{13}C NMR data, see Table 2; HRFABMS *m/z* [M + H]$^+$ 737.4460 (calculated for $C_{41}H_{61}O_8N_4$, 737.4489).

Homodolastatin 16 (42): white amorphous powder; $[\alpha]^{32}_D$ +3.1° (*c* 0.2, MeOH); IR (neat) 3394, 3321, 2965, 2931, 2877, 2362, 1745, 1733, 1651, 1638, 1509, 1460, 1426, 1388, 1298, 1185, 1091, 753, 702 cm $^{-1}$; ^{1}H and ^{13}C NMR data, see Table 4; HRFABMS *m/z* [M + Cs]$^+$ 1025.4364 (calculated for $C_{48}H_{73}O_{10}N_6$ Cs 1025.4364).

3.3 Biological assays

The brine shrimp larvae (*Artemia nauplii*) toxicity assays were performed at concentrations of 25 μg mL, $^{-1}$ 50 μg mL $^{-1}$ and 100 μg mL $^{-1}$ as described in Section 2.1.2. The biological activity studies of homodolastatin 16 (**42**) (Section 2.7) against two oesophageal cancer cell lines (WHCO1 and WHCO6) were performed at the Department of Medical Biochemistry at the University of Cape Town. The IC_{50} values of 42 in the WHCO1 and WHCO6 cell lines was 4.31 and 10.05 μg mL $^{-1}$ respectively.

3.4 Determination of the absolute stereochemistry of antanapeptin A (7) and homodolastatin 16 (42)

A known amount of **7** (1.5 mg) and **42** (2.5 mg) was dissolved in $CHCl_3$ to afford two solutions of a concentration of 1 mg mL $^{-1}$ (1 μg μL $^{-1}$). A portion (200 μL) of each solution was transferred into a round bottomed flask (10 mL) and the $CHCl_3$ removed by evaporation under nitrogen. The resulting residue was hydrolysed under reflux with 6N HCl (1 mL, 110 °C, 14 h).

3.4.1 Derivatization and analysis of the α-amino acids in 7 and 42 by chiral GC

To the hydrolysate obtained above in a 1 mL thick-walled Reactivial® was added dry 2-propanol (400 μL) and acetyl chloride (100 μL). The Reactivial was immediately securely capped. The solution was heated to 110 °C for 45 minutes in a copper block

following which the solution was dried under nitrogen. Pentafluoropropionic anhydride (PFPA, 400 μL) in dry CH_2Cl_2 (400 μL) was added to the residue and the vial capped immediately prior to further heating (100 °C for 15 minutes). The solvent was removed under a stream of dry nitrogen, the residue dissolved in EtOAc (300 μL) and the resultant solution analysed by GC using a ChirasilVal® column (0.16 μm x 25 m, i.d. 0.25 mm). The oven temperature was ramped from 30 °C to 120 °C at 4 °C min^{-1}. The helium gas flow was 32.6 mL min^{-1}. The respective α-amino acids were identified as being of the *L*- configuration by comparison of the retention times of similarly derivatized authentic amino acid standards (Section 2.5).

3.4.2 Marfey's analysis of antanapeptin A and homodolastatin 16

The acid hydrolysates of antanapeptin A and homodolastatin 16 obtained above were evaporated to dryness and resuspended in H_2O (100 μL). Into the aqueous hydrolysate was added 1% 1-fluoro-2,4-dinitrophenyl-5-*L*-alaninamide in acetone (*L*- Marfey's reagent, 100 μL) and 1 N $NaHCO_3$ (20 μL). The mixture was heated at 40 °C for one hour, cooled to room temperature, neutralised with 2 N HCl (10 μL) solution and evaporated to dryness under a stream of dry nitrogen. The residues were resuspended in DMSO (500 μL) and analysed by reversed phase HPLC [Zorbax SB C18, 5 μm, 4.6 x 250 mm, i.d., 5 μm, UV detection at 340 nm] using a linear gradient elution from H_2O/TFA (100:0.05) to MeCN/H_2O/TFA (10: 90: 0.05) in 60 minutes at a flow rate of 1 mL min^{-1}. The retention times of the hydrolysates matched those of similarly derivatised *L*- valine, *L*-proline and *N*-Methyl-*L*-phenylalanine (see Table 3 Section 2.5.3 and Table 5 Section 2.7.1).

3.4.3 Attempted synthesis of 1-fluoro-2,4-dinitrophenyl-5-*D*-alaninamide (D- Marfey's reagent)

A sample of *D*-Ala-NH_2.HCl (236.0 mg) was dissolved in 1 N NaOH (1.95 mL) and acetone (30 mL) and anhydrous $MgSO_4$ (5 g) added. The mixture was stirred (3 h) and the $MgSO_4$ removed by filtration. The filterate was washed with 3 mL acetone. 1, 5-difluoro-2,4-dinitrobenzene (FFDNB, 334.0 mg) was dissolved in 7.5 mL acetone and the acetone solution of *D*-Ala-NH_2 added drop-wise with magnetic stirring. After addition of the *D*-Ala-NH_2, the contents were stirred for an additional 30 minutes. H_2O (30 mL) was added, resulting into the formation of a golden yellow precipitate which was filtered, washed with 2:1 H_2O-acetone mixture (5 mL), H_2O (5 mL) and finally dried in a desiccator and kept in the dark. NMR analysis revealed that the precipitate was unchanged FFDNB.

3.4.4 Preparation of diazomethane

A solution of KOH (1.5 g), H_2O (3 mL) and ethyl digol (6 mL) was stirred at 70-75 °C. An etheral solution (20 mL) of Diazald® (1.5 g) was added carefully to the basic ethyl digol solution. Diazomethane distilled over as a yellow liquid and was trapped in ice cold ether (20 mL). The diazomethane was used for the methylation of the α-hydroxyisovaleric acid moieties in **7** and **42** and of the lactic acid moiety in **42**.

3.4.4 Chiral GC analyses of the α-hydroxyisovaleric acid moieties in antanapeptin A (7) and homodolastatin 16 (42) and of the lactic acid moiety in 16

A portion (200 μg) of each of hydrolysates of **7** and **42** was separately diluted in MeOH (50 μL) and etheral diazomethane (1 mL generated as *per* the procedure described above) added. The MeOH solvent and excess etheral diazomethane were removed under a stream of dry nitrogen, and the residues resuspended in MeOH. The GC chromatograms of the derivatized hydrolysates were obtained using a ChirasilVal®

column (0.16 μm x 25 m, i.d. 0.25 mm). The oven temperature was raised from 30 °C to 40 °C at 1 °C min $^{-1}$, held for 3 minutes and then ramped to 180 °C at 30 °C min $^{-1}$ for 32.66 minutes. The helium gas flow was 32.6 mL min $^{-1}$. The retention time of the methylated α-hydroxyisovaleric acid (Hiv) residues in **7** (t_R = 13.08 minutes) matched that of the methylated *L*- α-hydroxyisovaleric acid standard (t_R = 13.07 minutes).

However, the retention time of the methylated α-hydroxyisovaleric acid (Hiv) residue in **42** (t_R = 13.88 minutes) compared favourably with the *D*- α-hydroxyisovaleric acid standard (t_R = 13.67 minutes) (Table 3 Section 2.5.3 and Table 5 Section 2.7.1). Likewise, the retention time of the methylated lactate in **42** (t_R = 6.32 minutes) matched that of the *R* (*D*-)isomer (t_R = 6.29 minutes).

REFERENCES

1. Flam, F. *Science* **1994**, *266*, 1324-1325.
2. Andersen, R. J.; Williams, D. E. In Chemistry in the Marine Environment; Hester, R. E and Harrison, R. M., Ed.; Cambridge, U.K, **2000**; pp 55-79.
3. Look, S. A.; Fenical, W.; Matsumoto, G. K.; Clardy, J. *J. Org. Chem.* **1986**, *51*, 5140-5145.
4. Gerwick, W. H.; Tan, L.K.; Sitachitta, N. In The Alkaloids; Cordell, G. A., Ed.; Academic Press: San Diego, **2001**; Vol. 57, pp 75-184.
5. Fenical, W (1996). *Trends in Biotechnology*. **1997**,*15*, 339-341.
6. Burja, A. M.; Banaigs, B.; Abou-Mansour, E.; Burgess, J. G.; Wright, P. C. *Tetrahedron* **2001**, *57*, 9347-9377.
7. Davidson, B.S. *Current. Opinion in Biotechnology*. **1995**, *6*, 284-291.
8. Pietra, F. A. In Secret World: Natural Products of Marine Life 1st ed.; Birkhauser: Basel, Switzerland, **1990**; pp 4-6.
9. Pulz, O. In Biotechnology; Rehm, H. –J.; Reed, G., Ed.; Wiley-VCH: Weinheim, **2001**; Vol. 10, 105-136.
10. Moore, R. E. In Marine Natural Products: Chemical and Biological Perspectives; Scheuer, P. J., Ed.; Academic Press: New York, **1978**; Vol. 1, pp 43-123.
11. Jaspars, M.; Lawton, L. A. *Current Opinion in Drug Discovery and Development*. **1998**, *1*, 77-84.
12. Gerwick, W. H.; Proteau, P. J.; Nagle, D. G.; Hamel, E.; Blokhin, A.; Slate, D. L. *J. Org. Chem.* **1994**, *59*, 1243-1245.
13. Orjala, J.; Gerwick, W. H. *J. Nat. Prod.* **1996**, *59*, 427-430.
14. Luesch, H.; Yoshida, W. Y.; Moore, R. E.; Paul, V. J. *Tetrahedron*. **2002**, *58*, 7959-7966.
15. Nogle, L.; Gerwick, W. H. *J. Nat. Prod.* **2002**, *65*, 21-24.
16. Rinehart, K.L. *Med. Res. Rev*. **2000**, *20*, 1-27.
17. Mittelman, A.; Chun, H.G.;Puccio, C.; Coombe, N.; Lansen, T.; Ahmed, T. *Investigational New Drugs*. **1999**, *17*,179-182.
18. Tsunoo, A.; Kamijo, M. *J. Pharmacol. Exp. Ther*. **1999**, *290, 3*, 1006-1012.

19. Ngoka, L. C. M.; Gross, M. L.; Toogood, P. L. *J. Mass Spectrom.* **1999**, *182 / 183,* 289-298.
20. Rao, M.; Alving, C.R. *Adv. Drug Deliv. Rev.* **2000**, *41,*171-188.
21. Sitachitta, N.; Williamson, R.T.; Gerwick, W.H. *J. Nat. Prod.* **2000**, *63*,197-200.
22. Nakao, Y.; Yoshida, W. Y.; Szabo, C. M.; Baker, B. J.; Scheuer, P. J. *J. Org. Chem.* **1998**, *63,* 3272-3280.
23. Reese, M.T.; Gulavita, N.K.; Nakao, Y.; Hamann, M.T.; Yoshida, W.Y.; Coval, S.J.; Scheuer, P. J. *J. Am. Chem. Soc.* **1996**, *118,*11081-11084.
24. Carter, D. C.; Moore, R. E.; Mynderse, J. S.; Niemczura,W. W. P.; Todd, J. S. *J. Org. Chem.* **1984**. *49,* 236-241.
25. Williams, D. E.; Burgoyne, D. L.; Rettig, S. J.; Andersen, R. J.; Fathi-Afshar, Z. R.; Allen, T. M. *J. Nat. Prod.* **1993**. *56*, 4, 545-551.
26. Bates, R. B.; Gangwar, S. *Tetrahedron: Asymmetry,* **1993**, *4,* 69-72.
27. Mynderse, J. S.; Hunt, A. H.; Moore, R.E. *J. Nat. Prod.* **1988**, *51,*1299-1301
28. Harrigan, G. G.; Yoshida, W.Y.; Moore, R. E.; Nagle, D. G.; Park, P. U.; Biggs, J; Paul, V. J.; Mooberry, S. L.; Corbett, T. H.; Valeriote, F.A. *J. Nat. Prod.* **1998**, *61*, 1221-1225.
29. Pettit, G. R.; Kamano, Y.; Kizu, H.; Dufresne, C.; Herald, C. L.; Bontems, F. E.; Schmidt, J. M.; Nieman, R. A. *Heterocycles,* **1988**, *28,* 553-558.
30. Luesch, H.; Williams, P. G.; Yoshida, W. Y.; Moore, R. E.; Paul, V. J. *J. Nat. Prod.* **2002**, *65*, 996-1000.
31. Luesch, H.; Yoshida, W. Y.; Moore, R. E.; Paul, V. J.; Corbett, T. H. *J. Am. Chem. Soc.* **2001**, *123*, 5418-5423.
32. Horgen, F. D.; Yoshida, W. Y.; Scheuer, P. J. *J. Nat. Prod.* **2000**, *63,* 461-467.
33. Fernandez, R.; Rodriguez, J.; Quinoa, E.; Riguera, R.; Munoz, L.; Fernandez-Suarez, M.; Debitus, C. *J. Am. Chem. Soc.* **1996**, *118,* 11635-11643.
34. Luesch, H.; Yoshida, W. Y., Moore, R. E.; Paul, V. J. *J. Nat. Prod.* **2000**, *63, 8*, 1106-1112.
35. Pettit, G. R; Xu, J.; Hogan, F.; Williams, M. D.; Doubek, D. L.; Schmidt, J. M.; Cerny, R. L.; Boyd, M. R. *J. Nat. Prod.* **1997**, *60,* 752-754.

36. Luesch, H.; Pangilinan, R.; Yoshida, W. Y.; Moore, R. E.; Paul, V. J. *J. Nat.* Prod. **2001**, 64, 304-307.

37. Luesch, H.; Yoshida, W. Y.; Moore, R. E.; Paul, V. J.; Mooberry, S. L. *J. Nat. Prod.* **2000**, *63,* 611-615.

38. Luesch, H.; Yoshida, W. Y.; Moore, R. E.; Paul, V. J. *J. Nat. Prod.* **2000**, *63,*1437-1439.

39. Sone, H.; Kondo, T.; Kiryu, M.; Ishiwata, H.; Ojika, M.; Yamada, K. *J. Org.* Chem. **1995**, 60, 4774-4781.

40. Luesch, H.; Yoshida, W. Y.; Moore, R. E.; Paul, V. J. *J. Nat. Prod.* **1999**, *62,*1702-1706.

41. Mutou, T.; Kondo, T.; Ojika, M.; Yamada, K. *J. Org. Chem.* **1996,** *61*, 6340- 6345.

42. Murata, M.; Matsuoka, S.; Matsumori, N.; Paul, G. K.; Tachibana, K. *J. Am. Chem. Soc*. **1999**, *121*, 870-871.

42. Wu, M.; Okino, T.; Nogle, L. M.; Marquez, B. L.; Williamson, R. T.; Sitachitta, N.; Berman, F. W.; Murray, T. F.; McGough, K.; Jacobs, R.; Colsen, K.; Asano, T.; Yokokawa, F.; Shioiri, T.; Gerwick, W. H. *J. Am. Chem. Soc*. **2000**, *122*, 12041-12042.

43. Orjala, J.; Nagle, D. G.; Hsu, V. L.; Gerwick, W. H. *J. Am. Chem. Soc.* **1995**, *117*, 8281-8282.

44. Yokokawa, F.; Fujiwara, H.; Shioiri, T. *Tetrahedron Lett.* **1999**, *40*, 1915-1916.

45. Yokokawa, F.; Shiori, T. *J. Org. Chem.* **1998**, *63*, 8638-8369.

46. White, J. D.; Hanselmann, R.; Wardrop, D. J. *J. Am. Chem. Soc*. **1999**, *122*, 1106-1107.

48. Nogle, L. M.; Williamson, T. R.; Gerwick, W. H. *J. Nat. Prod*. **2001**, *64*, 716-719.

49. Harrigan, G. G.; Luesch, H.; Yoshida, W. Y.; Moore, R. E.; Nagle, D. G.; Paul, V. J. *J. Nat. Prod*. **1999**, *62*, 655-658.

50. Pettit, G. R. *Prog. Chem. Org. Nat. Prod.* **1997**, 70, 1-79. **2000**, *63*, 279-282.

51. Mitchel, S. S.; Faulkner, D. J.; Rubins, K.; Bushman, F. D. *J. Nat. Prod.*
52. Marfey, P. *Carlsberg Res. Comm.* **1984**, *49*, 591-596.
53. Manning, J. M.; Moore, S. *J. Biol. Chem.* **1968**, *243*, 5591-5597.
54. Chromatographic methods, Braithwaite, A.; Smith, F. J.; Ed; 4th Edition. Chapman and Hall pp 254-267
55. Pirkle, W. H.; House, D. W. *J. Org. Chem.* **1979**, *44*, 1957.
56. Alltech Associates, Inc. 2051 Waukegan rd, Deerfield, IL U.S.A. 60015-1899.
57. Debeer, T. J.; Backer, H. J. *Organic Synthesis.* **1956**, *16*, 16-19.
58. Obura, D. *Mar. Poll. Bullet.* **2001**, *42*, *12*, 1264-178.
59. Mwangi, S.; Kirugara, D.; Osore, M.; Njoya, J.; Yobe, A.; Dzeha, T. M. In Status of Marine Pollution in Mombasa Marine Park and Reserve and Mtwapa Creek, Kenya. Kenya Wildlife Service report. **2001**; p 11.
60. Moorjan, S. In Sea weeds of the Kenya Coast. Gunston, A.; Ed. Oxford University Press, Nairobi, **1998**; p 31.
61. Ruwa, K. In East African ecosystems and their conservation. McClanahan, T. R.; Ed Oxford University Press, New York, **1996**; pp101-130.
62. Anderson, J. E.; Goetz, C. M.; McLaughlin, J. L. Suffness, M. *Phytochem. Anal.* **1991**, *2*, 107-111.
63. MarinLit, Marine literature database. Munro, M. H.; Blunt, J. W. Department of Chemistry, University of Canterbury, Christchurch, New Zealand, February **2002**.
64. Desikachary, T. V. Cyanophyta; Indian council of Agricultural Research: New Delhi, **1959**; p 313.
65. Annual Health Report for the City of Port Elizabeth, 1 July 1997 –30 June **1998**, pp 28 – 34.
66. Dr. Denver Hendricks, Department of Medical Biochemistry, University of Cape Town – *personal communication.*